AD-760 627

FLUID MOTION PROBLEMS IN WIND TUNNEL DESIGN

Advisory Group for Aerospace Research and Development
Paris, France

April 1973

AGARD

ADVISORY GROUP FOR AEROSPACE RESEARCH & DEVELOPMENT

7 RUE ANCELLE 92200 NEUILLY SUR SEINE FRANCE

AGARD-R-602

AGARD REPORT No. 602

on

Fluid Motion Problems in Wind Tunnel Design

NORTH ATLANTIC TREATY ORGANIZATION

DISTRIBUTION AND AVAILABILITY ON BACK COVER

NORTH ATLANTIC TREATY ORGANIZATION

ADVISORY GROUP FOR AEROSPACE RESEARCH AND DEVELOPMENT

(ORGANISATION DU TRAITE DE L'ATLANTIQUE NORD)

AGARD Report No.602

FLUID MOTION PROBLEMS IN WIND TUNNEL DESIGN

This Report is sponsored by the Fluid Dynamics Panel of AGARD as a complementary paper to AGARD Advisory Report No.60 of the Large Wind Tunnels Working Group.

The AGARD Fluid Dynamics Panel wishes to thank Professor A.Heyser, Mr J.Y.G.Evans, and Professor D.Küchemann for their contribution in editing papers included in this Report.

THE MISSION OF AGARD

The mission of AGARD is to bring together the leading personalities of the NATO nations in the fields of science and technology relating to aerospace for the following purposes:

- Exchanging of scientific and technical information;
- Continuously stimulating advances in the aerospace sciences relevant to strengthening the common defence posture;
- Improving the co-operation among member nations in aerospace research and development;
- Providing scientific and technical advice and assistance to the North Atlantic Military Committee in the field of aerospace research and development;
- Rendering scientific and technical assistance, as requested, to other NATO bodies and to member nations in connection with research and development problems in the aerospace field;
- Providing assistance to member nations for the purpose of increasing their scientific and technical potential;
- Recommending effective ways for the member nations to use their research and development capabilities for the common benefit of the NATO community.

The highest authority within AGARD is the National Delegates Board consisting of officially appointed senior representatives from each member nation. The mission of AGARD is carried out through the Panels which are composed of experts appointed by the National Delegates, the Consultant and Exchange Program and the Aerospace Applications Studies Program. The results of AGARD work are reported to the member nations and the NATO Authorities through the AGARD series of publications of which this is one.

Participation in AGARD activities is by invitation only and is normally limited to citizens of the NATO nations.

Published April 1973

533.6.071

Printed by Technical Editing and Reproduction Ltd
Harford House, 7–9 Charlotte St, London. W1P 1HD

PREFACE

The Large Wind Tunnels Working Group (LaWs) of the Fluid Dynamics Panel of AGARD has been helped considerably in its deliberations by a large number of non-member scientists and engineers from the participating countries, who investigated particular problems, provided specially-written papers, or took part in the discussions. This help was very much appreciated by the members of the Group, and the information contained in the LaWs Papers, in particular, has proved to be very valuable. However, the number of LaWs Papers is so large (over 130) that it was not possible to publish them all or to include them in full in the Report of the Group (AGARD Advisory Report 60 entitled "The Need for Large Wind Tunnels in Europe"). On the other hand, some of the LaWs Papers present substantial surveys of particular fields and others describe possible options for future wind tunnels in detail. These papers supplement the Report of the Group in essential respects. The Group decided, therefore, to publish a selection of the LaWs Papers in AGARD Reports, so that they are generally available and can be read in conjunction with the Report of the Group.

As a result, four AGARD Reports are being published, collecting a number of papers together on subjects related to the design and operation of low-speed and transonic wind tunnels, with particular reference to possible future large wind tunnels in Europe. There are thus three further Reports in addition to the present Report. Their contents are listed in Appendix I at the end of this Report.

Wherever appropriate, the individual papers have been edited by a member of the LaWs Working Group. On behalf of the members of the LaWs Group, the undersigned wishes to thank all those who helped the Group and especially the authors of the papers published here.

D.Küchemann
Chairman, LaWs Working Group

November 1972

CONTENTS

THE INFLUENCE OF THE FREE-STREAM REYNOLDS NUMBER ON TRANSITION IN THE BOUNDARY LAYER ON AN INFINITE SWEPT WING

by

E. H. Hirschel
DFVLR-Institut für Angewandte Gasdynamik
5050 Porz-Wahn, Linder Höhe
W. Germany

SUMMARY

The three-dimensional compressible laminar boundary layer on an infinite swept wing at different sweep angles is calculated and stability and transition criteria are applied to it for free-stream Reynolds numbers ranging from values possible nowadays in transonic wind tunnels to values typically for full-scale flight. The distribution of the inviscid flow is taken from experiments on airofoils, and exhibits for subsonic free stream Mach numbers supersonic regions terminating in shock waves at about 20 percent chord length. Results are given for four different wing sections. The techniques employed and their shortcomings are discussed.

1. INTRODUCTION

Scale effects are present in the flow field about an airofoil at transonic speed. In order to determine this flow field theoretically, knowledge is needed of the transition processes in the boundary layer from laminar to turbulent state and vice versa. On a swept wing the boundary layer is three-dimensional, and this feature of the flow field adds further to the already large problems of the "simple" two-dimensional case.

The present paper is concerned with the prediction of transition in three-dimensional compressible boundary layers on swept wings. Little is actually known about the physical process of transition and its mathematical approach [1]. BEASLEY and TREADGOLD [2] have applied the currently known stability and transition criteria to the flow on an infinite swept wing, so reducing the effort necessary for the calculation of the boundary layer. The pressure distribution was taken from experiments on unswept wings at transonic conditions. The boundary-layer calculation was carried out for the incompressible case, using a finite difference method developed by BEASLEY [3]. The present work is based essentially on the same method of approach as in [2]. However, the boundary-layer calculations are made for the compressible case and an attempt is made to account for the compressibility in some of the criteria.

Calculating the compressible boundary layer on an infinite swept wing, one has to take somewhat more pain over the incompressible case, since the independence principle no longer holds due to the coupling of the momentum equations with the energy equation. The solution method of [4] has been adapted, and it proved to be usefull in this problem where supersonic outer flow conditions are present, and high pressure gradients occur, both favourable and adverse.

Four different airofoil sections (normal to the leading edge) are considered at free stream Mach numbers of about $M_\infty = 0.6$ to 0.65. All have supersonic flow regions with terminating shock waves at about 20 percent of the chord length. Sweep angles of the wing are generated by superimposing a velocity component parallel to the leading edge of the wing.

The calculations of the stability and transition parameters are made with different free stream Reynolds numbers, ranging from those achieved in existing transonic wind tunnels, to values which may be obtained in full-scale flight.

Certain flow features, present on finite swept wings, are not accounted for in this study. The methods used to predict the instability and the transition are based on crude assumptions in most cases [2]. Infact, it is doubtable in some cases, wether it is justified at all, to employ them for the boundary layer considered.

2. APPROACH TO THE PROBLEM

2.1 INVISCID FLOW

Fig. 1 shows the schematic of the flow field on an infinite swept wing. q_∞ is the undisturbed free-stream velocity, φ the sweep angle, and u_∞ and v_∞ are the resulting free-stream velocity components normal and parallel to the leading edge, respectively. At the leading edge the velocity component normal to the leading edge is zero, but assumes velocities $u_e(x)$ far larger than the free-stream value u_∞ while expanding around the upper surface of the wing which is only considered here. The velocity component in y-direction is constant and equal to v_∞ over the whole flow field.

The velocity distribution $u_e(x)$ is calculated from the pressure distribution shown in Fig. 2. The circles indicate the points at which the pressure is actually known from experiments. The measurements were made at the airofoils shown in Fig. 3. The free-stream Mach numbers were: $M_\infty = 0.603$ for section A, $M_\infty = 0.601$ for section B, and $M_\infty = 0.649$ for sections C and D. The Reynolds number was approximately $3 \cdot 10^6$. The coordinates in Fig. 3, and the pressure distribution in Fig. 2 are taken from [2]. The sweep angles $\varphi = 30^\circ$ and $\varphi = 60^\circ$ are obtained by adding vectorially an appropiate v_∞-component to the $u_e(x)$-distribution. The corresponding free-stream Mach numbers are:

a) $\varphi = 30^\circ$: $M_\infty = 0.696$, 0.694, 0.749 and 0.749
b) $\varphi = 60^\circ$: $M_\infty = 1.206$, 1.202 1.298 and 1.298

for the four sections, respectively. The velocity $u_e(x)$, as also the temperature $T_e(x)$, and the density $\varrho_e(x)$, is calculated from the measured pressure distribution under the assumption of constant specific heats, equal to the free-stream values, with a ratio of the specific heats of $\gamma = 1.4$.

2.2 BOUNDARY LAYER CALCULATION

Since an infinite swept wing is considered, all derivatives in y-direction of the flow variables are identical to zero. The three-dimensional boundary layer equations reduce therefore to a system with two independent variables x and z (if z is the direction normal to the wings surface). As in [2], the coordinate z and the velocity component w in this direction are transformed by employing the Blasius transformation . The two momentum equations and the energy equation are solved simultanously for u, v, and T in the boundary layer, while the normal velocity component w is obtained from the continuity equation [4]. The viscosity-temperature relation used is $(\mu/\mu_{ref}) = (T/T_{ref})^{0.76}$, and the heat conductivity is computed from this data with a Prandtl number $Pr = 0.75$. In the boundary layer calculations the specific heats are also considered as constant and equal to the free-stream values.

For all results presented here the boundary condition at the wall for the temperature is $T = T_\infty$. Boundary conditions at the wall: $T_w = 0.8\, T_\infty$, $T_w = 1.2\, T_\infty$, and the adiabatic wall condition $q_w = 0$ were also employed in some calculations in order to study their effect on the results. In this paper, however, only the dependence of the momentum thickness and the cross-flow-displacement thickness of section A for the different sweep angles on these boundary conditions is reported. The boundary-layer calculations were carried out over the first 20 percent of the chord to the position of the shock wave.

2.3 STABILITY AND TRANSITION

The free-stream Reynolds number in the stability and transition parameters is varied between $3 \cdot 10^6$ and $72 \cdot 10^6$. The Reynolds number is defined by $R = q_\infty c^*/\nu_\infty$ (q_∞ is the free-stream velocity, ν_∞ the free-stream kinematic viscosity, and $c^* = c/\cos\varphi$ the chord length measured in the free-stream direction, Fig. 1).

Although, as pointed out before, the validity of the criteria employed is only preliminary in nature, it can be concluded from [1] that at the present time only the criteria already employed in [2] exist for the problem studied. The following discussion of the stability and transition criteria, is therefore a shortened rendition of that in [2], partly expanded where the compressibility of the flow is considered.

2.3.1 LEADING-EDGE CONTAMINATION AND RE-LAMINARISATION

Any local turbulent contamination at the leading edge will tend to spread along the leading edge, when a critical value of the Reynolds number (see e. g. CUMPSTY and HEAD [5]):

$$R_\Theta = \frac{0.4\, v_\infty}{\sqrt{\nu (du_e/ds)_a}} \tag{2.1}$$

is exceeded. The term $(du_e/ds)_a$ is the velocity gradient of the inviscid flow at the leading edge in the direction normal to it. The coordinate s is measured around the surface of the wing in that direction (Fig. 1). Following [2] $R_\Theta = 100$ is considered as critical value, with a range of uncertainty of from 80 to 120. If R_Θ exceeds 240, turbulent contamination is considered as present in any case.

It appears that these values are essentially deduced from experiments in incompressible flows [2]. With regard to the compressible flow considered in this study the kinematic viscosity is taken as the local value at the leading edge. It cannot be decided at this point whether this is justified or not.

The possibility of re-laminarisation following turbulent leading edge contamination can be deduced from the parameter

$$K = \frac{\nu}{u_e^2} \frac{du_e}{dx} \quad . \tag{2.2}$$

LAUNDER and JONES [6] suggest that, in two-dimensional flow, re-laminarisation begins when $K > 2 \cdot 10^{-6}$, but to obtain effectively laminarised flow K has to exceed $5 \cdot 10^{-6}$. In the present study it is assumed that this criterion can be used if K is calculated along the stream line. The kinematic viscosity is considered firstly as local and then as free-stream value.

2.3.2 CROSS-FLOW INSTABILITY

HALL has discussed the current knowledge about the transition phenomena in three-dimensional boundary layers [1]. It appears that at the present time the only theoretical approach concerning the stability of the three-dimensional boundary layer flow is to investigate the cross-flow instability, and, if the cross flow is small, the Tollmien-Schlichting instability for adverse pressure gradients in the stream-wise direction (For this approach, the boundary-layer velocity components parallel to the surface u and v are transformed in a component parallel to the inviscid streamline (streamwise-component v_s), and a component normal to it (cross-flow-component v_c)).

OWEN and RANDALL [7] have proposed that the cross-flow instability and subsequent transition will occur when a cross-flow Reynolds number defined by

(2.3) $$\chi = \frac{v_{c_{max}} \delta_c}{\nu}$$

exceeds a definite value. $v_{c_{max}}$ is the maximal value of the cross-flow velocity in the boundary layer, and δ_c a not precisely defined boundary layer thickness. In the present study, as in [2], this boundary layer thickness is calculated from

(2.4) $$\delta_c = \int_0^\infty \frac{v_c}{v_{c_{max}}} dz \quad .$$

The critical value of χ is assumed to be $\chi = 120$, with a range of uncertainty of from 100 to 140 [2]. The kinematic viscosity again is considered both as local and as free-stream value.

2.3.3 TOLLMIEN-SCHLICHTING INSTABILITY

In [2], for the incompressible case, the Tollmien-Schlichting instability location was calculated using the empirical curve given in [8]. The curve gives the critical Reynolds number R_2 as function of the pressure gradient parameter λ_2. Since the instability was not considered for the stream-wise direction, but only in x-direction, the Reynolds number R_2 is defined by

(2.5) $$R_2 = \frac{u_e \delta_2}{\nu}$$

with $u_e(x)$ as the local outer velocity, and δ_2 as the momentum thickness in x-direction.

The pressure gradient parameter is

(2.6) $$\lambda_2 = \frac{\delta_2^2}{\nu} \frac{du_e}{ds} \quad .$$

The effect of the compressibility and the heat transfer at the wall has been taken into account in the work of LEES and LIN [9]. However, the only flow considered there is the flow past flat plates. SCHLICHTING [10] gives reference to work of this kind, including the influence of pressure gradients, but this results are not included in the present analysis.

From the results of [9] given in [10] it can be concluded that, as a first approximation, the effects of compressibility and heat transfer at the wall can be neglected, assuming, admittedly without further justification, that no strong coupling between these effects and the effect of the pressure gradient exists.

All that is done in the present work to take into account the compressibility is that in eqs. (2.5) and (2.6) the momentum thickness is calculated using the appropiate formula, and that the influence of the local and the free stream kinematic viscosity, respectively, is studied.

2.3.4 TRANSITION

For the transition due to cross-flow instability HALL [1] presents values for χ (eq 2.3), for which transition is completed. Because of large uncertainties in these values, transition following cross-flow instability is not considered.

Transition following the Tollmien-Schlichting instability is determined by using the method of GRANVILLE [11]. He gives a relationship between the change of values of the Reynolds number at the instability point R_i to that at the transition point R_t, and the average pressure gradient parameter. The latter is defined by

(2.7) $$\bar{\lambda}_2 = -\left[\int_{s_i}^{s_t} \left(\frac{\delta_2^2}{\nu} \frac{du_e}{ds}\right) ds\right] / (s_t - s_i)$$

Fig. 4 shows the relationship $R_{2t} - R_{2i} = f(\bar{\lambda}_2)$. Included is another curve, based on experiments on swept wings, which seems to be a necessary alteration of Granville's relation [1, 2]. Both curves are used for the sake of comparison in the present work.

3. RESULTS

3.1 GENERAL REMARK

Calculations were made for both the compressible and the incompressible case, the latter in order to check the programme against the results in [2]. In contrast to the results of the calculation of the incompressible boundary layer in [2] and in the present work, the calculation of the compressible boundary layer indicates for section D a separation at about 7 percent of the chord length for all sweep angles considered.

Although the pressure distribution shows a strong adverse pressure gradient in that region (Fig. 2), it is quite possible that the separation calculated is only due to inaccuracies of the interpolation process employed in order to get the pressure at the different points of calculation, and does not occur in reality.

3.2 LEADING-EDGE CONTAMINATION AND RE-LAMINARISATION

Figs. 5 to 8 show, for the four sections and the two sweep angles considered, the Reynolds number indicating leading edge contamination R_{Θ} vs. the free-stream Reynolds number R. Indicated is also the value $R_{\Theta_1} = 100$, which is considered as the critical value, and the value $R_{\Theta_2} = 240$, at which turbulent contamination is considered as beeing present in any case. For $\varphi = 30^\circ$ R_{Θ_1} is exceeded on sections A to C at about $R = 12 \cdot 10^6$, whereas R_{Θ_2} is exceeded only at much higher free-stream Reynolds numbers. For the larger sweep angle $\varphi = 60^\circ$ R_{Θ_1} is exceeded in all cases at least at $R = 6 \cdot 10^6$, and R_{Θ_2} at $R = 20 \cdot 10^6$, pointing to the conclusion that in experiments at low free-stream Reynolds numbers the probability of turbulent contamination is small, whereas it will be present at higher Reynolds numbers for all four sections and both sweep angles considered. The different defined kinematic viscosity has no strong influence. Concerning the reliability of the results, it should be emphasized that R_{Θ} depends on the only approximately known velocity gradient at the leading edge, which was determined from the experiments [2] to $d\,(u/u_e) / d\,(s/c) = 40$, 70, 50, and 20 for the four sections, respectively.

The possibility of re-laminarisation exists if $K_1 = 2 \cdot 10^{-6}$ is exceeded, but effective relaminarisation will be present only for values of K larger than $K_2 = 5 \cdot 10^{-6}$. Both values are exceeded at Reynolds-numbers lower than $R = 10 \cdot 10^6$ and at sweep angles $\varphi = 30^\circ$ for sections A to D as seen in Figs. 5 to 7, where the maximum values of K existing in the flow-field are shown. At $\varphi = 60^\circ$ the possibility of re-laminarisation is present, if at all, only at much lower Reynolds numbers. Section C is an exception in so far as here a strong influence exists depending on whether the flow is compressible or incompressible.

In Figs. 9 to 12 the location of the maximum values of K_{max} can be deduced from the peaks of the curves $K = 3 \cdot 10^{-6} = \text{const}$, and $K = 7 \cdot 10^{-6} = \text{const}$. In all cases considered K is too small to suggest the possibility of re-laminarisation for s/c larger than 0.1. Transition induced by cross-flow or Tollmien-Schlichting instabilities seems to be possible only at larger values of s/c. Turbulent contamination at low Reynolds numbers will be laminarised in some of the cases. As pointed out before, the data lie in a region where the velocity gradients are not exactly known, and therefore the results have to be interpreted with care.

3.3 CROSS-FLOW INSTABILITY

The cross-flow Reynolds number χ is given in Figs. 13 to 20 for both sweep angles $\varphi = 30^\circ$, and $\varphi = 60^\circ$, and all four sections considered, as functions of x/c with the free-stream Reynolds number as parameter. The maximum values of χ increase with the free-stream Reynolds number, and with the sweep angle. The critical value $\chi = 120$ is exceeded only in the incompressible case for $R \geq 36 \cdot 10^6$. In the compressible case $\chi = 120$ is always exceeded at $R = 18 \cdot 10^6$. For the compressible case shown here the kinematic viscosity was always taken as equal to its free-stream value ($\nu = 1$). If one takes, this being more realistic, ν as the local value, one arrives at results lieing almost halfway between both the results of the cases shown in Figs. 13 to 20. This also can be seen in Figs. 5 to 8, where the maximum values of χ are plotted.

The range of uncertainty is shown in Figs. 9 to 12. If one considers the compressible case with $\nu = 1$ cross-flow instability is possible already at very small Reynolds numbers, and at a chord length smaller than $s/c = 0.05$. It can be concluded that the position where the critical cross-flow Reynolds number is exceeded is closer to the leading edge for higher Reynolds numbers, but that it is not greatly affected by the sweep angle. The sweep angle influences the minimum Reynolds number at which cross-flow instability will occur.

3.4 TOLLMIEN-SCHLICHTING INSTABILITY AND TRANSITION FOLLOWING IT

Fig. 21 shows the position of transition x_t/c following the Tollmien-Schlichting instability for $\varphi = 0^\circ$. For both the other sweep angles $\varphi = 30^\circ$, and $\varphi = 60^\circ$ these positions are given in Figs. 9 to 12 (the relation between x/c and s/c is reported in [2]). In general it can be said, that for higher free-stream Reynolds numbers the transition will occur nearer the leading edge. The modified Granville data shift, except for section D, the transition point back from the leading edge to positions further downstream.

The calculations made for the compressible boundary layer with $\nu = 1$, yield points of transition nearer the leading edge, than those for the incompressible boundary layer. In Fig. 21, the case for $\varphi = 0$ with the locally taken kinematic viscosity (local ν), which is included for the non-modified Granville data, yields positions downstream from those for the incompressible case. Four cases of transition are possible at the wing. In general [2]: 1) transition following Tollmien-Schlichting instability, 2) leading-edge contamination followed, possibly, by relaminarisation and then transition through Tollmien-Schlichting instability, 3) leading edge contamination, followed, possibly, by re-laminarisation and then transition through cross-flow instability, and 4) transition following from cross-flow instability if leading-edge contamination is absent.

3.5 INFLUENCE OF THE DIFFERENT TEMPERATURE BOUNDARY CONDITIONS AT THE SURFACE OF THE WING

Calculations have been made in order to study the influence of the temperature boundary conditions on the transition properties of the boundary layer. Here only the results concerning the boundary-layer parameters which govern the cross-flow instability (δ_c), and the Tollmien-Schlichting instability (δ_3) are presented. As seen from Fig. 22, the cross-flow displacement thickness δ_c has larger values in the whole flow-field considered when the wall temperature T_w is higher. This indicates that the critical cross-flow Reynolds number will be reached at points closer to the leading edge, if the surface temperature is increased. For $\varphi = 60^\circ$ this trend is still stronger (not shown in Fig. 22). For the adiabatic wall the resulting

curve lies between those for $T_w = T_\infty$, and $T_w = 1.2\ T_\infty$.

Opposite trends are observed for the momentum thickness δ_2. δ_2 becomes smaller when T_w is larger. In the incompressible case, all sweep angles yield the same function δ_2 (s/c), because the momentum equation in y-direction is decoupled from the other equations. In all compressible cases considered, the functions δ_2 (s/c) belonging to different sweep angles are different from each other, which is due to the coupling of the equations. The results for $\varphi = 30^\circ$ lie closely underneath the values for $\varphi = 0^\circ$, whereas the curves for $\varphi = 60^\circ$ (not shown here as for 30°) are still further beneath it, but not much. The position of transition is shifted slightly nearer to the leading edge for higher wall temperatures.

4. CONCLUSION

With the present work an attempt has been made to predict transition in compressible boundary layers on swept wings. Conclusions can be drawn from the results of the calculations, but one has to keep in mind that the work rests partly on poorly justified assumptions. Considered in this study were: a) leading-edge contamination and re-laminarisation, b) cross-flow instability, c) Tollmien-Schlichting instability in the streamwise direction, and d) transition following Tollmien-Schlichting instability, all on an infinite swept wing. Not considered were the effects of roughness and free stream turbulence on the transition process.

Three groups of problems became apparent during the course of the work, and it seems to be necessary to discuss these problems briefly here:

1) The inviscid flow

Although only the flow in the first 20 percent of the chord on an infinite swept wing was considered, it became evident that the data of the inviscid flow-field must be known to a higher degree of accuracy than was known in this study. Nearly all of the criteria employed depend strongly on velocities and velocity gradients of the inviscid flow, and some of the results are of a small degree of accuracy a priori, due to the small degree of accuracy of the inviscid flow-field data.

The boundary-layer flow, on the other hand, should be calculated with as small an error as possible, and this error depends fully upon the quality of the boundary conditions, considering the high accuracy of the calculation methods available nowadays for laminar boundary layers.

The demand for high accuracy applies to both experimentally and theoretically determined flow-fields if one wishes to study transition processes in the three-dimensional boundary layers developed by this flow-fields. Both experiments and theories set up for such studies should be reconsidered under these aspects and be improved if necessary, and possible.

2) Boundary-layer calculation

The numerical calculation methods for compressible laminar boundary layers in two and three dimensions seem to have reached a high degree of accuracy and reliability. Effort is necessary in order to reduce calculation time and storage requirements, especially for three-dimensional boundary layers. Both can perhaps be reduced, for instance, by employing higher order difference approximations (e. g. the Mehrstellen-method), at least for the direction normal to the surface. Work on this problem already started at different places in Germany, should be encouraged and directed in order to get as soon as possible quicker methods.

3) Stability and transition criteria

In order to get acquainted with the stand of the art in this field one should read M. G. HALL's detailed analysis [1]. The main problem in this field seems to be that a very large amount of work is necessary for only a basic understanding of the transition process in general compressible three-dimensional boundary layers. Criteria suitable for prediction purposes require even more work if one wishes and has to rely on the results.

Finally the author wishes to express his opinion that a theoretical prediction of the flow on arbitrary shapes at arbitrary flow conditions will be possible in say one decade. But this will only be possible if concerted work is spent on broader basis on problems such as transition, turbulence and separation. The calculation of the flow-fields, as such, seems to be more or less a matter of computers big enough.

5. REFERENCES

[1] HALL, M. G. Scale Effects in Flows over Swept Wings. RAE TR 71043 (1971).

[2] BEASLEY, J. A., TREADGOLD, D. A. Some Examples of the Application of Methods for the Prediction of Boundary-Layer Transition on Sheared Wings. RAE-Report to be published.*

[3] BEASLEY, J. A. Calculation of the Laminar Boundary Layer and the Prediction of Transition on a Sheared Wing. RAE-Report to be published.

[4] KRAUSE, E., HIRSCHEL, E. H., BOTHMANN, Th. Differenzenformeln zur Berechnung dreidimensionaler Grenzschichten. DLR FB 69-66 (1969).

[5] CUMPSTY, N. A., HEAD, M. R. The Calculation of the Threedimensional Turbulent Boundary Layer. Part III. Comparison of Attachment-Line Calculations with Experiment. Aero Quart., Vol. XX, 99-113 (1969).

[6] LAUNDER, B. E., JONES, W. P. On the Prediction of Laminarisation. ARC CP 1036 (1969).

*[and see Paper 2, R.602]

[7] OWEN, P. R., RANDALL, D. G. Boundary Layer Transition on a Sweptback Wing. Unpublished RAE Techn. Memo, 1952.

[8] STUART, J. A. Application of the Instability Theory to Twodimensional Boundary Layers. Lect. 5 of Chapter IX, "Hydrodynamic Stability" in Laminar Boundary Layers", ed. L. Rosenhead, Oxford University Press (1963), 540-544.

[9] LEES, L., LIN, C. C. Investigation of the Stability of the Laminar Boundary Layer in a Compressible Fluid. NACA TN 1115 (1946).

[10] SCHLICHTING, H. Grenzschicht-Theorie, Chapter XVII. G. Braun, Karlsruhe (1964), 5. Auflage, 484-491.

[11] GRANVILLE, P. S. The Calculation of Viscous Drag of Bodies of Revolution. Rep. No. 849, The David Taylor Model Basin (1953).

ACKNOWLEDGEMENT

The present theoretical work was commenced in January of 1972. Since the date for the presentation was fixed for July of the same year, and the author had to work without assistance in a field partly new to himself, only the first step of an investigation of the problem, especially concerning the stability and transition criteria, was possible. Even the results presented here could not have been obtained without the help recieved from the RAE. The author wishes to thank J. A. Beasley and D. A. Treadgold, who provided him with the results of their investigation of the same topic for incompressible flows, and together with M. G. Hall, for their helpfull discussions on all matters concerning the present work.

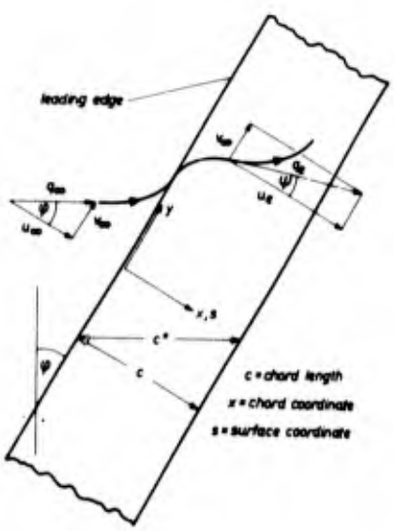

Fig. 1 Schematic of the flow at the infinite swept wing.

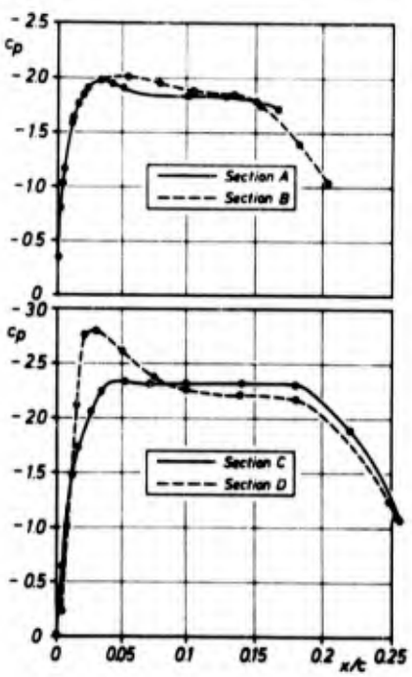

Fig. 2 The pressure distribution for the four sections near the leading edge [2].

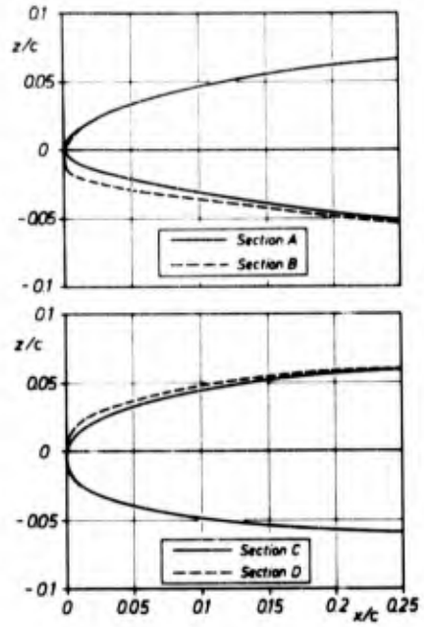

Fig. 3 The shapes of the four sections near the leading edge [2].

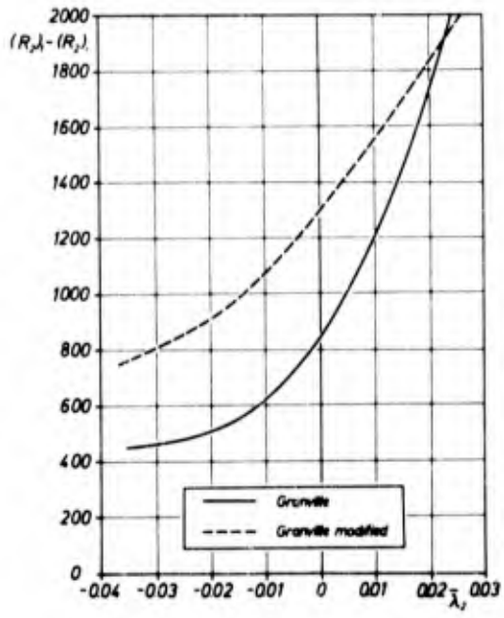

Fig. 4 Granville's relationship and the modified relationship [2].

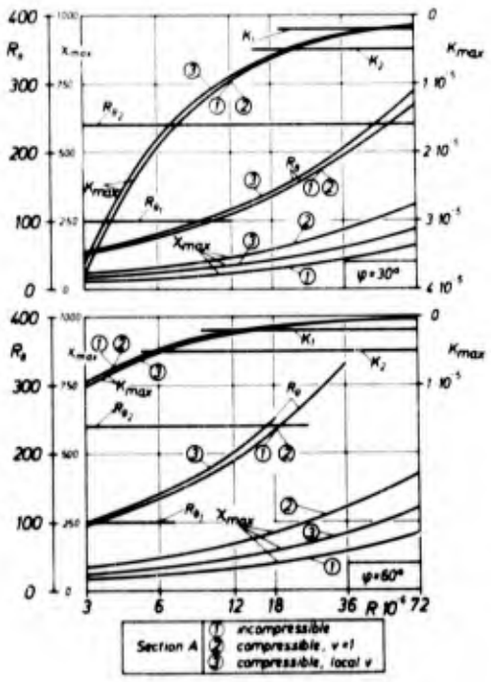

Fig. 5 Effect of free-stream Reynolds number on transition parameters, Section A.

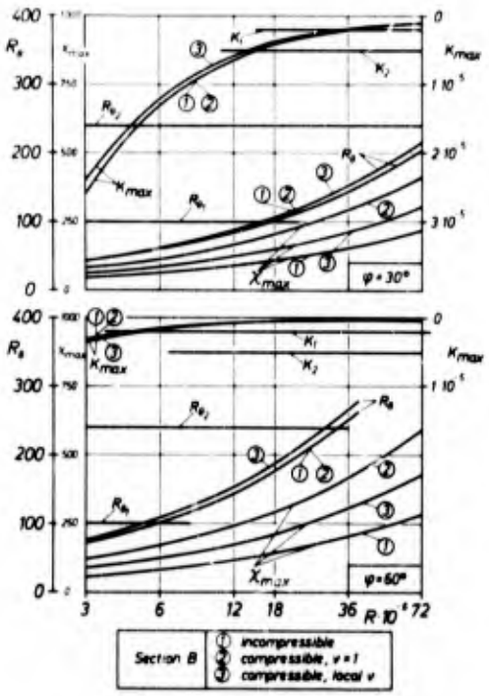

Fig. 6 Effect of free-stream Reynolds number on transition parameters, Section B.

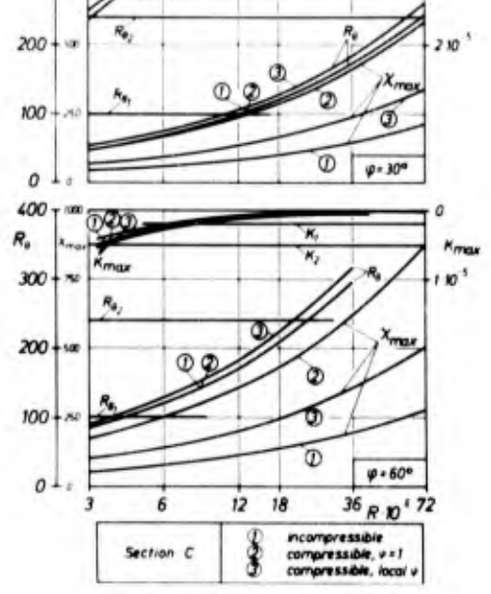

Fig. 7 Effect of free-stream Reynolds number on transition parameters, Section C.

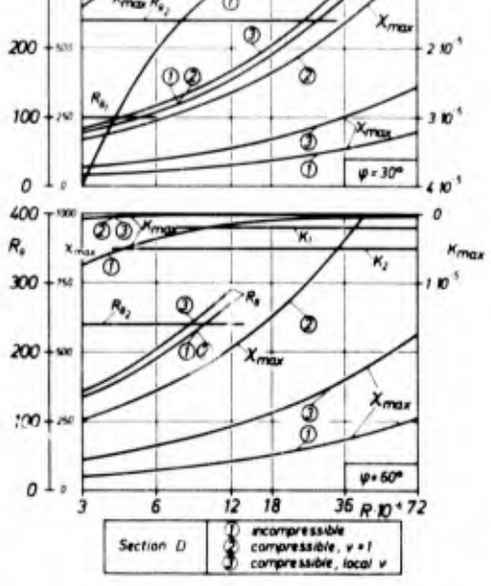

Fig. 8 Effect of free-stream Reynolds number on transition parameters, Section D.

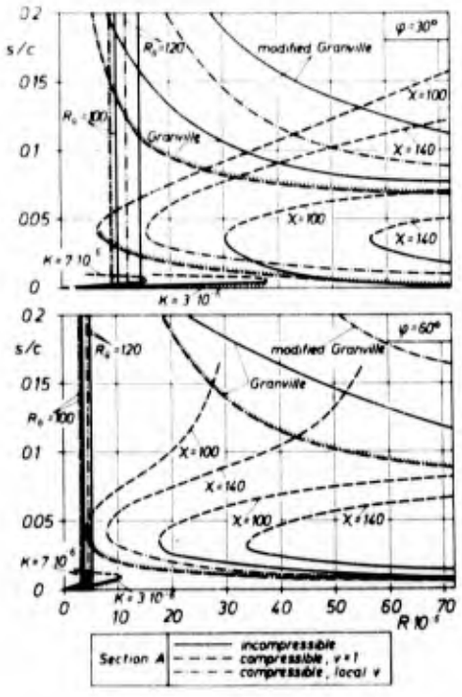

Fig. 9 Effect of free-stream Reynolds number on transition positions, Section A.

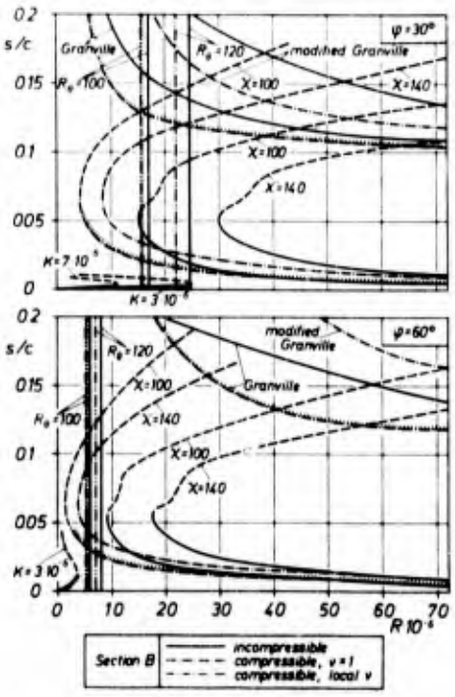

Fig. 10 Effect of free-stream Reynolds number on transition positions, Section B.

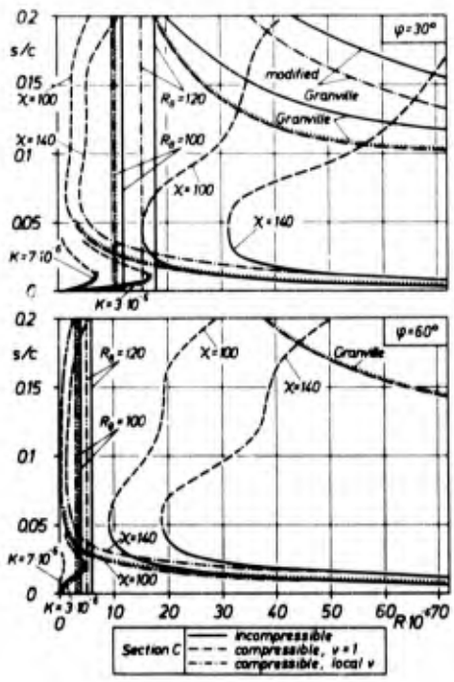

Fig. 11 Effect of free-stream Reynolds number on transition positions, Section C.

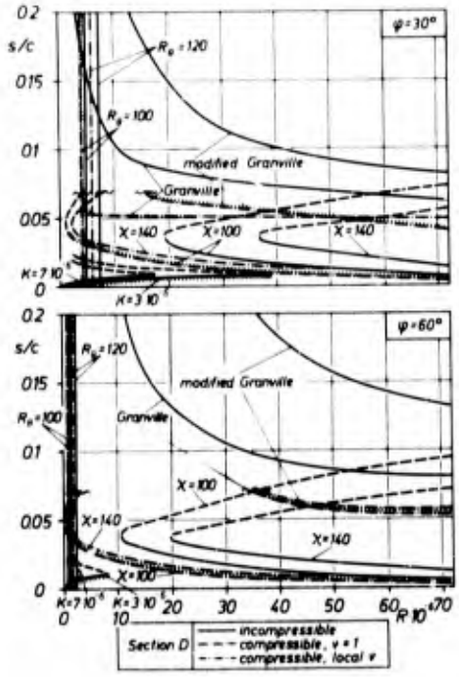

Fig. 12 Effect of free-stream Reynolds number on transition positions, Section D.

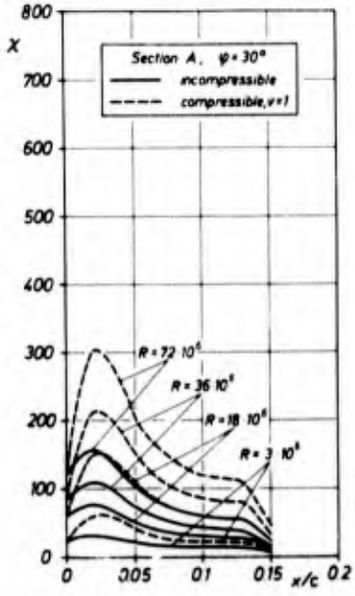

Fig. 13 Cross-flow instability criterion, Section A, $\varphi = 30^{\circ}$.

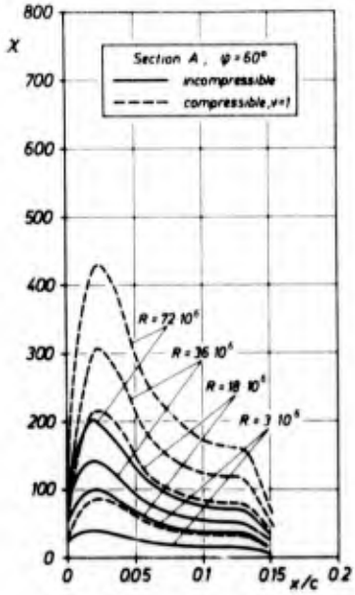

Fig. 14 Cross-flow instability criterion, Section A, $\varphi = 60^{\circ}$.

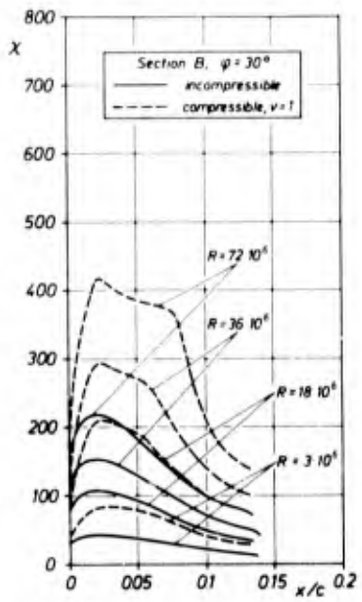

Fig. 15 Cross-flow instability criterion, Section B, $\varphi = 30^{\circ}$.

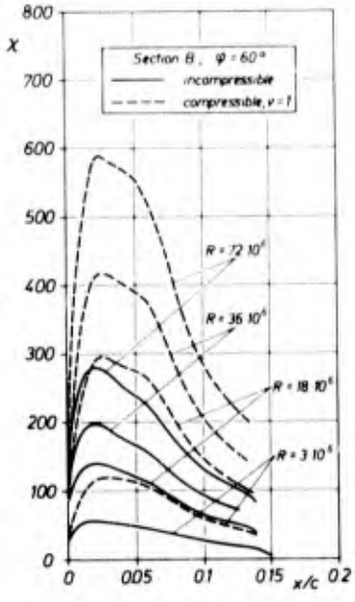

Fig. 16 Cross-flow instability criterion, Section B, $\varphi = 60^{\circ}$.

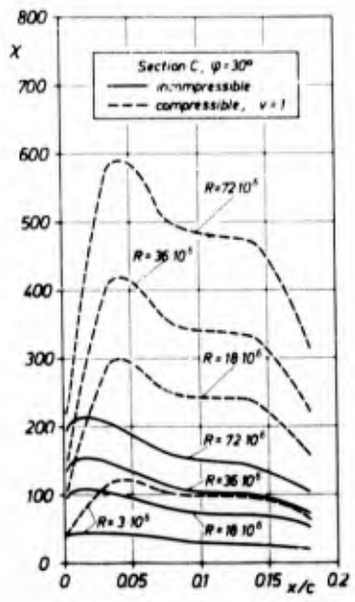

Fig. 17 Cross-flow instability criterion, Section C, $\varphi = 30^{\circ}$.

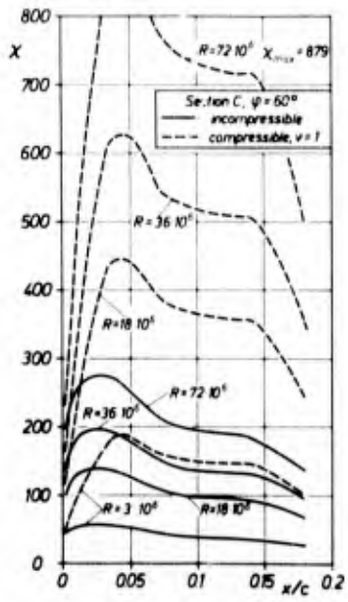

Fig. 18 Cross-flow instability criterion, Section C, $\varphi = 60^{\circ}$.

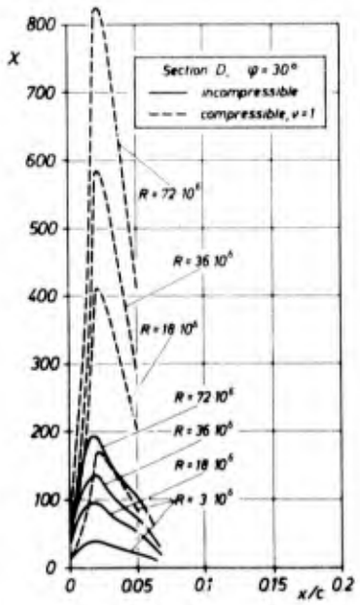

Fig. 19 Cross-flow instability criterion, Section D, $\varphi = 30^{\circ}$.

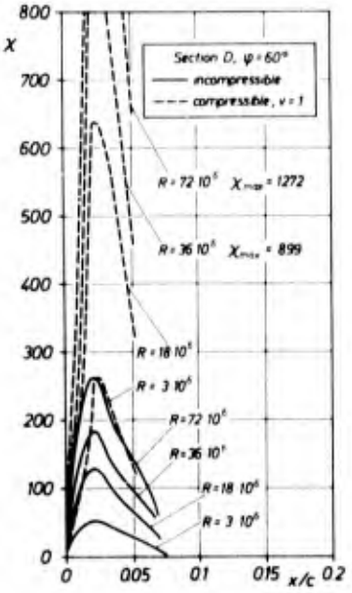

Fig. 20 Cross-flow instability criterion, Section D, $\varphi = 60^{\circ}$.

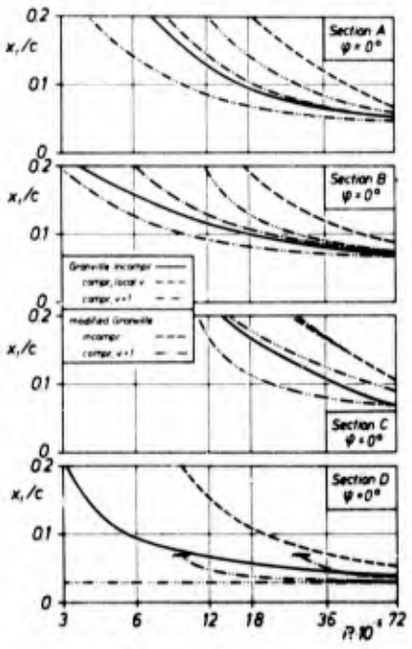

Fig. 21 Effect of free-stream Reynolds number on transition positions.

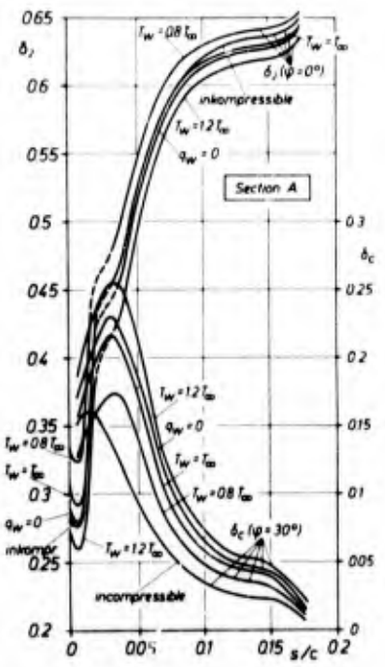

Fig. 22 Effect of temperature boundary conditions at the wing surface on momentum thickness δ_2 and cross-flow displacement thickness δ_c.

SOME EXAMPLES OF THE APPLICATION OF METHODS FOR THE PREDICTION OF BOUNDARY-LAYER TRANSITION ON SHEARED WINGS

by

D. A. Treadgold
J. A. Beasley
Royal Aircraft Establishment
Farnborough
Hampshire
England

SUMMARY

The laminar boundary layer has been calculated for the leading-edge region of four selected aerofoils for cases where the supercritical region is terminated by a shock wave at about 20% chord. The possibility of the boundary layer becoming turbulent before the shock wave is then considered according to four different criteria: leading-edge contamination, re-laminarisation, sweep instability and Tollmien-Schlichting instability. Many simplifying assumptions have had to be made, since the purpose of the Report is to demonstrate how the problem might be treated, rather than to present definitive results, and how the various mechanisms are seen in conjunction. It is concluded that much more needs to be known before predictions can be made confidently with any degree of precision.

SYMBOLS

a	suffix to denote value at the attachment line
c	chord length of wing, measured normal to the leading edge
C_p	pressure coefficient
i	suffix to denote value at point of instability
K	re-laminarisation parameter
R	Reynolds number, $\frac{U_\infty c (\sec \varphi)}{\nu}$
R_k	roughness Reynolds number, $\frac{u_k \sigma_k}{\nu}$
R_2	Reynolds number based on momentum thickness
R_θ	Reynolds number based on momentum thickness at the attachment line
S	distance measured around the surface in a plane normal to the leading edge
t	suffix to denote value at point of transition
u_k	velocity at the top of the roughness element
U	local velocity at edge of boundary layer
U_0	local velocity at edge of boundary layer perpendicular to leading edge
U_∞	free stream velocity at infinity
U'	component of the potential flow velocity in a plane normal to the leading edge
v_N	cross-flow velocity component within the boundary layer
V	component of the free stream velocity along the attachment line
x	Cartesian co-ordinate in the flow direction
X	distance measured along the wing chord from and normal to the leading edge
z	distance measured out from and normal to the wing surface
δ_c	cross-flow boundary layer thickness
σ_k	height of the roughness element
λ_2	parameter for Tollmien-Schlichting type of instability
$\bar{\lambda}_2$	average value of λ_2 over a region
ν	kinematic viscosity
φ	angle of sweep
χ	cross-flow Reynolds number
δ_c	momentum thickness

1 INTRODUCTION

One of the many problems that arise in investigations of the flow past swept wings is that of determining the state of the boundary layer. Hall[1] has reviewed the then current knowledge of the effects of variations in Reynolds number on the possible types of flow over a swept wing and the boundaries between them. Here, we are concerned only with where and how transition from the laminar to the turbulent state occurs, for a given wing shape and Reynolds number.

There are several general features of the flow over a swept wing which affect the problem, and which may be discussed in terms of the flow elements sketched in Fig.9 of Ref.2. The flow along the attachment line along the leading edge may be thought of as originating on the solid surface from a stagnation point at the apex of the wing or at the nose of the body. Flow separation may occur just upstream of the wing-body junction and lead to the formation of junction vortices (as described, for example, by East and Hoxey[3]) but, in any case, the flow along the attachment line may become turbulent on its own account by a mechanism which is commonly called 'leading-edge contamination'. If it does, there is a possibility that the flow may revert to the laminar state. This is commonly called 're-laminarisation'.

If the streamlines are viewed in a direction along the leading edge it is apparent that some concavity may exist near the attachment line; thus the possibility of an instability of the kind investigate by Görtler and Witting[4] must be admitted although it has not been possible to treat this quantitatively in this analysis. In planview, the streamlines downstream of the attachment line are curved as the component of the velocity of the external flow normal to the leading edge changes. This flow may be unstable due to cross-flow as described, for example, by Stuart[5]. There are some indications that the actual transition process is then fairly rapid. The curvature of the streamlines may also be such that the flow separates, as described by Maskell and Weber[6]. Finally, the flow may become unstable in the sense of Tollmien and Schlichting; this could occur at any point aft of the attachment line, given the right conditions.

The present Report is concerned with the prediction of transition on sheared wings of infinite span and consideration is given in turn to leading-edge contamination and the probability of re-laminarisation, cross-flow instability and the Tollmien-Schlichting type of instability. Available criteria are employed to predict transition but the calculation of the laminar boundary layer is performed using a method recently developed by Beasley[7]. This method allows the velocity profiles to be found accurately in any direction, which is believed to be of particular significance in the context of cross-flow instability, although at present the method takes no account of effects of compressibility*.

Four different aerofoil sections are considered which have pressure distributions fairly typical of flows that have a supersonic region terminating with a strong shock wave at about 20% chord. The free stream Reynolds number is varied from values which are representative of those that can be achieved in existing transonic wind tunnels, to values which may obtain in full-scale flight.

Of course, it must be appreciated that some of the effects observed in fully three-dimensional flows over finite wings are ignored in this analysis and, furthermore, that the omission of the effects of compressibility from the boundary-layer calculations can only be excused by the absence of a suitable method for calculating them at the present time. The methods used to predict transition are of uncertain accuracy, as discussed by Hall[1], so that the results themselves are subject to numerous and serious doubts. The main purpose of this Report in describing an attempt made to quantify the problem, is to demonstrate the various mechanisms in conjunction and thus to put them into perspective and to indicate where the main gaps in our knowledge are.

2 CASES CONSIDERED AND METHODS USED

2.1 Aerofoil sections and pressure distributions

Four different aerofoil sections were considered; they will be referred to as sections A, B, C and D respectively. The section shapes near the leading edge are shown in Fig.1 and the measured pressure distributions for zero sweepback on the upper surfaces over the forward part of the aerofoils, as used in the analysis described below, are shown in Fig.2. These are at a Mach number of 0.6 for sections A and B and a Mach number of 0.65 for sections C and D. The pressure distributions are similar in that they all have a supersonic region extending over the first 20% or so of the wing chord, but are different in detail within the supersonic regions. From these pressure distributions, velocity distributions were determined. The velocity distribution on the corresponding sheared wing, with the appropriate Mach number, was obtained by simply compounding the velocity normal to the leading edge with the component parallel to the leading edge. Sweep angles of 30° and 60° were considered; the corresponding free stream Mach numbers were 0.693 and 1.2 respectively for wings A and B, and 0.751 and 1.3 respectively for wings A and B, and 0.751 and 1.3 respectively for wings C and D.

2.2 Boundary-layer calculations

Making use of the velocity distributions described above, calculations were made of the three-dimensional laminar boundary layers on the corresponding sheared wings of infinite span at sweep angles of 30° and 60°. The method[7] used solves the equations of momentum and of continuity for an infinite cylinder, using finite difference substitutions and integrating across the boundary layer by a matrix method. It can be expected that the results are much the same as would have been obtained by the method

---

* Since this Report was initially drafted the computer program used has been extended to include compressible flow by Dr. Hirschel of DFVLR, but the associated problem of extending the criteria for transition to include compressibility remains.

of Jaffa and Smith[8]. The boundary-layer calculations were carried out only over the first 20% of the chord length, that is to the position of the shock wave. Upstream of this point, the adverse pressure gradients were small and the calculations indicated no likelihood of laminar separation.

The Reynolds number was varied between 3×10^6 and 72×10^6. It is defined by

$$R = \frac{U_\infty c(\sec \varphi)}{\nu}$$

where U_∞ is the free steam velocity at infinity, c the chord, ν the kinematic viscosity, and φ the angle of sweep.

2.3 Tests for instability of the laminar boundary layer

2.3.1 Leading-edge contamination and re-laminarisation

The Reynolds number based on momentum thickness at the attachment line was computed from

$$R_\theta = \frac{0.4V}{\sqrt{\nu\left(\frac{dU'}{ds}\right)_a}}$$

(as given for example, by Cumpsty and Head[9]), where V is the component of the free stream velocity along the attachment line, U' is the component of potential flow velocity in a plane normal to the leading edge, s is the distance measured around the surface in the same plane, and the suffix a refers to the value at the attachment line. The value of R_θ is clearly sensitive to the accuracy with which $\left(\frac{dU'}{ds}\right)_a$ was computed. Since, in the present exercise, this was deduced from the meagre experimental data available near the nose of the aerofoil, no great accuracy can be expected.

Experimental work by Gregory[10], Pfenninger[11], Gaster[12] and Landeryou and Trayford[13] suggests that, if the value of R_θ is below about 100, then the flow along the attachment line will have a strong tendency to remain laminar or to revert to laminar if it should have become locally turbulent for any reason. For values of R_θ significantly greater than 100, any local turbulent contamination will tend to spread along the attachment line so that, in practice, transition will occur. It was assumed here that a value of R_θ of 100 could be used as a critical value, with a range of uncertainty of from 80 to 120.

The possibility of re-laminarisation of the boundary layer following turbulent contamination at the attachment line was considered. Launder and Jones[14] have investigated the correlation between the occurrence of re-laminarisation in accelerating flows and the value of the parameter K, defined by

$$K = \frac{\nu}{U^2}\frac{dU}{dx},$$

where U is the local velocity at the edge of the boundary layer and x is the Cartesian co-ordinate in the flow direction. They have suggested that in two-dimensional flow a degeneration from turbulent to laminar flow might begin when K exceeds about 2×10^{-6}. But it is likely that much higher values, say in excess of 5×10^{-6}, are needed for the flow to revert effectively to laminar form. In the present exercise, it is assumed, admittedly without any direct experimental justification, that values of K of this order would be relevant if K were evaluated along the streamline. Again, it should be emphasised that the value of K is only as accurate as the velocity distribution and, since the maximum values of K occurred very close to the leading edge where the velocities were not accurately known, there was some element of uncertainty here. The calculations showed that the value of K falls off rapidly after reaching a maximum. In all cases, K was too low to suggest any possibility of re-laminarisation aft of about 1% chord. Hence, re-laminarisation had only to be considered when transition was due to turbulent contamination along the attachment line.

2.3.2 Cross-flow instability

Owen and Randall[5] have proposed that the onset of instability should be indicated when the cross-flow Reynolds number, given by

$$\chi = \frac{(v_N)_{max}\delta_c}{\nu},$$

exceeds a certain value. Here $(v_N)_{max}$ is the maximum value of the cross-flow velocity component and δ_c is a boundary-layer thickness not precisely defined. In the present work, δ_c was defined by

$$\delta_c = \int_0^\infty \frac{v_N}{(v_N)_{max}}\,dz,$$

where z is the Cartesian co-ordinate perpendicular to the aerofoil surface. The value of χ was computed at each step in the boundary-layer calculations and should be reliable since the velocity profiles were accurately computed. But there is considerable uncertainty about the critical value itself, bearing in mind that this is only a criterion for the onset of instability and that the actual development of a turbulent flow may be influenced by other factors. Using the present methods of calculating the boundary layer and evaluating χ, an analysis of the results of an experiment on a sheared wing by Boltz, Kenyon

and Allen[15] has suggested a critical value for χ of about 120, but there was some evidence that transition occurred also where the value of χ was as low as 100, or as high as 140. In the work reported here, the critical value of χ was therefore assumed to be 120, with a range of uncertainty of from 100 to 140.

2.3.3 Tollmien-Schlichting instability

The position, S_i, of the instability point was calculated using the empirical curve given in Ref.16. This is a plot of the critical value of a Reynolds number based on the momentum thickness, given by

$$R_2 = \frac{U_0 \delta_2}{\nu}$$

against a parameter λ_2, given by

$$\lambda_2 = \frac{\delta_2^2}{\nu} \frac{dU_0}{ds},$$

where U_0 is the local velocity at the edge of the boundary layer perpendicular to the leading edge and δ_2 is the momentum thickness. The values of R_2 and λ_2 were computed at each step in the boundary-layer calculation and the value of R_2 was compared with the critical value deduced from the curve of Ref.16 for the corresponding value of λ. Subsequently, Granville's method[17] was used to estimate the point, S_t, where transition can be expected to be completed. Granville introduced a relationship between the change in Reynolds number from instability to transition and the average value of λ_2 over that region, that is between

$$(R_2)_t - (R_2)_i$$

and

$$\bar{\lambda}_2 = -\left[\int_{S_i}^{S_t} \left(\frac{\delta_2^2}{\nu} \frac{dU_0}{ds}\right) ds\right] \Big/ (S_t - S_i),$$

where suffices t and i denote values at the transition point and the instability point respectively. He has deduced a relationship, as shown by the full line in Fig.3, between these two parameters, based on experimental results, and this was used here to predict the transition point in the first instance.

However, a further analysis, calculating the boundary layer by the present method, was made of the experimental results of Boltz, Kenyon and Allen[15]. This showed considerable scatter of the experimental points, as can be seen from Fig.3. A new curve was therefore drawn which, together with Granville's curve, encloses nearly all the experimental points. In the results below, two sets of values according to these two curves are given.

In the above approach, any influence of cross-flow was ignored and it is arguable whether it might have been more appropriate to have applied the criteria along the streamlines.

3 PRESENTATION OF THE RESULTS OF THE CALCULATIONS

The main results of the calculations made are given in Table 1. These are supplemented in Figs.4 and 5 by some specific results from the calculations of the cross-flow instability parameter. The results of the calculation of the critical parameters are presented in Figs.6 to 9 to show the variation with Reynolds number for the four pressure distributions considered. The three scales used for the ordinates in these figures have been chosen in such a way that the critical values of each parameter fall on the same line. Instability leading to transition to turbulence is likely above the line whereas laminar conditions should exist below the line. The horizontal dashed lines in the figures for swept conditions indicate the possible margin of error in the critical values based on present evidence.

Figs.6 to 9 also show for the case of zero sweep the significance of the modification to Granville's curve, mentioned in section 2.3.3, on the predicted location of the transition point. To indicate the position of the point of transition or point of instability for the examples considered the form of presentation explained in the sketch given in Fig.10 has been adopted. For sweep angles of 30° and 60° these positions are shown for the four wing sections in Figs.11 to 14.

4 SOME REMARKS ON THE EFFECTS OF SURFACE ROUGHNESS

In the analysis given in the previous section the effects of surface roughness have not directly been taken into consideration, although, of course, in many practical applications, it must be appreciated that its effect on the criteria assumed may be of great significance.

Hall[1] quotes some of the conclusions reached by Cumpsty and Head following from their study of the effects of roughness elements on the flow along the attachment line. The governing parameter for such flows is the Reynolds number $R_\theta = V\theta/\nu$, which as mentioned above is given by

$$R_\theta = \frac{0.4}{\left(\nu \frac{dU'}{ds}\right)_a^{\frac{1}{2}}}$$

For $R_\theta < 100$, the flow remains laminar irrespective of the size of the roughness element used; in their case a wire wrapped around the leading edge. A critical diameter of trip wire exists below which the flow can remain laminar up to a value of R_θ of at least 245. This critical diameter is given by

$$\left(\frac{Vd}{\nu}\right)_{crit} = 47R_\theta^{\frac{1}{2}},$$

for conical forms of excrescence. However, 65 might be a more appropriate value to assume for the empirical constant in this expression when the diameter d is replaced by the height of the element. For wire diameters exceeding this critical size, there is a transitional regime for values of R_θ in the range roughly between 100 and 150, whilst above this range the velocity profiles of the boundary layer assume a form characteristic of a fully turbulent layer.

Table 2 gives values of the critical diameters for the four wing sections under consideration. Taking, for example, sea-level conditions, a sweep of 30°, and a mean chord of 2.5 m (approximately 8 ft), then the critical diameter would be of the order of 100 μm (or 0.004 in), and at 3500 ft would be about four times this. Imperfections of this order may well be present on most operational aircraft; thus it is not unreasonable to assume that this critical roughness level is exceeded in most instances. In the case of model testing in a wind tunnel, the situation is somewhat different. For example, assuming a fifth scale model, that is a chord of 0.5 m, and a Reynolds number of 18×10^6, then the critical diameter would be about 25 μm (or 0.001 in), and imperfections of this magnitude would not normally be present.

Consideration of the conditions when transition is provoked by roughness downstream of the attachment line is more difficult. Some guidance may be provided by a crude generalisation of two-dimensional information by using a roughness Reynolds number R_k, based on height of the roughness and the resultant velocity at the top of the roughness. Experiments in two-dimensional flow appear to be insufficient to formulate reliable rules for other than zero pressure gradients, but they indicate critical values of R_k ranging from about 100 to 800, depending on the form of the roughness elements. Also, as stated in Ref. 1, quoting the experimental work of Potter and Whitfield, the effects of compressibility are great when the Mach number at the roughness height reaches high subsonic or supersonic values. Nevertheless, to give an impression of the order of roughness heights which are significant in the context of the examples considered here, curves are shown in Fig.15 based on a value of R_k of 200. The curves do not indicate any high degree of sensitivity to pressure distribution for the range covered by the examples considered.

5 DISCUSSION

Even at first glance, it is clear that the results are not very definite and cannot be readily interpreted. Consider first transition following Tollmien-Schlichting instability, which may be regarded as the main criterion for unswept wings. The chordwise station where transition is supposed to be complete varies greatly from one section to another, as does the change with Reynolds number, even though the pressure distributions would not appear to differ much. Further, the differences between the two estimates are considerable in some cases. Altogether, the uncertainties seem to be too great for engineering purposes; to narrow them down needs further work.

In all cases where the angle of sweep is high, matters appear to be more clear cut, if the present criteria are to be believed. Leading-edge contamination appears to be the dominant effect, even at relatively low Reynolds numbers, and there seems to be little likelihood of re-laminarisation in the cases considered. This would imply that the boundary layer would be turbulent right from the attachment line onwards. If leading-edge contamination is really such a powerful effect, the possibility of sweep instability need not be taken very seriously at high angles of sweep. It would be extremely useful to have adequate experimental confirmation of this fact.

Matters appear to be very complex at moderate angles of sweep. At the low Reynolds numbers of many existing wind tunnels, the boundary layer appears to be laminar over the whole of the supersonic region, except possibly in the case of section D where spanwise contamination might occur, but it might be suppressed by re-laminarisation. This is, of course, assuming that no artificial means are used to provoke transition prematurely. Conversely, at the higher Reynolds numbers considered here, the flow is likely to be turbulent right from the leading edge. So there is a Reynolds number range over which it is very difficult to forecast with certainty what type of flow to expect and which of the modes of transition would predominate. Some carefully planned tests and numerical experiments would seem to be necessary to sort out what the conditions are under which the flow will have settled down to the type expected in full-scale flight, so that subsequent changes might be smooth and monotonic, permitting confident extrapolation from tunnel to flight conditions.

The results presented also illustrate the difficulties that must be overcome if the conditions that obtain at the higher Reynolds numbers are to be simulated at lower Reynolds numbers where the boundary layer is naturally laminar over extensive regions of the surface. It is difficult to see how simple simulation devices can be expected to reproduce the desired flow in any reasonably representative manner.

The results further give an indication of a rather disturbing possibility that the flow itself can be so sensitive that it is dependent on the fine detail of the pressure distribution and profile shape. This would imply, in the first place, that these two must be known fairly completely and accurately, which places great demands on both the theoretical and experimental techniques. In the second place, other sections different from those considered here might yield different results and lead to quite different conclusions.

To sum up, it would appear that much more work is needed to determine the transition criteria more precisely, or determine new criteria if necessary. A larger number of representative cases needs to be investigated, and some consideration given to cases where laminar separation is a possibility. Lastly

and most importantly, the work should be extended beyond the rather artificial cases of sheared wings of infinite span to include a proper treatment of fully three-dimensional wings.

REFERENCES

No.		
1	M.G. Hall	Scale effects in flows over swept wings. RAE Technical Report 71043 (1971)
2	D. Küchemann	Fluid mechanics and aircraft design. J. Aero. Soc., India, 22, 141-156 (1970)
3	L.F. East R.P. Hoxey	Low speed threedimensional turbulent boundary layer. ARC R & M 3653 (1970)
4	P. Čolak-Antic	Visuelle Untersuchungen von Laengswirbeln im Staumpunktbegiet eines Kreiszylinders bei Turbulenter Anstroemung. Deutsche Luft-und Raumfahrt, DLR MITT 71-13, Mitteilung, pp.194-221 (1971)
5	J.T. Stuart	The instability of three-dimensional boundary layers. Section 6 of Chapter IX 'Hydrodynamic stability' in 'Laminar boundary layers' (edited by L. Rosenhead), 549-555, Oxford University Press (1963)
6	E C Maskell J. Weber	On the aerodynamic design of slender wings. J. Roy. Aero. Soc., 61, 37 (1957)
7	J.A. Beasley	Calculation of the laminar boundary layer and the prediction of transition on a sheared wing. RAE Report to be published.
8	N.A. Jaffe A.M.O. Smith	Calculation of laminar boundary layers by means of a differential difference method. Progress in Aerospace Sciences, 12, 49-212, Pergamon Press (1971)
9	N.A. Cumpsty M.R. Head	The calculation of the three-dimensional turbulent boundary layer. Part III. Comparison of attachment-line calculations with experiment. Aero. Quart. Vol.XX, 99-113 (1969)
10	N. Gregory	Transition and the spread of turbulence on a 60° swept-back wing. J. Roy. Aero Soc., 64, 562 (1960)
11	W. Pfenninger	About some flow problems in the leading edge region of swept laminar flow wings. Northrop Norair Report BLC-160 (1964)
12	M. Gaster	On the flow along swept leading edges. College of Aeronautics Note Aero 167 (1965)
13	R.R. Landeryou R.S. Trayford	Flight tests of a laminar flow swept wing with boundary layer control by suction. College of Aeronautics Report Aero 174 (1964)
14	B.E. Launder W.P. Jones	On the prediction of laminarisation. ARC CP 1036 (1969)
15	F.W. Boltz G.C. Kenyon C.Q. Allen	Effects of sweep angle on the boundary-layer stability characteristics of an untapered wing at low speeds. NASA TN D-338 (1960)
16	J.T. Stuart	Application of the instability theory to two-dimensional boundary layers. Section 5 of Chapter IX 'Hydrodynamic stability' in 'Laminar boundary layers' (edited by L. Rosenhead), 540-544, Oxford University Press (1963)
17	P.S. Granville	The calculation of viscous drag of bodies of revolution. Report No. 849, The David Taylor Model Basin (1953)

Table 1

CALCULATED VALUES OF THE POSITIONS OF INSTABILITY AND TRANSITION AND OF PARAMETERS OF SWEEP INDUCED INSTABILITY OR TRANSITION

	$\varphi = 30^\circ$						$\varphi = 60^\circ$					
	X_i	$X_t(i)$	$X_t(ii)$	R_θ	$K \times 10^6$ (max)	χ_{max}	X_i	$X_t(i)$	$X_t(ii)$	R_θ	$K \times 10^6$ (max)	χ_{max}
					$R = 3 \times 10^6$							
Section A	0.036	>0.2	>0.2	55	40.0	34	0.037	>0.2	>0.2	96	10.4	46
Section B	0.032	>0.2	>0.2	42	22.6	47	0.060	>0.2	>0.2	72	3.9	65
Section C	0.044	>0.2	>0.2	49	16.6	43	0.051	>0.2	>0.2	86	4.2	56
Section D	0.024	>0.2	>0.2	78	40.5	40	0.026	>0.2	>0.2	136	7.6	54
					$R = 18 \times 10^6$							
Section A	0.028	0.089	0.175	136	6.7	84	0.031	0.174	>0.2	235	1.7	113
Section B	0.029	0.093	0.135	102	3.8	116	0.032	0.138	>0.2	178	0.6	159
Section C	0.035	0.164	>0.2	121	2.8	106	0.040	>0.2	>0.2	210	0.7	138
Section D	0.023	0.068	0.122	192	6.8	98	0.024	0.121	>0.2	333	1.3	132
					$R = 36 \times 10^6$							
Section A	0.026	0.063	0.113	192	3.3	118	0.029	0.109	>0.2	332	1.9	159
Section B	0.027	0.081	0.103	144	1.9	164	0.030	0.103	0.159	251	0.3	224
Section C	0.032	0.123	0.168	171	1.4	150	0.036	0.173	>0.2	297	0.3	195
Section D	0.023	0.054	0.077	271	3.4	139	0.024	0.077	0.183	470	0.6	187
					$R = 72 \times 10^6$							
Section A	0.023	0.052	0.077	271	1.7	167	0.028	0.076	0.143	470	0.4	225
Section B	0.025	0.085	0.085	204	1.0	232	0.028	0.087	0.121	353	0.2	317
Section C	0.027	0.089	0.127	242	0.7	212	0.034	0.154	0.179	420	0.2	275
Section D	0.022	0.044	0.061	384	1.7	196	0.023	0.061	0.096	665	0.3	265

Table 2

CRITICAL ROUGHNESS HEIGHT FOR TURBULENT FLOW AT THE ATTACHMENT LINE

Section	$R_c \times 10^{-6}$	$\varphi = 30^\circ$		$\varphi = 60^\circ$	
		R_θ	$\sigma_k/c \times 10^3$	R_θ	$\sigma_k/c \times 10^3$
A	3	55	0.232 (0.321)	96	0.177 (0.245)
	18	136	0.061 (0.084)	235	0.046 (0.064)
	36	192	0.036 (0.051)	332	0.028 (0.038)
	72	271	0.022 (0.030)	470	0.016 (0.022)
B	3	42	0.203 (0.281)	72	0.153 (0.211)
	18	102	0.054 (0.075)	178	0.040 (0.056)
	36	144	0.031 (0.043)	251	0.024 (0.033)
	72	204	0.019 (0.026)	355	0.014 (0.020)
C	3	49	0.219 (0.303)	86	0.168 (0.232)
	18	121	0.057 (0.079)	210	0.044 (0.060)
	36	171	0.034 (0.033)	297	0.026 (0.036)
	72	242	0.020 (0.028)	4 0	0.015 (0.021)
D	3	78	0.277 (0.383)	136	0.211 (0.292)
	18	192	0.072 (0.100)	333	0.055 (0.076)
	36	271	0.043 (0.060)	470	0.033 (0.045)
	72	384	0.026 (0.035)	665	0.019 (0.027)

Note: σ_k refers to the critical diameter of a wire wrapped around the leading edge, but figures in parenthesis relate to conical roughness elements.

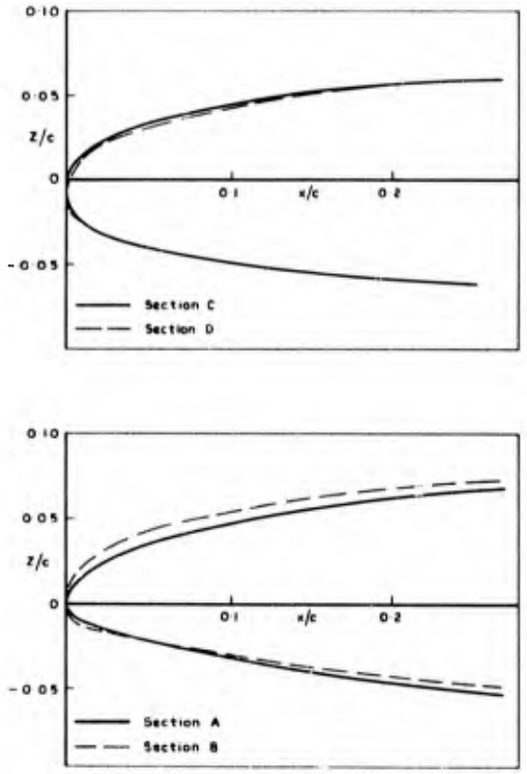

Fig. 1 Shapes of the aerofoil sections near the leading edge

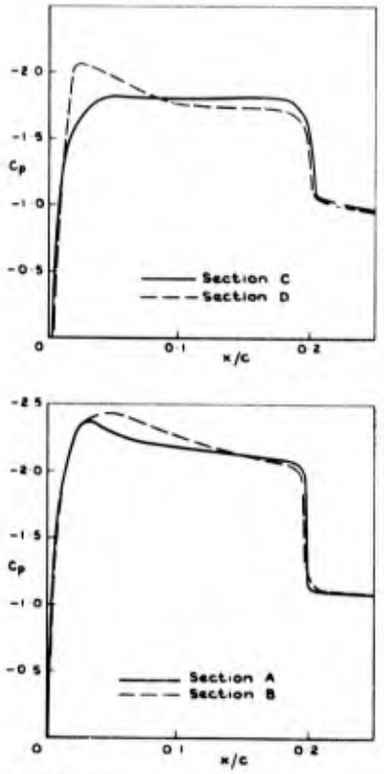

Fig. 2 Pressure distributions over the forward part of the aerofoils at zero sweepback

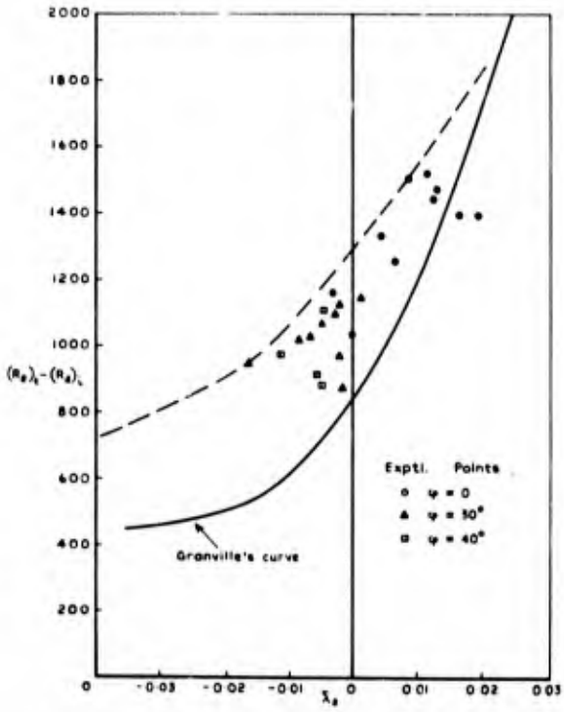

Fig. 3 Values of Granville's transition parameter deduced from experimental swept wing data compared with Granville's curve

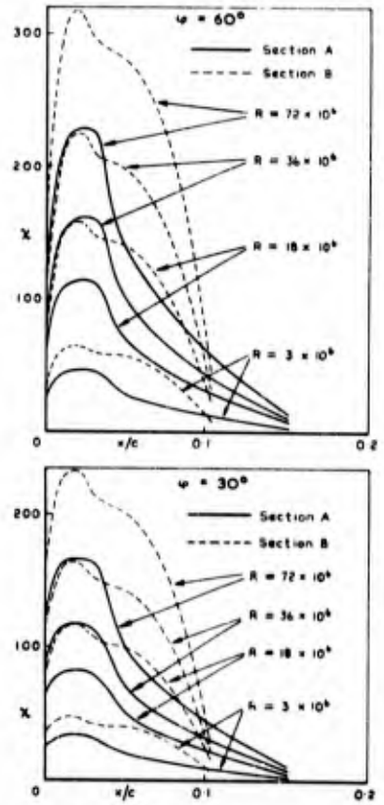

Fig. 4 Variation of cross-flow Reynolds number with chordwise position, sections A & B

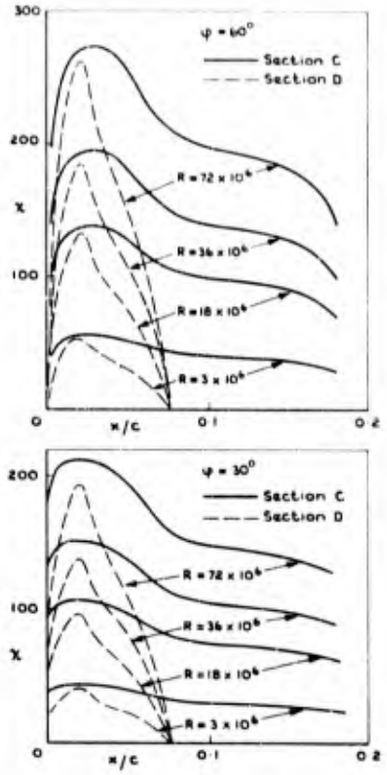

Fig. 5 Variation of cross-flow Reynolds number with chordwise position; sections C and D

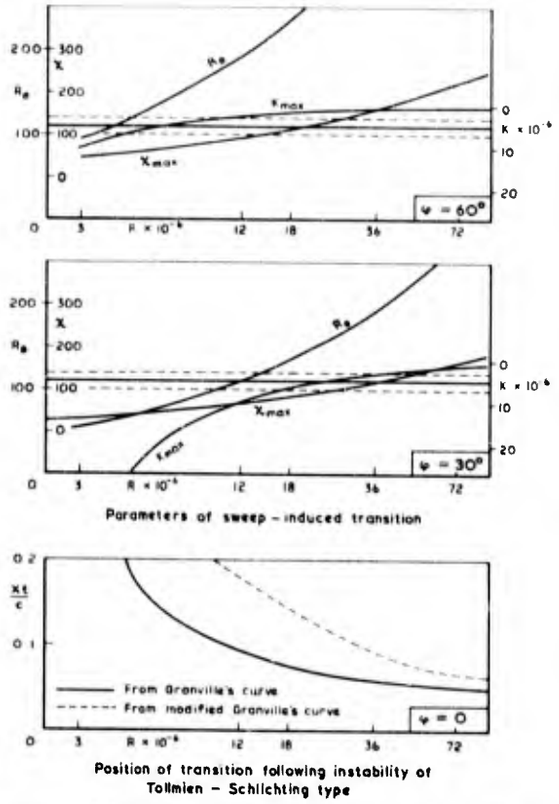

Fig.6 Parameters of sweep-induced transition and the estimated position of transition following viscous instability; section A

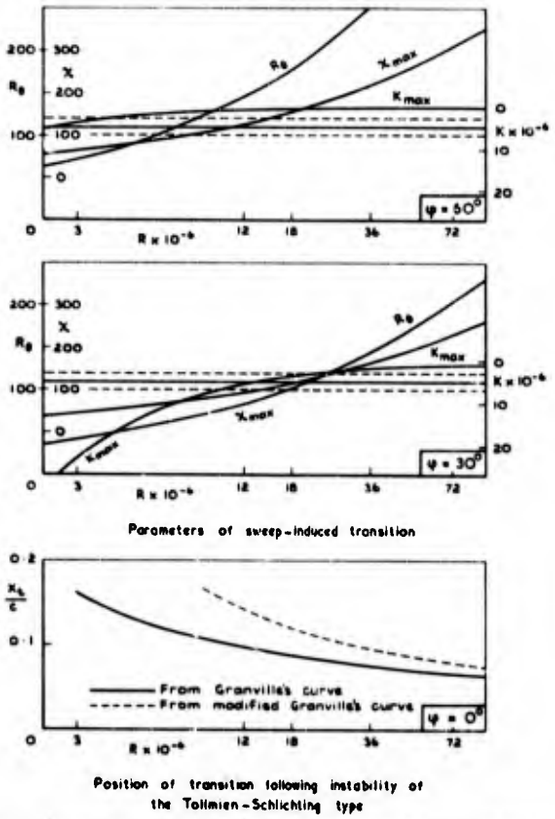

Fig.7 Parameters of sweep-induced transition and the estimated position of transition following viscous instability; section B

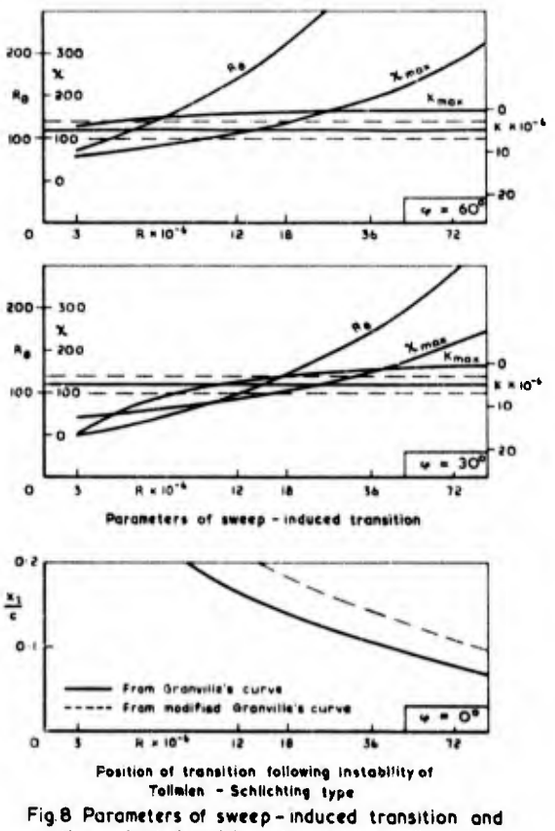

Fig.8 Parameters of sweep-induced transition and the estimated position of transition following viscous instability; section C

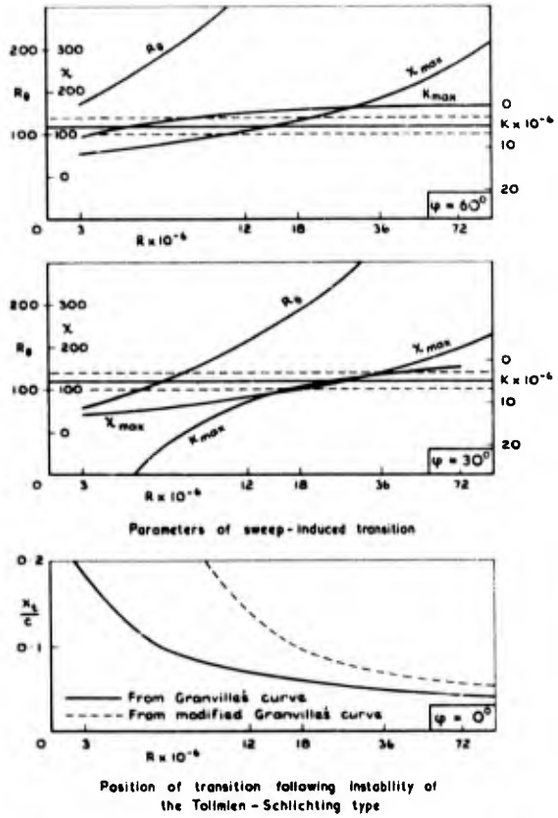

Fig.9 Parameters of sweep-induced transition and the estimated position of transition following viscous instability; section D

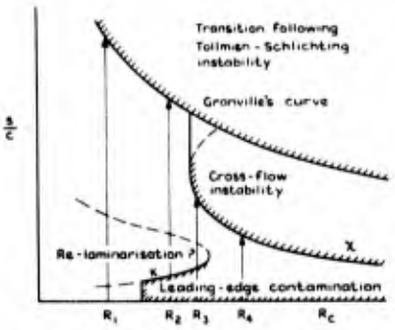

At R_1 Transition follows from Tollmien-Schlichting instability

At R_2 Leading-edge contamination, followed possibly by re-laminarisation and then transition through Tollmien-Schlichting instability

At R_3 Leading-edge contamination, followed possibly by re-laminarisation and then transition through cross-flow instability

At R_4 Transition follows from cross-flow instability if leading-edge contamination were absent

Fig.10 Schematic sketch of the movement with Reynolds number of the predicted point of transition or of instability

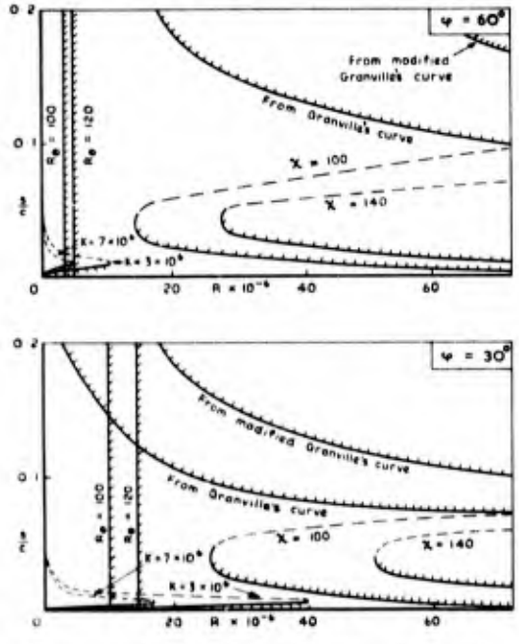

Fig.11 The movement with Reynolds number of the predicted point of transition or of instability; section A

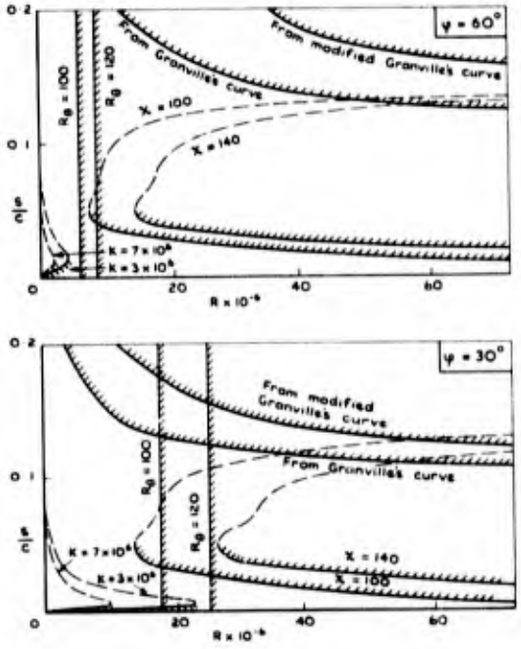

Fig.12 The movement with Reynolds number of the predicted point of transition or of instability; section B

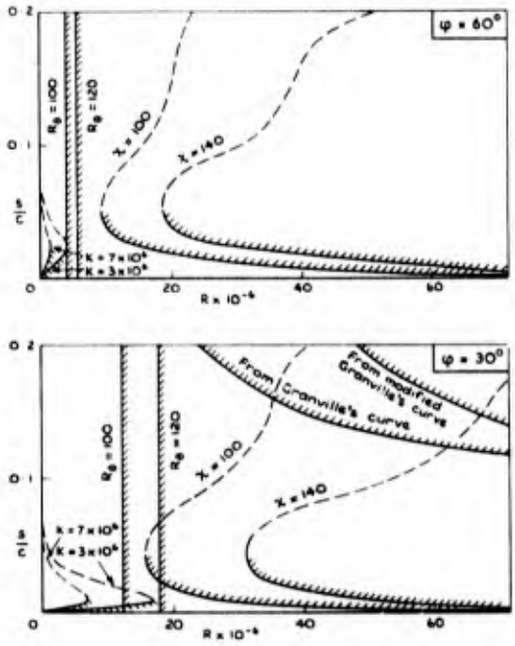

Fig. 13 The movement with Reynolds number of the predicted point of transition or of instability; section C

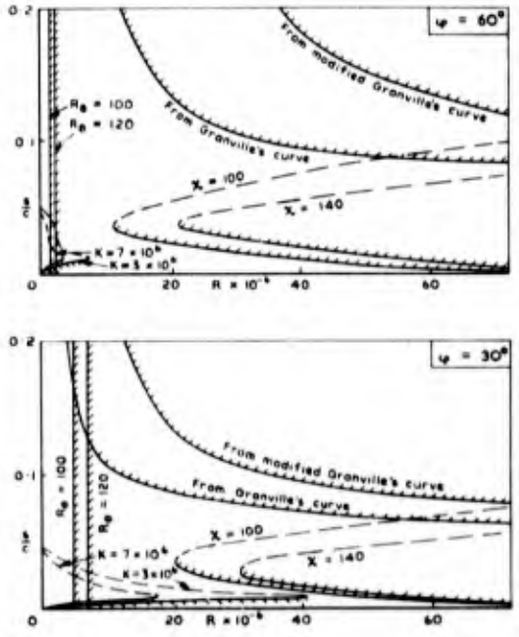

Fig. 14 The movement with Reynolds number of the predicted point of transition or of instability; section D

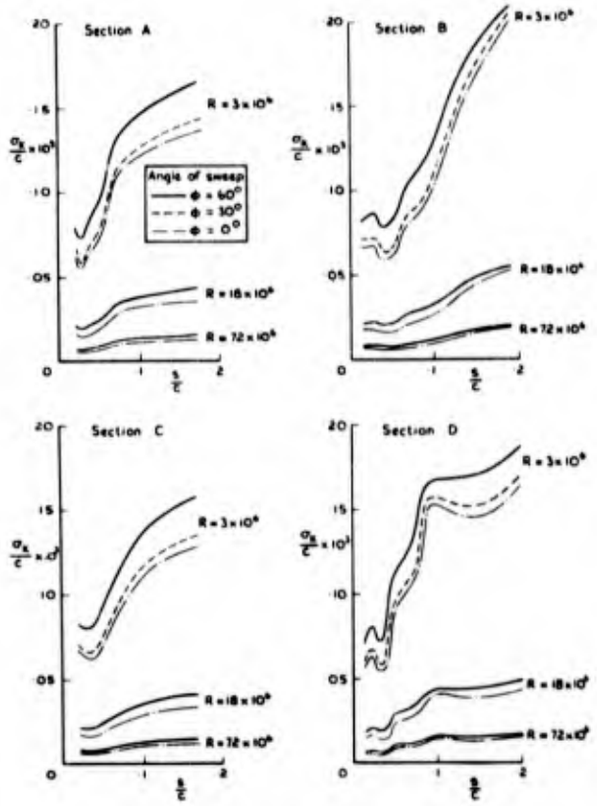

Fig. 15 Variation of critical roughness height with chordwise position and Reynolds number

THE NEED FOR HIGH-REYNOLDS-NUMBER TRANSONIC TUNNELS

by

C. R. Taylor

Royal Aircraft Establishment, Bedford, England

SUMMARY

The role of wind-tunnels in research and as aircraft-design tools requires that they should provide aerodynamicists with the capability of measuring full-scale flows in model tests and the historical development of wind-tunnels has been determined by this requirement. The present generation of transonic tunnels cannot simulate full-scale flows at critical points of the flight envelope for many current aircraft designs and there is an urgent need for new tunnels which would permit model tests to be made at much higher Reynolds numbers. The new tunnels should allow good simulations of aircraft shape to be made for a wide range of model tests; this limits the maximum tunnel total pressure to about 8 bars. A Reynolds number range which covers about half the full-scale range is advocated, demanding a working section area of about $25m^2$. The tunnels should have low levels of free-stream turbulence and be capable of operation under conditions giving little heat transfer to the model. Running times of at least 10 secs are required.

NOTATION

$\bar{c}$	wing mean chord (m)	M_D	wing-design Mach number
c_T	wing tip chord (m)	R_{FS}	full-scale Reynolds number
C_L	wing lift coefficient	R_M	model Reynolds number
F	see Fig 1	S_T	cross-section area of tunnel (m^2)
H_o	tunnel total pressure (bars)	T_r	model recovery temperature
p	tunnel static pressure (bars)	γ	ratio of specific heats for air
M	Mach number	σ	wing stress (bars)

1 INTRODUCTION

Aircraft aerodynamics is an amalgam of science and engineering, in which the improvement of aircraft performance and safety is heavily dependent on research and its applications. It is only the fundamentals of the subject which are understood in any depth, the detailed analyses of aerodynamic flows of practical interest and the prediction of aircraft performance and design data lean heavily on experiment.

Wind-tunnels are the principal sources of experimental data, both for aerodynamic research and for aerodynamic design and development of aircraft. They provide a means of producing airflows over aircraft shapes under controlled conditions and enable a wide range of aerodynamic measurements to be made. These data, which typically include forces and pressures on models and air velocities near the surface of models, are the raw material of aerodynamics. Hence, a wind-tunnel, with its measuring equipment, is as essential to an aerodynamicist as is a microscope to a biologist or a laboratory balance to a chemist.

As instruments for aerodynamic research, wind-tunnels have provided facilities for careful experimental investigations of basic flow phenomena and for checking the validity of various approximate solutions of the equations of motion of air. Basic research has frequently indicated the directions in which further work, aimed at improving the aerodynamic design and performance of aircraft, would be most effective. In this "aimed" research wind-tunnels have an even more important role, since much of this work is concerned with flows which are well beyond the scope of theoretical solutions.

An essential difference between the experimental methods used in aircraft aerodynamics and those employed in other branches of science and technology lies in the aerodynamicists use of measurements on small-scale models. This technique is fairly common in hydrodynamic and aerodynamic research and when it can be used it affords considerable economy and flexibility. Other branches of technology in which models are not used rely on very expensive and time-consuming experiments on full-scale test specimens. Aircraft engines, structures and systems are examples of these. However, tests on scale models in wind-tunnels seldom reproduce flight conditions exactly and, in general, it is necessary to "extrapolate" the tunnel measurements to full scale. The validity of this procedure is critically dependent on certain essential features of the airflow being correctly represented in the wind-tunnel and it is due to this that the size and complexity of wind-tunnels have increased with the size, speed and wing loading of aircraft. The history of this process is outlined in section 2.

During the periods when wind-tunnels have had the capability of providing an adequate simulation of flight conditions aircraft performance has improved at a very impressive pace. This has been possible because aircraft designers have been able to rely on wind-tunnels for measurements of aerodynamic design data and hence they have been able to exploit advances in aerodynamic design principles at the earliest opportunity - long before they were thoroughly understood.

However, there is now evidence that wind-tunnels cannot provide aerodynamic design data to the accuracy needed, because adequate simulations of flight conditions cannot be obtained. The problem is most severe

for transonic speeds and there is a need for a new generation of transonic tunnels which will enable full-scale conditions to be approached more closely. The case for this is argued in section 4.1. This is followed, in section 4.2, with a discussion of the broader aspects of a specification for these tunnels.

2 THE PAST

(An outline of the historical development of wind-tunnels up to 1960)

The use of wind-tunnels, for experiments on scale models, dates back over 100 years, to the work of Wenham[1], in the wind-tunnel which he and Browning built at Greenwich with the support of the Aeronautical Society of Great Britain*. Wenham experimented with wings of various shapes in order to "ascertain the fundamental relationship between velocity and pressure on surfaces of different areas and inclinations"[2] - perhaps the earliest example of basic research in aerodynamics. Many others followed Wenham's example by building wind-tunnels for aerodynamic research[1], but the distinction of being the first to use a wind-tunnel as a tool for aircraft design and development must be given to the Wright brothers. They made a systematic study of wings of various shapes and chose one of these shapes for their third glider, which they flew successfully in 1902 [3,4]. In the years following the first powered flight in 1903, the use of wind-tunnels became more widespread[5], replacing the whirling arm and model gliders as the principal experimental tool for aerodynamic research and development.

It is also established that the Wright brothers took the precaution of calibrating their wind-tunnel, by comparing measurements of the aerodynamic performance of their third glider with predictions based on the data from tests of models in the tunnel[4]. In this way they established a sound engineering approach to the use of wind-tunnel data in aircraft design, which has persisted up to the present time.

Some of the factors governing the equivalence of model and full-scale flows have been recognised for a long time. For example, the significance of the ratio of the aircraft speed (or air speed) to the speed of sound in air, was pointed out by Ernst Mach in 1887[6]. This ratio, which is a measure of the importance of the effects of the compressibility of air, is now called Mach number**.

The existence of a non-dimensional parameter which takes account of the viscosity of air was first deduced by Osborne Reynolds, from the results of his observations of the flow of water on pipes in 1883[7]. Reynolds number, as this parameter is now known, is defined as the product of a characteristic length, the air density and the airspeed divided by the viscosity of air. It is usually of the order of several millions. In the early days of aviation, when aircraft flew at comparatively low altitudes and tunnels ran at near-atmospheric pressures, the ratio of full-scale Reynolds numbers to model Reynolds numbers was very nearly the same as the ratio of aircraft size to model size (ie of the order 50 : 1). However, it is unlikely that this difference in Reynolds number was a major cause of worry to aircraft designers, since they were not required to predict the performance of their aircraft with much accuracy and scale effects on the flows over their models were comparatively small. Similarly, since flight speeds were very low, Mach number was not a significant parameter.

This state of affairs did not persist for very long. Perhaps the first significant change was brought about by the realisation that a large part of the power of the engine was being absorbed by the effects of flow separations from bluff shapes. This resulted in a gradual move to the "streamline aeroplane"[8] and hence to flows which showed a greater sensitivity to Reynolds number. It was during this period (1925 to 1935) that several wind-tunnels were built in which the air could be pressurised to give higher Reynolds numbers in model tests[9,10]. Several large atmospheric tunnels, for tests of full-scale aircraft, were also constructed[11,12]. The causes of scale effects were associated with changes in the boundary layer (this is the shallow region of air, adjacent to the aircraft surface, in which the effects of viscosity are concentrated) and research was directed to the study of the development of the boundary layers on aircraft wings and fuselages. Also the accuracy of tunnel data was improved, by the use of better measuring equipment and an understanding of the constraining effects of the tunnel walls on the flow past the model[13,14]. The development of streamlined aircraft and of more powerful engines led to increases in flight speeds, up to Mach numbers at which the effects of compressibility became significant. Research in the early high-speed tunnels showed that, at flight speeds greater than about three-quarters the speed of sound, the flows over wings and bodies could be very sensitive to small changes in Mach number and hence that precise duplication of Mach number was needed in simulating full-scale flows. By about 1939 most aircraft designers had access to tunnels in which they could test models of aircraft at high subsonic speeds[15,16,17]. In these tunnels the flow could be adjusted to give the desired Mach number, provided this was less than about 0.85 but the Reynolds numbers were still lower than full-scale, by a factor of ten or more.

It was thought that provided the model tests were made at a high enough Reynolds number (ie not less than 2×10^6 based on wing mean chord) and the boundary layer over most of the model surface was turbulent, the model data could be extrapolated to full scale, with an accuracy which was consistent with the tolerances in the aircraft requirements. Comparisons of flight measurements with tunnel data provided post-hoc validations of the extrapolation procedure and, since most new aircraft were developments of earlier types, this validation was assumed to carry over to the new design. In effect, this was a development of the engineering approach to the use of model data which was used by the Wright brothers in 1902.

By 1933 scientists had begun to think about the problems of manned supersonic flight. Small supersonic tunnels had already been used for basic research and by 1946, when the development of the jet engine had reached a stage which made the prospect of sustained supersonic flight of aircraft seem a very real possibility, large supersonic wind-tunnels had been built in most of the major research establishments[18,19,20] and a great deal was known about the techniques of measurement[21]. The foundations of gas dynamics were well established and some important types of inviscid supersonic flow had been shown to be amenable to theoretical solution[22,23]. Moreover, much of the wartime work of German scientists on high-speed flows had been disseminated and discussed. There was, however, one major obstacle. It was known that supersonic aircraft could experience potentially dangerous changes in stability when passing through the transonic speed range (ie

*The Royal Aeronautical Society since 1918

**The term Moisson number has been used in France[6].

between M = 0.85 and M = 1.20). Several means of overcoming this difficulty had been proposed but, since existing types of wind-tunnel could not be used for tests at transonic speeds, the means of studying the problem were very limited. The difficulties of making model tests at transonic speeds are due to the constraining effects of the walls of the tunnel[24]. These effects are present at low speeds but they can be allowed for by adding small corrections to the measured speed of the flow and to the incidence of the model. As the tunnel speed is increased, to values approaching the speed of sound, the constraining effect of the walls increases to such an extent that its influence on the measurements cannot be allowed for.

For the first time since 1870 research workers were deprived of the means of studying an important class of flows in the laboratory and aircraft aerodynamicists could no longer rely on wind-tunnel data to help them design new projects. The only available means of obtaining experimental data were very expensive and considerably less convenient than wind-tunnels. German aerodynamicists working on supersonic missiles during the war had used rocket powered models to develop shapes for stabilising surfaces which would minimise the stability changes occurring in the transonic speed range. Their methods of measurement were not very accurate - but the impetus provided by the absence of transonic wind-tunnels encouraged the development of improved techniques and facilities for testing models in free flight were established in many countries. The models could either be launched by rocket from the ground[25,26] or dropped from aircraft[27,28]. Various other techniques for obtaining aerodynamic data at transonic speeds were brought into use. These included flight tests of partial models, fixed to the wings of aircraft, in positions where the local airspeed became transonic or supersonic in subsonic flight[29] and, for a time, there was even a revival of the whirling arm[30], the early rival to the wind-tunnel[1]. None of these methods of testing matched the wind-tunnel in economy and versatility but the best that could be done in tunnels was to test small partial models in localised regions of transonic flow. These flows were generated by a bump fixed to one wall of the tunnel working section. The "transonic-bump" technique[31] provided a cheap means of obtaining data in existing wind-tunnels but, due to small size of the models, the Reynolds numbers were much too low for the data obtained to be used for predicting full-scale flows with any confidence. It was during this period, before the development of transonic working sections, that NACA and the American armed forces initiated contracts for the design and construction of special research aircraft which could explore the problems of transonic flight. At that time it was thought that full-scale flight tests would be the only means of obtaining comprehensive design data for aircraft which were required to be capable of sustained flight at near-sonic speeds[32,33].

The constraint problem was eventually overcome, to a large extent, by the use of partially-open walls in the working section of the tunnel. The open areas were in the form of either streamwise slots or uniformly distributed perforations[24]. Large transonic tunnels with ventilated walls started coming into service during the early 1950s. At the same time, because the main obstacle to supersonic flight had now been cleared, a new generation of large supersonic tunnels was also built. The period following this phase of re-equipment is outlined in the next section.

The history of the development of wind-tunnels demonstrates quite clearly that they have an essential role in research and in the design process of advanced aircraft. It also shows that the continued development of aviation has been dependent on the proper simulation of flight conditions in wind-tunnels. Given the capability to provide this, wind-tunnels offer the most economical and effective means available for obtaining essential aerodynamic design data for aircraft.

3 THE PRESENT

Most of the tunnels which are now used for aircraft research and development were built more than 15 years ago, in the period of equipment which followed the development of ventilated walls for testing at transonic speeds. These tunnels enable model tests to be made over a continuous range of speeds from low subsonic through transonic to high supersonic (ie $0.1 \leq M \leq 5$). The transonic tunnels, and some of the supersonic tunnels, can also be used for testing models at subsonic speeds and, in some cases, a range of Reynolds numbers can be obtained at constant Mach number. However, the highest Reynolds numbers that can be achieved in tests of models of complete aircraft is, at most, one fifth of full-scale values[34] and aircraft designers still have to extrapolate the experimental results to full-scale. The practice of checking the validity of the extrapolation method, by comparisons of tunnel data with flight measurements, has been continued. From time to time, the routine checks which are made using prototype aircraft have been supplemented by special experiments with research aircraft which have been specially designed to explore particular flight regimes[35], or utilise novel forms of airflow[36].

The 1950s and early 1960s were years of considerable challenge, optimism and achievement in aerodynamics. The theory of supersonic flow was greatly expanded and widespread advances were made in fluid mechanics, flight mechanics, propulsion aerodynamics and project analysis. There were also many significant developments in tunnel technique which enabled wind-tunnels to play a more active part in research and improved the accuracy of measurements of aircraft design data. Although certain problems were recognised, such as simulation of engine flows in model tests, the correlations of tunnel and flight data encouraged aircraft designers to increase their use of (and dependence on) experiments in wind-tunnels. The advances that have been made since 1950 are quite spectacular and fully justify the expenditure on tunnels and research. To quote only a few examples:- the maximum speeds of fighter planes have increased from high subsonic values to well over twice the speed of sound and research aircraft now fly at Mach numbers up to six; the concepts of variable sweep and vertical take-off and landing have been realised; in civil aviation subsonic turbojets have come into worldwide service and their payload fraction, at medium ranges, has been doubled, now the supersonic transport stands poised to introduce a new era in commercial aviation.

In the design of advanced aircraft the aerodynamicist now relies on wind-tunnel experiments for a wide range of data. He will probably base his initial design on aimed research and then work towards an optimisation using tunnel measurements from a range of model tests. Once an aircraft geometry has been chosen wind-tunnel experiments are needed to provide almost all the aerodynamic design data. These include the following:-

1. For calculations of the aircraft's stability and handling characteristics - measurements of variations of overall forces and moments with slow changes of attitude, measurements of rates of change of forces

and moments during oscillatory variations of attitude, at frequencies which are typical of those experienced in flight, and measurements of aircraft attitude and control settings for all conditions of flight.

2. For checking that the design is capable of meeting the operational requirements of the specification - measurements of overall forces and of unsteady forces on wings and stabilising surfaces, measurements of the performance of the air intakes, measurements of the effects of variations of intake flow on overall forces and moments, measurements of the effects of exhaust flow, measurements of the effects of external stores, measurements which enable the trajectories of stores just after release to be determined.

3. For calculations of the effects of the elastic distortion of the structure and the structural stresses - measurements of pressures and loads (both steady and unsteady) on wings and stabilising surfaces up to extreme flight conditions, measurements of heat transfer.

4. For checks on engine/airframe compatibility - measurements of steady and unsteady pressures and velocities in and near the air intake, and at the position of the engine face, for a range of intake flows, including simulated engine surging.

5. For checking the dynamic stability of the structure - measurements of unsteady forces, moments and pressures due to oscillatory control deflections, measurements of the critical flutter speeds for wings and stabilising surfaces using models having dynamically similar structural characteristics to those of the aircraft.

6. For the design of control systems - measurements of aerodynamic loads on the control surfaces, over a wide range of control settings and flight conditions, measurements of surface pressures at possible locations for control sensors.

7. For understanding the aerodynamic performance and for investigations of possible improvements in performance - observations of surface flows, measurements of surface pressures and measurements in the boundary layer.

In general, the present generation of wind-tunnels has provided aircraft designers with all the aerodynamic data they asked for. There have been problems of course, but technological innovation has often provided an acceptable solution - the representation of high-bypass-ratio fan engines is an example. There have also been instances in which aircraft have failed to meet their design targets, either because available tunnel data was ignored or because certain tunnel tests, which were within the capabilities of existing techniques, were not made. With hindsight, aircraft designers consider that they have not used wind-tunnels as much as they should have done[37].

It was not until 1966 that flight tests gave evidence that, for certain types of flow, tunnel data could be seriously in error for measurements of vital design data[38]. The problem concerned transonic flows. At much the same time, research work began to show that these flows offered a valuable potential for further advances in aircraft design. By then, various external factors had begun to influence the role of wind-tunnels. These aspects are discussed in the following section.

4 THE FUTURE

4.1 The need for new transonic tunnels

In the last ten years many countries have seen changes in their social and economic structures which have had a far reaching influence on their aerospace industries and on their methods of aircraft procurement, both civil and military. Increased industrial competition has made the economics of aircraft manufacture more vulnerable to technical errors. At the same time, successive generations of aircraft have grown larger and more complex - increasing the investment needed for design, development and production. These factors have generated a movement towards much tighter specification of the performance of aircraft projects in the operational requirements and there is now an expectation that each new generation of aircraft should embody significant aerodynamic advances and meet the specification with the minimum of flight development. Because of these trends, aircraft designers no longer have the opportunity to develop projects by gradual stages. Their accumulated experience is less relevant to advanced designs and for their aerodynamic design data they have become even more dependent on wind-tunnel experiments in which a good simulation of flows at flight conditions can be achieved.

In this context, a good simulation is one which provides a secure basis for extrapolation to full scale. Either the experiment must reproduce full-scale conditions in every respect or, more realistically, it must achieve conditions which are sufficiently close to full scale for the changes with scale to be monotonic. If this latter condition is realised, then the extrapolation can be based on the results from controlled variations of scale in experiments. The accuracy of the extrapolation should be consistent with that of the basic measurements.

The problems of extrapolation are most severe for transonic flows with shockwaves. With modern swept-winged aircraft, locally-transonic flows can occur over a wide range of flight speeds. For example, it is now known that compressibility effects can be significant at Mach numbers as low as 0.15[39] and, with wings of high sweep, transonic flows may occur at flight speeds in the supersonic range[40]. At present, it is the flows which occur at, and near, the extremes of the flight envelope which are most difficult to simulate in existing wind-tunnels and hence give the greatest risk of errors in extrapolating to flight conditions. The best known case, for which design data was seriously wrong, is the C-141 transport aircraft[41], other less serious examples which have been documented are the Caravelle and FD2[42]. Hence we have reached another stage in the history of the development of wind-tunnels where they cannot provide an adequate simulation of flight characteristics at critical points in the flight envelope and, as in similar situations in the past, there is a need for a new generation of tunnels. In this case it is necessary to reduce the gap between wind-tunnel and flight Reynolds numbers.

The gains which would result from the use of new high-Reynolds-number transonic tunnels would not be confined to improvements in the accuracy to which aerodynamic design data can be extrapolated to flight conditions, although this, by itself, would lead to substantial increases in the safety and performance of new aircraft. It is now recognised that some of the full-scale flows which cannot be simulated in existing wind-tunnels offer a rich source of aerodynamic advancement which should be exploited by research and development, involving experiments at high Reynolds numbers. The advantages of designing for high Reynolds numbers can be exploited in many ways. Compared with present day designs, wings could be made smaller or thicker, or they could have lower angles of sweep. These benefits would be applicable to a wide range of aircraft types and would lead to lighter structures with improved aircraft take-off, landing, manoeuvre and cruise performances. The research needed to improve our understanding of high-Reynolds-number flows over wings and bodies should not be underestimated and it has been predicted that the full exploitation of the facilities for research, which would be offered by the correct choice of new tunnels, would take at least 20 years.

The alternatives to an investment in new wind-tunnels are:-

1. To accept the present risk of errors in aerodynamic design data, with its attendant risk of project failure or high flight-development costs, or

2. To deliberately design for low Reynolds number flows so as to reduce the risk of serious errors in extrapolation, and to accept the consequent degradation in aircraft performance, or

3. To undertake a programme of research aimed at achieving a sufficient understanding of the fluid mechanics of full-scale flows and those in wind-tunnel experiments (including those with artificial simulation of higher Reynolds numbers) for scale effects between model and aircraft to be predicted with the accuracy needed for the design of advanced aircraft.

The first two alternatives are obviously unacceptable in the present climate of commercial competition and would seriously prejudice defence capabilities and costs. The third may appear to merit consideration. The principal objection to it is the high risk involved. The fluid mechanics of the flows which occur at limiting lift conditions are extremely complex[43] and, as has already been suggested, a full understanding of their behaviour would require a great deal of research, involving experiments at high-Reynolds-number. Without a new tunnel these would need to be made in flight. It would also be necessary to have an equal understanding of low-Reynolds-number flows with artificial simulations of higher Reynolds numbers. On balance it would appear to be more cost effective to provide a new tunnel and to aim the research effort at other topics, having greater chances of reaching successful conclusions and providing possibilities for direct improvements in aircraft performance and safety.

4.2 The right choice of tunnel

It is to be expected that any new large tunnel, which is planned now, could not be completed before 1980. This would be too late for it to be used in the design and development of the next generation of aircraft and hence the main benefits from the proposed new tunnels would come from 1985 onwards. The specification for these tunnels should be based on the anticipated needs for research and aircraft design during that period.

The advances in aerodynamic design, which have already been referred to, would find their most beneficial applications on aircraft with swept wings of moderate-to-high aspect ratio and it must be anticipated that these types of aircraft will continue to fulfil a substantial part of both civil and military requirements for this period. Also, environmental considerations will accentuate the importance of the transonic and low-supersonic speed ranges[44].

The choice of tunnel and its technical specification must depend on:-

1. The type of experiments which will be needed to support future research and aircraft design.

2. The Reynolds number range which is needed to provide an adequate basis for extrapolating to flight conditions.

3. The range of tunnel pressures which will allow representative simulation of flight shapes and permit model tests to be made up to limiting lift conditions.

Preliminary studies of the feasibility and cost of new high Reynolds number transonic tunnels have shown that continuous flow tunnels are not a practical option for Europe[45]. Several types of intermittent tunnels have been proposed[46] and the choice of the most suitable type is, to some extent, dependent on the requirements for flow steadiness and flow duration. These requirements arise from consideration of types of experiment and experimental techniques. However, the main factors which influence the overall specification are the Reynolds number and the allowable degree of pressurisation. These two aspects have been considered in some detail in a paper presented at the AGARD Specialists' Meeting on "Facilities and Techniques for Aerodynamic Testing at Transonic Speeds and High Reynolds Number" in April 1971[47]. The essential points, which have not been seriously challenged, are summarised in the next two sections. These are followed by a discussion of other factors, leading to a choice of tunnel size, pressure and running time.

Since the problems of achieving a good simulation of full-scale conditions are greatest for swept wings of medium-to-high aspect ratio at high lift conditions (when the flow is locally transonic) it is these cases which are considered in the discussions.

4.2.1 Limitations on tunnel pressure

The use of high tunnel pressures offers the cheapest way of obtaining high model Reynolds numbers. The limiting factors are the strength of the model, its aeroelastic distortion and the difficulty of holding the model in the tunnel without seriously disturbing the flow.

In Ref 47 it was shown how the ratio of the maximum stress, in a model wing, to the free-stream static pressure could be expressed as the product of an aerodynamic loading ($\gamma/2\ M^2\ C_L$) and a geometric parameter F (see Fig 1). To first order the maximum aerodynamic loading on the outer wing is independent of the angle of sweep of the wing and is primarily dependent on wing-section thickness and design, a typical maximum value for high-speed wing sections without boundary layer control is 0.35 or 0.45 for wings of low sweep with manoeuvre flaps and slats. Current developments in wing-section design could increase the wing thickness or the design Mach number (at constant wing sweep) without reducing the maximum loading. The use of boundary-layer control and/or high-lift devices for high-speed manoeuvres could increase the maximum aerodynamic loading to about 0.5 (Fig 1). For most current aircraft the value of F is about 2500 and there are good reasons for believing that this value may be typical for future STOL/VTOL transports and for future variable-sweep combat aircraft. Advanced long-range transonic transport aircraft[44] are expected to have values approaching 4000. Hence it should be anticipated that models will need to be designed to stress/pressure ratios (σ/p) of:-

1400 for advanced long-range transports

1250 for combat aircraft with manoeuvre devices

or 875 for short-range STOL/VTOL transports.

Consideration of the strength of high-tensile steels suitable for model making, unsteady aerodynamic loadings and material fatigue leads to the conclusion that the maximum design stress for models with solid wings will be about 66 h bar (43 tons/in^2). This gives maximum tunnel static pressures of:-

4.7 barsfor models of long-range transports.

5.3 barsfor models of combat aircraft

and 7.6 barsfor models of short-range transports.

For the model of a combat aircraft, the flaps, slats and supporting brackets would have to be machined integral with the wing. However, these pressures are higher than would seem desirable from other considerations. The examples of model support interference given in Ref 47 show that the stings needed for tests of models of slender-bodied long-range transports at 4.7 bars, or of wide-bodied short-range transports at 7.6 bars, would be nearly as big, in diameter, as the fuselages of the models. Clearly, this would prevent the fitting of tailplanes, fins and rear nacelles and tests of complete aircraft configurations would have to be made with smaller stings at lower pressures. Wing plus body tests would be subject to gross sting interference. For models of combat aircraft, tests at 5.0 bar static pressure could only be made without internal flow and a small amount of after-body distortion may be needed. A gross distortion of the rear fuselage would be necessary if the model was required to have representative intake flows at transonic speeds. Since the techniques of measuring support interference are restricted to comparatively low tunnel pressures[48] the model support, in high-Reynolds-number tests, should not be so big that it affects the flow over the wing or seriously changes the mean downwash at the tailplane. As a rough guide this would limit tunnel static pressures to about 70% of the values quoted above.

The other factor which should influence the choice of maximum tunnel pressure is the matching of model and aircraft shapes. The shape of an aircraft wing changes with changes of payload and fuel and with variations in flight attitude, Mach number and normal acceleration. These shape changes cannot be matched exactly in tunnel tests at high Reynolds number. However, in the case of swept-winged transport-aircraft the wind-tunnel model could be designed so that at one tunnel pressure, it assumes a shape which is reasonably representative of range of aircraft loading and flight conditions, with the same Mach number and lift coefficient. It is obviously desirable that the changes in effective model shape, with variations of Mach number and lift coefficient, should follow those of the aircraft. Otherwise, the advantages of testing the model at high Reynolds number may be lost by the inadequacy of the shape simulation, or several models of differing shapes will need to be tested. The comparisons of model and aircraft distortions given in Refs 47 and 48 show that, for this matching to be feasible, the tunnel pressures should not exceed those given above as model strength limits. The lower pressures suggested as the upper limits for tests of complete aircraft configurations with restricted support interference offer the prospect of matching model and aircraft distortions over a much wider range of conditions[48]. They would also enable many more of the measurements listed in section 3 to be made, should they require high Reynolds numbers.

The conclusion of this section is that the tunnel should be big enough to allow the target Reynolds numbers to be obtained at tunnel static pressures not exceeding:-

3.5 bars for models of transonic transports.

4.0 bars for models of combat aircraft

and 5.0 bars for models of short-range STOL transports.

The tunnel total pressure needed to allow tests to be made up to these limits is about 8 bars, corresponding to p = 5 bars at M = 0.85 or p = 3.5 bars at M = 1.15. A total pressure of 12 bars would allow partial models to be tested up to their strength limits.

4.2.2 Reynolds number requirement

In recent years full-scale Reynolds numbers have tended to increase. Successive generations of transport aircraft have grown larger and military combat aircraft also tended to increase in size as flight speeds increased. It is not yet clear whether large transport aircraft will continue to get bigger since aircraft about the size of the C5A or 747 offer very convenient stowage arrangements for military vehicles or combinations of passengers and freight. Moreover, it now requires quite substantial increases in aircraft weight to make significant increases in Reynolds number and it can be shown that increases in cruising speed alone will not lead to higher values[47]. With military combat aircraft there is a current tendency towards smaller aeroplanes. It seems likely, therefore, that the past rate of increase of the higher flight Reynolds numbers will not be maintained but the range of flight Reynolds numbers, for the complete spectrum of advanced designs,

will be larger than at present. If this turns out to be the case, we must expect that there will be a large range of fluid-mechanic situations which will need to be simulated in tunnel tests.

A guide to future full-scale Reynolds numbers, for transport aircraft in cruising flight, can be obtained using the prediction given in Ref 47, that unit Reynolds numbers for advanced long-range transonic transports will be around 6×10^6 m^{-1} and for short/medium range STOL aircraft 10^7 m^{-1}. These values give mean-chord Reynolds numbers of about 67×10^6 for a long-range transport 30% larger than a 747 and 58×10^6 for a STOL aircraft the same size as the A300B. A small fighter aircraft ($\bar{c}$ = 2.5m) would have a mean-chord Reynolds number of about 33×10^6 in high-g manoeuvres at an altitude of 3.5 km.

The range of Reynolds numbers needed to provide an adequate basis for extrapolation to full scale must be determined from consideration of the fluid mechanics of transonic flows over swept wings, since it is these flows which show the most significant scale effects. The range required is one for which the flows will be governed by the same mechanisms as full-scale flows, so that changes with Reynolds number will be monotonic. Experience, so far, shows that there are two basic types of flow, which represent the ends of the spectrum of observed flows, and pose somewhat different problems of flow simulation. A range of Reynolds numbers which is adequate for both these should also provide satisfactory conditions for intermediate cases.

The first type is found on wings at high incidence when the component of the free-stream velocity in a direction normal to the leading edge is low, compared with the velocity of sound. At these conditions, the flow round the leading edge of the wing (or slat) expands rapidly to low supersonic speeds and then almost immediately, decelerates to subsonic speeds. This rapid recompression which may, or may not, contain a shockwave, is completed within a few per cent chord of the leading edge and it is followed by a more gradual deceleration to free-stream velocity near the trailing edge. At low Reynolds numbers the boundary layer under the steep recompression will be laminar and hence it will be more susceptible to separation than the turbulent boundary layers found at very high Reynolds numbers. Different boundary layer states give very different flows irrespective of whether the recompression involves a shockwave[48] or not[49] and a first-order requirement for flow similarity is that this state should be the same in the tunnel as in flight. The Reynolds number should also be high enough to avoid complicated interactions between the separation under the recompression and that at the trailing edge[50]. A good simulation requires that the boundary layer on the model at the beginning of the recompression should have a profile shape which is similar to that in flight.

The boundary layer state and profile are very sensitive to the location of the transition front and possibly to the mechanism of transition. The several mechanisms of transition have been discussed in a recent review by Hall[51]. Calculations of the development of laminar boundary layers close to the leading edge of swept wings for some typical cases show that the mechanism and location of transition will change with Reynolds number and may change with incidence[52]. Also, if the expansion round the leading edge is very rapid, as is often the case at high incidence, transition of the boundary layer to a turbulent state may be followed by a reversion to a laminar state close to the leading edge. This phenomenon has not yet been observed on swept wings but it is known to occur in two-dimensional flow.

If flight Reynolds numbers are low enough for the transition front to vary with incidence and attitude, as may be the case for small combat aircraft, flow similarity could only be obtained by testing at full-scale Reynolds numbers, in a tunnel with low turbulence levels. First-order similarity with flows at higher Reynolds numbers could be achieved if the tunnel Reynolds number was high enough for the transition front to be very close to the leading edge even though the transition mechanism differed from that in flight. Tests over a range of Reynolds numbers should then provide a basis for extrapolating to flight conditions. The arguments presented in Ref 47 suggested that a minimum chord Reynolds number for these tests is about 15 million.

The second type of flow which needs to be considered occurs at higher Mach numbers and necessarily lower lift coefficients, when the flow over the upper surface develops a large supersonic region which is terminated by a shockwave well back on the chord. The initial flow separation can occur either at the shockwave or at the trailing edge. Observations of these types of flow in tunnel experiments show that, when separation first occurs at the shockwave, the reversed flow may be contained in a recirculating bubble of air which allows the boundary layer to reattach itself to the surface a short distance downstream of the shock. When the shock is fairly weak and unswept, this bubble does not have a marked effect on the overall flow until at higher incidences or Mach numbers there is an abrupt spread of the separation. When the shock has appreciable sweep the bubble will develop into a part-span vortex. This leads to very complicated flow developments[43]. At low Reynolds numbers it is more likely that the initial flow separation will occur at the trailing edge - this gives an immediate effect on the overall flow, which grows with increasing incidence, as the separation locus moves forward on the wing surface. For this type of flow a good simulation of flight conditions requires that the flow separation in the tunnel experiment should start in the same way as in flight and should develop in the same way. For this to happen the boundary layer thicknesses and profiles at the shockwave and at the trailing edge should be close to full scale.

The development of the turbulent boundary layer downstream of the transition front is mainly determined by the Reynolds number and the pressure distribution. Other factors which have a significant influence are:- the mechanism of transition, surface shape and roughness, heat transfer, noise and free stream turbulence. The surface roughness needed to influence the growth of the boundary layer is smaller than that which provokes transition and many aircraft are believed to have aerodynamically rough surfaces. By contrast models made to current standards of surface finish will be aerodynamically smooth, except at very high pressures[47]. Little is known about the effects of in-flight noise or of discrete-frequency noise radiated from the wall perforations of transonic tunnels[53]. The turbulence levels of most transonic tunnels are high compared with the better solid-wall tunnels or the levels which might be expected in expansion-tube tunnels[54]. It is not clear what effects these forms and levels of turbulence have but much higher levels of turbulence are known to modify the mean velocity profile in the direction of higher Reynolds numbers[55] and increase the skin friction. A similar effect is obtained from surface cooling[56]. Taken together these factors imply that it would be very difficult to achieve a precise simulation of full-scale boundary layer growth in transonic tunnels and that, by itself, the attainment of full-scale Reynolds numbers would not be sufficient.

Loving and Blackwell of NASA Langley have suggested a means by which a first-order simulation of the initial stages of full-scale flow separation can be achieved in model tests at low Reynolds number[57,58]. They postulate that the boundary layer should be turbulent at the shock (as recommended by Haines, Holder and Pearcey)[59] and that at the wing trailing edge its thickness and profile should match full-scale values. They achieve these conditions by using transition trips located further aft on the chord than the full-scale transition front. This technique, which is sometimes rather misleadingly referred to as 'underfixing', has since been used very extensively in model tests, although in many applications it is not possible to achieve the trailing-edge condition. Until better transonic tunnels are available it provides a method of obtaining a qualitative guide to the magnitude of possible scale effects. Its limitations have been widely commented on. Firstly, it can only be used to obtain the correct form of initial separation, when that occurs at the shock, and not the subsequent flow development. This is because extensive laminar regions can only be obtained at low Reynolds numbers[38,44] and then the rate of growth of the boundary layer is very different to full scale[38]. This is an important restriction since the limiting lift conditions of many modern aircraft are well beyond separation onset. Secondly, it cannot be used in cases where the shock is well forward on the wing, or where there are strong recompressions ahead of the shock[50,43]. Haines[43] has identified several more subtle but equally powerful limitations.

Other methods of synthetic simulation have been suggested which could perhaps, find applications in experiments on two-dimensional flows in existing wind-tunnels. These include the use of vortex generators[60], or glass beads[61], and the use of boundary layer control by suction[62,63] or surface cooling[38]. The principal objection to these methods (and also to the use of high tunnel turbulence) is that their successful application must depend on an understanding of the fluid mechanics of boundary layers and separation which is very much better than that now available. This would need to cover the complications introduced into the model flows, as well as full-scale flows, and would need to yield quantitative methods of determining the synthetic equivalence of the two flows. In the absence of high-Reynolds-number tunnels it would be difficult to identify the fluid mechanics of the full-scale flows, other than by post-hoc observation. This would be of limited value if, as seems inevitable, advanced aircraft are designed to exploit new types of flow.

A good simulation of full-scale flows should allow extrapolation to flight conditions to be made by controlled variation of significant parameters in tunnel experiments. A first-order simulation, such as that provided by underfixing, does not allow this. Synthetic simulations are also unsatisfactory for the reasons just given. As regards Reynolds number, there is no clearly defined lower limit, apart from that provided by consideration of transition mechanisms and, as has already been shown, these require that model test Reynolds numbers should approach full-scale values. A minimum chord Reynolds number of 15 million should be aimed for[47]. The upper end of the range can be deduced if it is assumed that the ratio of the maximum flight Reynolds number to the maximum tunnel value should be the same as the ratio of the end values of the tunnel range. Thus, extrapolation to a flight value of 60 millions would require a tunnel-tests at Reynolds numbers from 15 to 30 million.

From what has been said already about synthetic simulations, it follows that the tunnel should have low free-stream turbulence and should allow the model to be tested under conditions of zero, or low, heat transfer. The restriction of low heat transfer limits the extent to which low tunnel total temperatures can be used to increase unit Reynolds number[56]. In the following sections of this paper it will be assumed that model recovery temperature is maintained at 290°K (an average ambient temperature for NW Europe) with zero heat transfer.

4.2.3 Tunnel size and running time

The Reynolds numbers quoted at the end of 4.2.2 should be interpreted as minimum values for the model wing. Somewhat lower values can be accepted for the stabilising surfaces, in tests of complete-aircraft configurations, since these are not usually near limiting lift conditions at transonic speeds. To translate these values into equivalent tunnel size and conditions requires consideration of likely wing planforms and the permissable model size.

Model size is normally limited by the non-uniformity of tunnel interference. This depends on many factors but for models of swept-winged aircraft a convenient rule which fits current practice is

$$\bar{c} = 0.1\, M_D \sqrt{S_T}$$

where $\bar{c}$ is the mean chord of the model wing

M_D is the aerodynamic-design Mach number of the wing

and S_T is the cross-sectional area of the tunnel working section.

Using this rule, the size of tunnel needed to achieve the target Reynolds number (R_M), at the static pressure limits suggested in section 4.2.1 can be determined. The relevant data for three types of aircraft which have been considered in earlier sections are set out in Table 1. Both model and full-scale Reynolds numbers are based on wing mean chord; the model recovery temperature is 290°K and the tunnel Mach number is taken as M_D. It can be seen that a tunnel of 25 m^2 area is needed to meet these requirements. This figure would be reduced if research on ventilated walls could be relied on to show ways of obtaining more uniform tunnel interference. The recommended size of tunnel would allow models of all but the very large aircraft to be tested up to full-scale Reynolds numbers (Fig 2).

The requirements for wind-tunnel tests in support of future advanced aircraft will not be less demanding than those listed in section 3, although not all testing will require high Reynolds numbers. At the present time it is the conditions near limiting lift which are most demanding but it must be anticipated that the existence of high-Reynolds-number tunnels will encourage aircraft aerodynamicists to design for conditions which can be obtained in the tunnels and this will extend the range of conditions for which low-Reynolds-number tests may be misleading. Current trends indicate that greater accuracy of measurement and more extensive testing will be asked for. Another trend is towards more measurements of unsteady quantities. In general, these demand longer tunnel running times than steady measurements.

A problem at high lift is the determination of the manoeuvre limits of an aircraft. In the past it has often been suggested that buffet onset should limit the manoeuvre capability but now a degree of buffet penetration is accepted. This means that the limiting factor may be either the dynamic response of the aircraft structure to the buffet excitation or a form of dynamic instability[64]. The measurement of buffet excitation and damping requires that the model should have similar structural modes to those of the aircraft, at least for the lower frequencies, and, of course, high Reynolds numbers are needed. It has been estimated that wings having ratios of torsional to bending stiffnesses which are typical of aircraft structures could be made in a way which would give them 60% to 75% of the strength of solid wings[48] and hence these models could be tested at pressures up to those suggested at the end of section 4.2.1. Current experience of measurements of unsteady wing strain on models in buffet conditions suggests that quite long sampling times are needed to get consistent results, principally because the level of excitation appears to vary from one level to another every ten seconds or so. This phenomenon is not properly understood but, since these time intervals are much longer than any which can be associated with unsteady flows generated by the model, it has been inferred that the change of level is due to unsteady flows in the tunnel. If this is true, the phenomenon may not be observed in expansion-wave tunnels operating with choked diffusers. In these cases, the sampling times needed will depend on the frequency of the model and the amount of aerodynamic noise - in a quiet tunnel a 100 cycle sample should be more than adequate. For the size of tunnel recommended above this would require about 5 seconds of running time for a model with solid wings. Aeroelastic models would have higher natural frequencies and hence could have shorter sampling times.

The dynamic instabilities which may limit aircraft manoeuvres vary with different aircraft. In some cases the problem has been wing dropping, in others wing rocking and in others a lack of stability which is difficult to define. The subject is receiving intensive investigation. The sorts of measurement which might be needed for future projects include the dynamic response to change in attitude at scaled aircraft frequencies and observations of stall hysterisis. Again high Reynolds numbers, a clean airflow and running times equivalent to several cycles of oscillation would be needed. With forced oscillations the number of cycles needed could be as low as 10 but, due to the low frequencies sample times could be as long as 10 seconds[65].

In intake testing unsteady measurements of engine-face pitot pressures are used to obtain samples of instantaneous flow distortions due to separations in the intake and ducting. Measurements of static pressures are also made to determine the unsteady loadings when the intake is in a buzz condition, or when an engine surge is being simulated. These measurements do not need more than 1 or 2 seconds recording time but in intermittent tunnels it may be necessary to repeat the same condition several times to ensure that the samples taken are representative.

In the long term, flutter experiments may also require high Reynolds numbers. The most critical flutter conditions usually occur in the transonic speed range but at low lift coefficients where, in the past, flows have not been very sensitive to scale effects. The low Reynolds number of most flutter experiments has not therefore given much cause for concern. However, developments in the structural design of wings are making the flutter aspects more critical and there is a need for greater accuracy. Also, the aerodynamic developments which can be foreseen will make the flows more susceptible to scale effects and we must expect that, in these flows, oscillatory variations of incidence and control angles will generate aerodynamic responses which cannot be described simply in terms of 'in-phase' and 'in-quadrature' components of a linear response. This means that the existing methods of calculating critical flutter speeds, using measurements of aerodynamic response will become unreliable and recourse will have to be made to more extensive use of aeroelastic models with true dynamic scaling. The need for greater accuracy will require that these models be tested in high-Reynolds-number tunnels. Very low turbulence levels will be necessary, to avoid spurious structural response. There will need to be significant development in model-making technique if the kinetic pressure range for testing dynamic models is to be increased to allow high Reynolds numbers to be obtained in pressurised tunnels but the use of aeroelastic flutter models will obviously be limited to lower pressures than those available for tests of models with solid steel wings. Again some development of technique will be needed if tests are to be made in intermittent tunnels and there will be some limit on the running time of the tunnel. Current ideas are that 10 secs may be adequate in "clean" tunnels[65].

It appears that a running time of 10 seconds would be adequate for a wide range of unsteady measurements, provided that the turbulence level of the tunnel flow is low. Fluid-dynamic research would also require low tunnel turbulence; a running time of 10 seconds would allow traverses to be made of boundary-layers and regions of separation.

In expansion-wave tunnels the principal source of aerodynamic noise will be the ventilated walls of the working section. Research into means of reducing the pressure fluctuations at the wall perforations (particularly at the lower frequencies) should be encouraged if the full benefits of high Reynolds number tunnels are to be sought.

5 CONCLUSIONS

Over the past 100 years wind-tunnel experiments, in association with methods of extrapolating measurements to flight conditions, have become an economical and effective means of obtaining aerodynamic data for aircraft design; today they play an essential part in the design and development process of any major new aircraft. During this period, as wind-tunnels have developed, both in their capability to simulate a wider range of flight conditions and in their contribution to each new aircraft project, there has been a continued need to increase the accuracy with which aerodynamic characteristics in flight can be predicted from tunnel tests.

We have now reached a stage at which, because of the gap between wind-tunnel and flight Reynolds numbers, aerodynamic characteristics at full scale can no longer be predicted with the required accuracy and, to meet the needs of the future, a new generation of wind-tunnels, providing substantially higher Reynolds numbers than available today, must be built.

In the transonic speed range (ie $0.5 < M < 1.4$), the new tunnels should provide Reynolds numbers, for

tests of complete models of aircraft, which cover the range from 20 to 45 millions, based on mean chord. These Reynolds numbers should be achieved at total pressures which allow realistic simulation of the aeroelastic distortion of aircraft and which permit models to be tested up to limiting lift conditions, ie 8 to 12 atmospheres. The tunnels should be suitable for the full (and ever widening) range of experiments needed for a new aircraft project and should have running times of at least 10 seconds, to allow measurements of those unsteady phenomena for which sampling over a fairly large number of cycles is required.

To take full advantage of these new tunnels, further improvements in wind-tunnel technique will have to be made. At the same time, we shall need to develop further and draw fully upon, our understanding of the basic fluid mechanics of transonic viscous flows, so that the process of extrapolation from wind-tunnel to flight has a solid and rational foundation.

The gains from a new generation of high Reynolds number tunnels would be increased performance and safety in new aircraft, achieved at lower flight-development cost and with less risk of a project failing for technical reasons. The exploitation of research into high-Reynolds-number transonic flows could sustain developments in aircraft design for a period of about 20 years.

REFERENCES

1. Pritchard, J.L., "The Dawn of Aerodynamics," Jour Royal Aero Soc, Vol 61, 1957.

2. Pritchard, J.L., "F.H. Wenham 1824-1908," Jour Royal Aero Soc, Vol 62, 1958.

3. Pritchard, J.L., "The Wright Brothers," Jour Royal Aero Soc, Vol 57, 1963.

4. McFarland, M.W.(Ed), "The Papers of Wilbur and Orville Wright," McGraw-Hill, New York, 1953.

5. Naylor, J.L., and E. Ower, "Aviation: Its Technical Development," Peter Owen/Orsion Press, London, 1965.

6. Black, J., "Ernst Mach - Pioneer of Supersonics," Jour Royal Aero Soc, Vol 54, 1950.

7. Reynolds, O., "An Experimental Investigation of the Circumstances which Determine Whether the Motion of Water shall be Direct or Sinuous, and of the Law of Resistance in Parallel Channels," Phil Trans 174, 1883.

8. Jones, M.B., "The Streamline Aeroplane," Jour Royal Aero Soc, Vol 33, 1929.

9. Jacobs, E.N., and I.H. Abbott, "The NACA Variable Density Wind Tunnel," NACA Report No 416, 1932.

10. "Variable Density Wind Tunnel - Report of Scale Effect Panel," ARC R&M 1149, 1927.

11. De France, S.J., "The NACA Full-Scale Wind Tunnel," NACA Tech Report 459, 1933.

12. Pope, A., and J.J. Harper, "Low-Speed Tunnel Testing," Wiley, New York, 1966.

13. Glauert, H., "Wind Tunnel Interference on Wings, Bodies and Airscrews," R&M 1566, 1933.

14. Toussaint, A., "Experimental Methods - Wind Tunnels," Part 1, Aerodynamics Theory Vol III, Div I Springer, Berlin, 1934.

15. Goethert, B., "The DVL High-Speed Wind Tunnel," Lilienthal-Ges Luftfahrtforsch No LGL 127, 1940.

16. Millikan, C.B., "High-Speed Testing in the Southern Californian Cooperative Wind Tunnel," Aero Conf London, 1947.

17. Thompson, J.S., and W.A. Mair, "The RAE High-Speed Tunnel and a Review of the Work Accomplished in 1942-1945," R&M 2,222, 1946.

18. Ackeret, J., "Windkannale für hohe Geschwindikeiten," Atti Accad d'Italia (5th Volta Congress), Rome, 1935.

19. Ferri, A., "The Guidonia High Speed Tunnel," Aircraft Engineering, Vol 12, 1940.

20. Smelt, R., "A Critical Review of German Research on High-Speed Airflow," Jour Royal Aero Soc, Vol 50, 1946.

21. Pankhurst, R.C., and D.W. Holder, "Wind-Tunnel Technique," Pitman & Sons, London, 1952.

22. Sauer, R., "Theoretischer Einführung in die Gasdynamik," Springer Berlin, 1943.

23. Liepmann, H.W., and A.E. Puckett, "Aerodynamics of a Compressible Fluid," John Wiley & Sons, New York, 1947.

24. Geothert, B.H., "Transonic Wind Tunnel Testing," Agardograph 49, Pergamon Press, 1961.

25. Shortal, J.A., "Techniques of Model Testing in Free Flight," Agard AG 15, (5th meeting of wind-tunnel and model testing panel), 1954.

26. Hamilton, J.A., and P.A. Hufton, "Free-Flight Techniques for High-Speed Aerodynamic Research," Jour Royal Aero Soc, Vol 60, 1956.

27. Goethert, B., "Drop Tests to Determine the Drag of Model SC-50 at High Velocities," DVL Tech Report ZWB 11 252, 1944.

28. Kurbjun, M.C., and J.R. Thompson, "Free-Flight Measurements of the Effects of Wing-Body Interference on the Transonic Drag Characteristics of Sweep-Wing-Slender-Body Configurations," NACA RM L53C51, 1953.

29. Johnson, H.J., "Measurements of Aerodynamic Characteristics of a 35° Swept-Back NACA-65-0009 Airfoil Model with a $\frac{1}{4}$ Chord Plane Flap by the NACA Wing-Flow Method," NACA-RM-L47F13, 1947.

30. Habel, L.W., J.H. Henderson and M.F. Miller, "The Langley Annular Transonic Tunnel," NACA Report 1106, 1952.

31. Weaver, J.H., "A Method of Wind Tunnel Testing Through the Transonic Range," Jour Aero Sci, Vol 15, 1948.

32. Heinemann, E.H., "Developments in High-Speed Aircraft," Mechanical Engineering, Vol 69, 1947.

33. Klein, D.B., "Research Aircraft," Mechanical Engineering, Vol 69, 1947.

34. Cahill, J.F., et al, "Feasibility of Testing a Large-Chord Swept-Panel Model to Determine Wing Shock Location at Flight Reynolds Number," AGARD CP-83-71, Paper 17, 1971.

35. Mellinger, G.R., "Design and Operation of the X-15 Hypersonic Research Airplane," AGARD Report 288, 1960.

36. Bisgood, P.I., "Stability and Control Tests on a Slender-Wing Research Aircraft," AGARD CP-85, 1972.

37. Mitchell, J.G., "The Test Facilities Role in the Effective Development of Aerospace Systems," AFSC-TR-71-01, 1971.

38. Cahill, J.F., "Simulation of Full-Scale-Flight Aerodynamics Characteristics by Tests in Existing Transonic Wind Tunnels," AGARD CP-83-71, Paper 20, 1971.

39. Isaacs, D., "Wind Tunnel Measurements of the Low Speed Stalling Characteristics of a Model of the Hawker Siddeley Trident 1C," ARC R&M 3608, 1969.

40. Lock, R.C., and J. Bridgewater, "Theory of Aerodynamic Design for Swept-Winged Aircraft at Transonic and Supersonic Speeds," Prog in Aero Sci, Vol 8, 1966.

41. "The High Reynolds Number Tunnel - A National Need," AEDC 72-84, 1972.

42. Poisson-Quinton, Ph., "Validite de la Soufflerie pour la Prevision des Performances et des Qualities de vol," AGARD CP-83-71,Paper 18, 1971.

43. Haines, A.B., "Possibilities for Scale Effects on Swept Wings at High Subsonic Speeds," AGARD CP-83-71, Paper 14, 1971.

44. Goodmanson, L.T., "Transonic Transports," Twelth Anglo-American Aeronautical Conference, Paper No 72/8, July 1971.

45. Baals, D.D., and G.M. Stokes, "A Facility Concept for High Reynolds Number Testing at Transonic Speeds," AGARD CP-83-71, Paper 28, 1971.

46. Pankhurst, R.C., "Technical Evaluation Report on Agard Specialists' Meeting on Facilities and Techniques for Aerodynamic Testing at Transonic Speeds and High Reynolds Number," AGARD Advisory Rept No 37, 1971.

47. Evans, J.Y.G., and C.R. Taylor, "Some Factors Relevant to the Simulation Full-Scale Flows in Model Tests and to the Specification of New High-Reynolds-Number Transonic Tunnels," AGARD CP-83-71, Paper 31, RAE Technical Report 71029, 1971.

48. Taylor, C.R., "The Design of Wind Tunnel Models for Tests at Transonic Speeds and High Reynolds Numbers, VKI Lecture Series 42, RAE Tech Memo 1443, 1972.

49. McCullough, G.B., and D.E. Gault, "Examples of Three Representative Types of Airfoil Stall at Low Speed," NACA TN 2502, 1951.

50. Osborne, J., and W.H. Pearcey, "A Type of Stall with Leading-Edge Transonic Flow and Rear Separation," AGARD CP-83-71 Paper 4, 1971.

51. Hall, M.G., "Scale Effects on Flow Over Swept Wings," AGARD CP-83-71 Paper 1, 1971.

52. Treadgold, D.A., and J.A. Beasley, "Some Examples of the Application of Methods for the Prediction of Boundary Layer Transition on Sheared Wings," RAE Technical Report 72135, AGARD Report R-602-72, 1972.

53. Freestone, M.M., and R.N. Cox, "Sound Fields Generated by Transonic Flows over Surfaces having Circular Perforations," AGARD CP-83-71 Paper 24, 1971.

54. Evans, J.Y.G., and P.G. Pugh, "The Development of a System for Generating Quiet Transonic Flow Suitable for Model Testing at High Reynolds Numbers, AGARD Report R-601-72, 1972.

55. Green, J.E., "On the Influence of Free-Stream Turbulence on a Turbulent Boundary Layer as it Relates to Wind-Tunnel Testing at Subsonic Speeds," RAE Technical Report 72201, AGARD Report R-602-72, 1972.

56. Green, J.E., D.J. Weeks and P.G. Pugh, "Some Observations upon the Influence of Charge-Tube Mach Number upon the Utility of Flows Generated by Expansion Waves," RAE unpublished, 1972.

57. Loving, D.L., "Windtunnel-Flight Correlation of Shock-Induced Separated Flow," NASA TN D-3580, 1966.

58. Blackwell, J.A., "Effect of Reynolds Number and Boundary-Layer Transition Location on Shock-Induced Separation," AGARD CP 35, 1968.

59. Haines, A.B., D.W. Holder and H.H. Pearcey, "Scale Effects at High Subsonic and Transonic Speeds and Methods for Fixing Boundary-Layer Transition in Model Experiments," ARC R&M 3271, 1960.

60. Pearcey, H.H., "Shock-Induced Separation and its Prevention by Design and Boundary Layer Control," in "Boundary Layer and Flow Control," (Ed G.V. Lachmann), Pergamon Press, 1961.

61. Vaucheret, X., "La Recherche Aerospatiale," No 6, 1971.

62. Bore, C.L., "On the Possibility of Deducing High Reynolds Number Characteristics using Boundary Layer Suction," AGARD CP-83-71 Paper 23, 1971.

63. Green, J.E., "Some Aspects of Viscous-Inviscid Interactions at Transonic Speeds and their Dependence on Reynolds Number," AGARD CP-83-71 Paper 2, 1971.

64. Jones, J.G., "The Dynamic Analysis of Buffeting and Related Phenomena," Paper at Agard Specialists' Meeting on Fluid Dynamics of Aircraft Stalling, Lisbon, 1972.

65. Coupry, G., R. Destuynder, H. Försching and J.W.G. von Nunen, "Measurement of Unsteady Phenomena in Wind Tunnels," AGARD Report R-601-72.

ACKNOWLEDGEMENT

This paper is British Crown Copyright reproduced by permission of the Controller of Her Brittanic Majesty's Stationery Office.

TABLE

Type of Aircraft	Long-Range Transonic	Swept-Winged Combat	Short/Medium-Range STOL
M_D	0.95	0.8	0.8
$\bar{c}$ (m)	11.2	2.5	5.8
$R_{FS} \times 10^{-6}$	67	33	58
$\bar{c}/c_T$	1.75	1.5	2.0
$R_M \times 10^{-6}$	42	27	42
p (bars)	3.5	4.0	5.0
A (m^2)	23.1	16.5	24.7

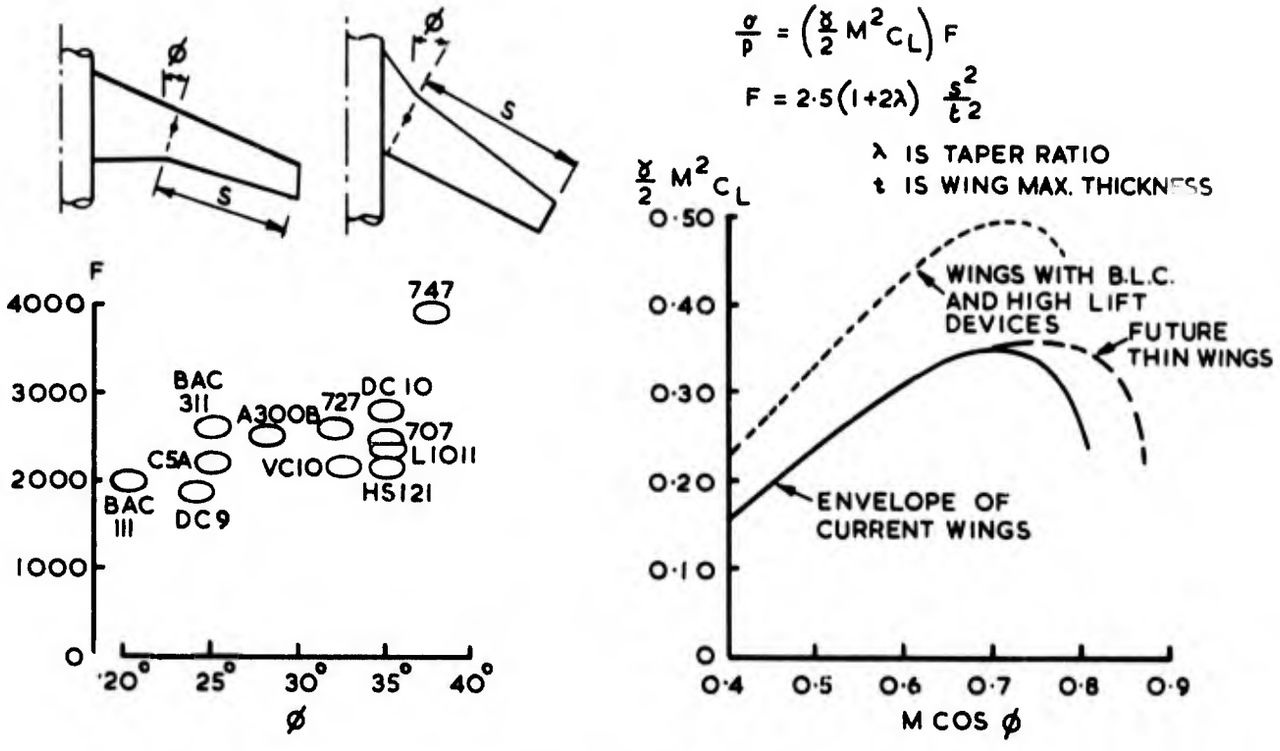

FIG. 1 FACTORS AFFECTING MAXIMUM MODEL STRESS

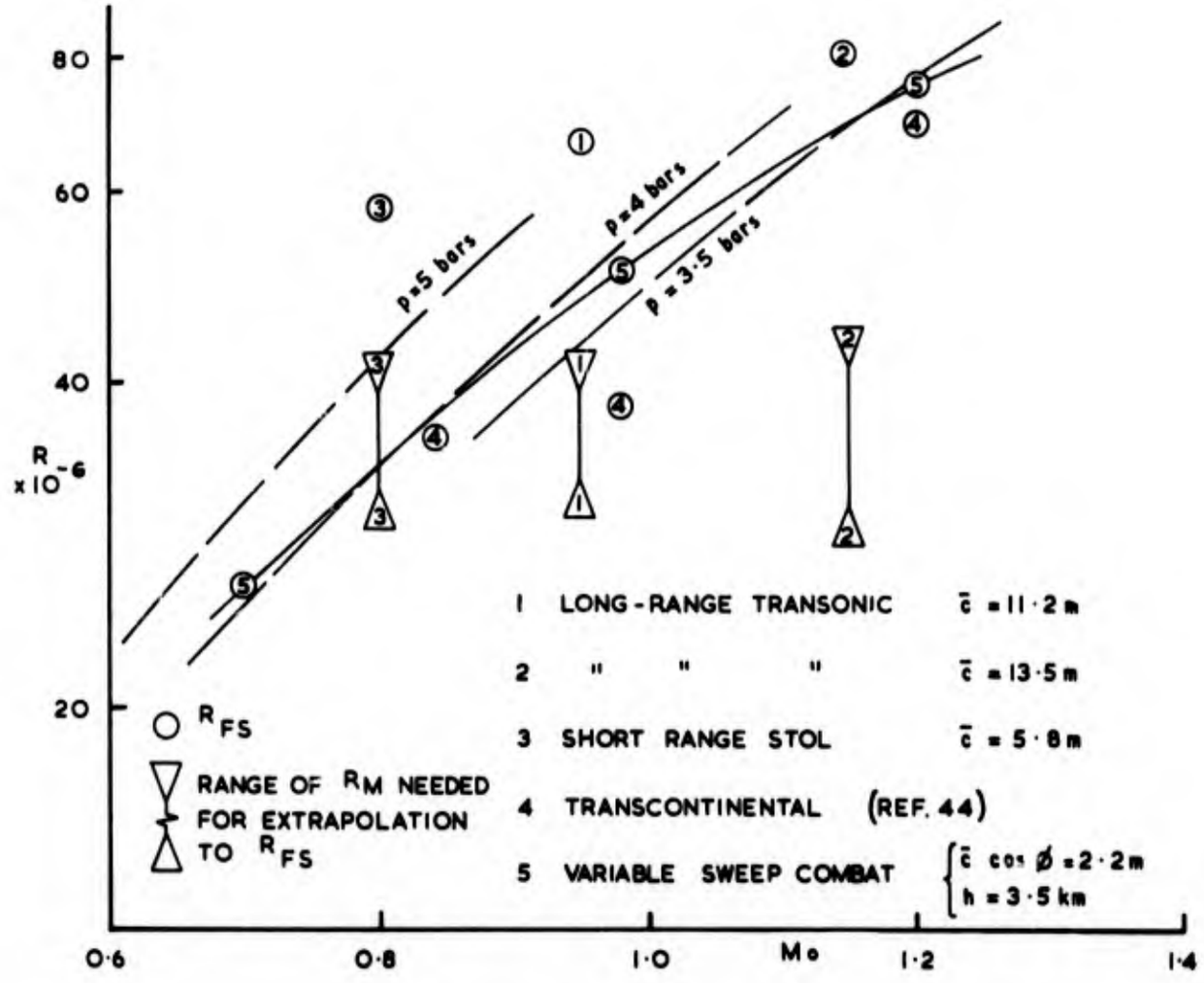

FIG. 2 TUNNEL CAPABILITY

ON THE INFLUENCE OF FREE STREAM TURBULENCE ON A TURBULENT BOUNDARY LAYER, AS IT RELATES TO WIND TUNNEL TESTING AT SUBSONIC SPEEDS

by

J. E. Green

Royal Aircraft Establishment, Bedford, England

SUMMARY

Published experimental measurements show the turbulent boundary layer to be highly sensitive to turbulence in the free stream. In zero pressure gradient, a small increase in the streamwise rms velocity fluctuation $\tilde{u}/u_e$ is found to have the same effect on the shape of the velocity profile as a fractional increase in Reynolds number $\Delta R/R$ roughly sixty times as great. This effect needs to be taken into account in planning new wind tunnels for subsonic and transonic testing at high Reynolds number. Meanwhile, further experimental work is needed to clarify:- the importance of turbulence scale; the influence of pressure gradients; the influence of radiated pressure (as opposed to convected vorticity) fluctuations.

NOTATION

A, B	constants in skin-friction law (equation (6))
c	aerofoil chord
C_f	local skin-friction coefficient
G	Clauser's shape parameter (equation (3))
H	conventional shape parameter = δ^*/θ
K	function of G in skin-friction law (equation (6))
ℓ	mixing length
R_θ	Reynolds number based on momentum thickness
x, y	coordinates along and normal to surface
u	streamwise velocity
u_τ	friction velocity $\left(=\sqrt{\tau_w/\rho_w}\right)$
$\tilde{u}$	rms fluctuating component of streamwise velocity
α	empirical constant (equation (2))
δ	boundary-layer thickness
δ^*	displacement thickness
θ	momentum thickness
ρ	density
τ	shear stress

Subscripts

e	denotes conditions at edge of boundary layer
0	denotes conditions with quiescent external flow
∞	denotes conditions far upstream
w	denotes conditions at the surface

1 INTRODUCTION

We are becoming more sharply conscious of the role of Reynolds number in aircraft aerodynamics, and the advantages which might be gained by fully exploiting our understanding of it. Swept wings for high subsonic speeds are being designed to operate at specific target Reynolds numbers, and boundary-layer prediction methods are being used to confirm that, at the design condition, the boundary layer is expected to be as close to separation as is judged prudent. These wings, wind tunnel tested at their design Reynolds numbers, will shed light on the accuracies of the design methods. Meanwhile, the same design methods are indicating quite clearly that there are substantial gains in aerodynamic performance to be had by designing wings up to full scale rather than wind tunnel Reynolds numbers. Such high performance wings cannot, however, be checked out in existing wind tunnels because, at the lower Reynolds numbers of the tunnel, premature boundary-layer separation will occur.

The shortfall in Reynolds numbers between current wind tunnels and full scale is inhibiting the exploitation of advanced wing design and, conversely, the pursuit of advanced design is undermining the value of testing in existing wind tunnels. In recent years, notably in the report of the HIRT Group[1], the papers presented at the AGARD Specialists Meeting on Transonic Testing at Göttingen in April 1971[2], and the subsequent discussions of the LaWs Group[3], the limitations imposed by the Reynolds numbers of our present wind tunnels have been brought into focus, and the case for building a new generation of wind tunnels providing substantially higher Reynolds numbers than currently available has been forcefully developed.

The villain of the piece is the turbulent boundary layer. It is primarily through the influence of Reynolds number on its development, interaction with shock waves, and separation that important differences between wind tunnel and full-scale flows arise. Hence, in framing our policies on building new tunnels, we must make full use of our existing understanding, such as it is, of the turbulent boundary layer. In particular, given the subtle but significant differences between the environments provided by the wind tunnel and by the atmosphere, and the fact that no model is a true replica of the aeroplane, we should avoid the

dangerous oversimplification of assuming that to build a wind tunnel which gives full-scale Reynolds numbers will ensure exact simulation of boundary-layer behaviour.

This paper is concerned with the influence of one aspect of the wind tunnel environment, free stream turbulence, on the properties of a turbulent boundary layer. Underlying the discussion are the questions (1) whether the turbulence in today's wind tunnels is having a significant influence on the 'effective' Reynolds number of the flow, and (2) whether there is any future in artificially increasing the turbulence level in a tunnel to increase the 'effective' Reynolds number. The available experimental results, though they do not go far enough to answer these two questions, do show the effect of turbulence on the boundary layer to be, in one respect, remarkably strong. In what follows, some of these experimental results are discussed and some general but rather speculative deductions made. Finally, in the context of wind tunnel testing, we note some aspects of the problem which merit further experimental investigation.

2 EXPERIMENTAL RESULTS ON FLAT PLATES AT LOW SPEEDS

Recently, Charnay, Compte-Bellot and Mathieu[4] and Huffman, Zimmerman and Bennett[5] have reported investigations of the influence of free stream turbulence on the turbulent boundary layer on a flat plate.

The two experiments were closely similar in layout: a relatively long flat plate was mounted across the full span of a small, low-speed wind tunnel; turbulence was generated by a grid a short distance upstream of the plate (in one case[4] the grid was a square lattice, in the other[5] only vertical rods were used); detailed hot-wire measurements were made in the boundary layer at a number of streamwise stations.

The results of the two experiments are also similar. An increase in free stream turbulence level leads to an increase in skin-friction coefficient, a fuller velocity profile (the shape parameter H is reduced), and a thicker boundary layer. Each set of authors discusses in detail the observed influence of free stream turbulence on the turbulence structure of the boundary layer. In the present context, however, it is sufficient for us to note the influence of free stream turbulence on the mean velocity profiles.

Charnay et al[4] find that the usual flat-plate velocity-defect law

$$\frac{u_e - u}{u_\tau} = f\left(\frac{y}{\delta}\right) \qquad (1)$$

does not correlate their measured profiles. However, if the profiles are rescaled in the form

$$\frac{u_e - u}{u_\tau - \alpha\tilde{u}} = f\left(\frac{y}{\delta}\right) \quad , \qquad (2)$$

where $\tilde{u}$ is the rms fluctuating component of streamwise velocity and α is an empirical constant, they may all be collapsed onto a single curve.

In terms of the shape parameter

$$G = \frac{H - 1}{H}\sqrt{\frac{2}{C_f}} \quad , \qquad (3)$$

equations (1) and (2) imply that the results of Charnay et al would satisfy the relation*

$$G = G_0\left(1 - \alpha\frac{\tilde{u}}{u_\tau}\right)$$

$$= G_0\left(1 - \alpha\sqrt{\frac{2}{C_f}}\frac{\tilde{u}}{u_e}\right) \qquad (4)$$

where G_0 is the value of G in the boundary layer of a quiescent flow with zero pressure gradient, generally accepted to be constant at 6.5 approximately.

Huffman et al[5] do not examine the applicability of the velocity-defect law as such, but they do tabulate H and C_f, from which G can be determined. In Fig 1, their values of G are plotted against $\tilde{u}/u_\tau$, and compared with the correlation of Charnay et al. An approximate scale for turbulence intensity $\tilde{u}/u_e$, appropriate to the Reynolds numbers of these two experiments, is also shown.

Agreement between the two experiments is remarkably close. In round terms, if we take G_0 as 6.4, we find that

$$G = G_0\left(1 - \frac{1}{3}\sqrt{\frac{2}{C_f}}\frac{\tilde{u}}{u_e}\right) \qquad (5)$$

is a reasonable fit to both sets of results for turbulence levels up to 5%, though it seems unlikely that the variation will remain linear at higher levels.

In correspondence with the author, Mr. P. Bradshaw has argued that the influence of free stream turbulence on gross boundary-layer properties should go as $1 + O(\tilde{u})^2$ rather than as $1 + O(\tilde{u})$, at least for small $\tilde{u}$ ($< 0.01u_e$). In condensed form, his argument is that uncorrelated disturbances add as mean squares rather

*This inference is based on standard bookwork, but depends on the Reynolds number being sufficiently high for the contribution of the viscous sublayer to the momentum and displacement thickness integrals to be negligible.

than as rms values and that, at sufficiently small $\tilde{u}$, the free stream fluctuations and the large boundary-layer eddies (which erupt from the inner layer where the turbulence energy >> $\tilde{u}^2$) are bound to be uncorrelated. He suggests, therefore, that any curve through the experimental data should be parabolic at the origin.

Although the linear fit to the data in Fig 1 looks convincing, Bradshaw's argument is appealing, and certainly has an important bearing on how much significance we attribute to turbulence levels of less than one per cent. A parabolic fit at low $\tilde{u}$ is sketched dotted in Fig 1, and we see from this that the shape of any such parabola will be determined by the value of G in a quiescent free stream.

A value of 6.1, as given by the parabolic curve in Fig 1, is lower than is generally expected in zero pressure gradient. However, we should remember that the more usual value of approximately 6.5 applies at high Reynolds numbers, when the velocity-defect law describes virtually the entire velocity profile and contributions from the viscous sublayer to displacement and momentum thickness integrals are negligible. In the experiments of Huffman et al[5], Reynolds number was not so high for us to be able to discount the contribution of the viscous sublayer, and the authors did in fact take it into account in analysing their data. Hence, to clarify behaviour at low $\tilde{u}$ and to assess the argument put forward by Bradshaw, we must attempt from the data available to estimate what value G would have taken in these experiments if zero $\tilde{u}$ had been achieved.

The integral boundary-layer properties presented by Huffman et al were obtained by numerically fitting the experimental velocity profiles with Coles's well known 'wall-plus-wake' family using a two-parameter optimisation routine. In the process, the strength of Coles's 'wake' component $\Delta u/u_\tau$ was evaluated and is tabulated by the authors. In Fig 2 we plot their values of $\Delta u/u_\tau$ against G. The value of G in quiescent flow is then taken to be the value at $\Delta u/u_\tau$ of 2.75, which is the asymptotic value proposed by Coles[6] for constant pressure flow at high Reynolds number. There are two reasons for placing reliance on this estimate: first, pressure gradient in the experiments was set to zero by means of a flexible tunnel wall, so a perturbation in G and $\Delta u/u_\tau$ due to pressure gradient can be discounted; second, the Reynolds numbers in the experiments were sufficiently high ($R_\theta \sim 4000$ to 5000) for $\Delta u/u_\tau$ to approach closely its asymptotic value at high Reynolds number[6].

From Fig 2, we infer that Huffman et al would have measured a value of 6.4 for G if they had performed their experiment with $\tilde{u}$ zero*. Hence, from Fig 1, it would seem that any parabolic variation of G is apparent only at very low values of $\tilde{u}/u_e$ (< 0.001, say). For our present purposes, the linear approximation to these results, equation (5), will therefore be adopted. At the low turbulence levels of high quality wind tunnels, the behaviour may well prove to be as suggested by Bradshaw, but a rather refined experimental technique will be needed to demonstrate this behaviour.

Given equation (5), the susceptibility to free stream turbulence of boundary-layer parameters other than G, in flows at constant pressure, may be derived analytically** from the skin-friction relation of Nash and MacDonald[7]. From their equation (1)

$$\sqrt{\frac{2}{C_f}} = A \ln R_\theta + B + K(G) \quad , \tag{6}$$

taking G as 6.4 on a flat plate in quiescent air, the sensitivities are found to be: at constant momentum thickness Reynolds number R_θ,

$$\frac{G}{C_f}\frac{dC_f}{dG} = -14.3\sqrt{\frac{C_f}{2}} \tag{7}$$

and

$$\frac{G}{H}\frac{dH}{dG} = \{7.17 - 0.77H\}\sqrt{\frac{C_f}{2}} \quad , \tag{8}$$

while, for H to remain constant,

$$\frac{G}{R_\theta}\frac{dR_\theta}{dG} = \frac{1}{A}\left[\frac{2}{C_f} - 7.17\sqrt{\frac{2}{C_f}}\right]\sqrt{\frac{C_f}{2}} \, . \tag{9}$$

If we assume that equation (5) can be applied to flows over a wide range of Reynolds numbers, equations (7) to (9) may be combined with equation (5), differentiated, to give: at constant R_θ,

$$\frac{\Delta C_f}{C_f} = 4.8\frac{\tilde{u}}{u_e} \tag{10}$$

and

$$\frac{\Delta H}{H} = -\{2.4 - 0.25H\}\frac{\tilde{u}}{u_e} \tag{11}$$

while, for H constant, taking A to be 2.47 as proposed in Ref 7,

---

*That the variation of G with $\Delta u/u_\tau$ is closely linear over the range of Fig 2 can readily be confirmed from Coles's[6] profile family.

**The derivation requires the assumption that the empirical constants in the law of the wall are insensitive to free stream turbulence. From our present knowledge of turbulent flows, and in the absence of evidence to the contrary, this seems justified.

$$\frac{\Delta R_\theta}{R_\theta} = -\left(\frac{0.27}{C_f} - 0.97\sqrt{\frac{2}{C_f}}\right)\frac{\tilde{u}}{u_e} \quad . \qquad (12)$$

Thus, a free stream turbulence level of 0.2% will result in a value of C_f roughly 1% greater than in quiescent air, and value of H roughly 0.005 lower. This value of H corresponds, in fact, to that in a quiescent flow with a value of R_θ 12% greater according to equation (12) (with values of C_f typical of Refs 4 and 5).

One point which emerges from equations (10)-(12) (and which depends therefore on the validity of equation (5)) is that, in zero pressure gradient, a change in free stream turbulence of a given magnitude will have the same proportional effect on skin friction at all Reynolds numbers, while on H its effect will increase marginally with increasing Reynolds number due to the fall in H. On the other hand, the fractional increment in R_θ given by (12) will increase appreciably as C_f falls with increasing Reynolds number.

For the sake of argument, let us take H to characterise the boundary layer; ie,in zero pressure gradient, let us define the 'effective' Reynolds number of the boundary layer in a turbulent stream as the Reynolds number at which the same value of H would obtain with a quiescent external flow. Then, from equation (12), we see that not only is the effective Reynolds number highly sensitive to turbulence - the fractional increment in R_θ is 60 times that in $\tilde{u}/u_e$ for the data of Refs 4 and 5, so that profiles at R_θ = 5000 and 1% $\tilde{u}/u_e$ have the same H as those at R_θ = 8000 in a quiescent stream - but also that this sensitivity increases with increasing Reynolds number.

3 CALCULATIONS FOR FLOWS WITH PRESSURE GRADIENT

To throw some light on the effect that free stream turbulence might have in flows with pressure gradient, some calculations have been made using a boundary-layer method speculatively modified to account for this effect. The lag-entrainment method of Ref 8 is formulated to include explicitly the mean mixing length ℓ in the outer part of the boundary layer. Although the ratio of this length to boundary-layer thickness δ is commonly assumed to be constant in boundary layers near equilibrium, the method is programmed in such a way that this ratio can easily be varied. Since variations in ℓ/δ, so long as they are not large, provide a good first-order means of representing changes in the turbulence structure due to extraneous influences, the method is well suited to a parametric investigation of the effects of any such changes.

Boundary-layer development has been calculated in flows with zero pressure gradient and also for an upper surface pressure distribution of the family of high lift aerofoils put forward by Weeks[9]. The calculations were made over a range of Reynolds number with the method in standard form and, at the lowest Reynolds number of the range, with the mixing length (ie ℓ/δ) increased to 10/9 and 10/8 times its normal value (for which it was expected that G in zero pressure gradient would be reduced by 10 and 20 per cent respectively).

The results for the calculations in zero pressure gradient are indicated in Fig 1 by the horizontal bars*. The computed reductions in G were 9.5% and 19%, corresponding to free stream turbulence levels of just over 1% and 2% in the experiments of Refs 4 and 5.

Fig 3 shows calculated boundary-layer development in the aerofoil pressure distribution (a) with mixing length ℓ/δ constant, at chord Reynolds numbers of 7×10^6, 12×10^6 and 21×10^6 and (b) with mixing length varied at a constant chord Reynolds number of 7×10^6. In Figs 3b and 3c we see that both momentum and displacement thicknesses decrease appreciably with increasing Reynolds number, their values at the trailing edge falling by 20 and 25 per cent respectively when Reynolds number is increased by a factor of three. By comparison, the effect of varying mixing length is relatively small: a 25% increase in ℓ/δ (ie a change from $\ell = \ell_0$ to $\ell_0/\ell = 0.8$) produces only a 2½% increase in momentum thickness and a 4½% reduction in displacement thickness at the trailing edge.

In contrast to these results, Fig 3d shows the shape parameter H to be quite sensitive to mixing length. In the region of sustained adverse pressure gradient over the rear of the aerofoil, the effect on H of increasing ℓ/δ by 25% is virtually the same as that of a threefold increase in Reynolds number.

4 DISCUSSION

Consider the results of these calculations in the context of wind tunnel tests on swept wings at high Reynolds number (either with a turbulent boundary layer along the wing attachment line or with transition fixed very close to the leading edge so that extraneous influences on transition are not important). At a given Reynolds number, variations in the wind tunnel environment which affect the turbulence structure in the boundary layer on the model seem likely to have only a small influence on drag (momentum thickness) and on reduction in slope of the lift curve due to viscous effects (displacement thickness).

On the other hand, the sensitivity to ℓ/δ of the shape parameter H over the rear of the aerofoil indicates that the tunnel environment might have an appreciable influence on the value of lift coefficient at which separation first appears. The calculations suggest that an increase in free stream turbulence level of 1% could have an effect on the conditions for separation onset very similar to the effect of increasing Reynolds number by 60 to 70 per cent (this result is very similar to that for zero pressure gradient given by equation (12)). On modern wings under conditions of high lift - ie when viscous effects are at their severest and experiment is the only reliable way to determine aerodynamic characteristics - the value of H over the upper rear of the wing has been argued[10,11] to be the single most important boundary-layer parameter. The calculations thus point up an effect which may well be not only surprisingly large but also of considerable practical importance.

---

*For simplicity, ℓ/δ is written as ℓ in all the figures; suffix zero denotes a quiescent free stream.

5 SOME UNCERTAINTIES

Let us, as in section 2, loosely define the 'equivalent' Reynolds number of a flow as the Reynolds number required to give approximately the same distribution of H in a quiescent stream with the same pressure distribution. Two questions of interest are then: whether the 'equivalent' Reynolds numbers in today's wind tunnels differ significantly from their nominal values; and whether the 'equivalent' Reynolds number of a tunnel could be artificially increased, by turbulence grids for example, without this gain being offset by deleterious side effects. No answer to these questions is offered here, but they serve as a useful background against which to list some further complications.

5.1 The effect of turbulence scale

In the experiments of Refs 4 and 5, on which all the deductions of this paper are based, the turbulence was generated with grids of similar spacing to the thickness of the boundary layer under investigation. As a result, the integral length scale of the turbulence (measured in Ref 4, crudely estimated for Ref 5 from other measurements[12] of the decay of grid turbulence) was of order $\frac{1}{2}$ to 1 times the boundary-layer thickness.

Neither experiment showed any clear influence of turbulence scale on the response of the boundary layer. Nevertheless, it seems unlikely that the correlation shown in Fig 1 will be applicable to flows in which the scale of the free stream turbulence and the scale of the energy-containing eddies in the boundary layer (ie δ) are different by an order of magnitude. For example, if the turbulence scale of the free stream in the experiments of 4 and 5 were increased by an order of magnitude, with the rms velocity fluctuation $\tilde{u}/u_e$ held constant, the turbulence energy at the boundary layer scale would be reduced by a factor of 50; we might expect the boundary layer in this situation to respond to the predominant fluctuations as large scale unsteadiness rather than as a source of turbulent energy.

Further experimental evidence is needed to clarify this point. Measurements similar to those of Refs 4 and 5 but over a much wider range of the ratio of free stream turbulence scale to boundary-layer thickness would be valuable. A fairly large wind tunnel would probably be required to enable this range to be covered.

Finally, if these speculations are correct, we should observe that the notion of an 'equivalent' Reynolds number cannot be applied to a wind tunnel in isolation, without reference to the scale of the boundary layer of interest. The thicknesses of boundary layers on a tunnel sidewall and on the wing of a model aircraft mounted in the tunnel will usually differ by an order of magnitude, and their responses to turbulence in the tunnel stream might well be quite different.

5.2 The effect on the turbulence of flow accelerations

Whereas the experiments of 4 and 5 are for a flow at constant pressure with nearly isotropic turbulence, the flow around the wing of a wind-tunnel model experiences large accelerations and decelerations. The result will be a local distortion of the turbulence[12], with different velocity components amplified and attenuated by an acceleration and the process reversed in the subsequent deceleration.

Broadly speaking, the rms fluctuation $\tilde{u}/u_e$ should be reduced in the high velocity regions over the forward upper surface of a wing, but should return to roughly its undisturbed value as the pressure returns towards the free stream value at the trailing edge. However, the greater the perturbation from free stream conditions, the more anisotropic will the turbulence become. It is possible that the interaction between this distorted turbulence and the mean shear of the boundary layer will differ appreciably from that observed in 4 and 5, but the question can be resolved only by further experiment.

5.3 Boundary layers in pressure gradients

It is not obvious that a given level of free stream turbulence will have as great an influence on a boundary layer in a strong adverse pressure gradient as it has on the flat plate boundary layer. The exercise of section 3 of using a calculation method to explore the effect of varying mixing length in flows with pressure gradient is thought to be valid, but it provides only a partial answer so long as the dependence of mixing length on the turbulence level is unknown.

On the assumption that the dominant parameter is the ratio of rms fluctuation in the free stream to rms fluctuation at some point in the outer part of the boundary layer, we can conjecturally extend the correlation of section 2 to include boundary layers in pressure gradient. For flows in zero pressure gradient, the velocity-defect law implies that the ratio of mixing length to boundary layer thickness varies inversely as G. Hence we may write equation (5)

$$\left(\frac{\ell}{\delta}\right)_0 = \frac{\ell}{\delta}\left(1 - \frac{1}{3}\sqrt{\frac{2}{C_f}}\,\frac{\tilde{u}}{u_e}\right) \quad , \tag{13}$$

which we assume can be applied in flows with zero pressure gradient. Combining the assumption of Bradshaw et al[13], that turbulent kinetic energy is proportional to shear stress in boundary-layer flows, with the mixing-length assumption (at y/δ = const, $\sqrt{\tau/\rho} \propto \partial u/\partial y, \propto u_e/\delta \times H/(H-1)$ if velocity-defect profiles have similar shapes such that $1 - u/u_e = \delta^*/\delta\ f(y/\delta)$), we may then* replace $\sqrt{2/C_f}$ in equation (13) by the term $G_0 H/(H-1)$ to give

$$\left(\frac{\ell}{\delta}\right)_0 = \frac{\ell}{\delta}\left(1 - \frac{2.1H}{H-1}\,\frac{\tilde{u}}{u_e}\right) \quad . \tag{14}$$

The right-hand term in the brackets is now, to first order, proportional to the ratio of rms fluctuations in the free stream to those at some characteristic point in the outer part of a boundary layer in a

*The derivation is straightforward but again requires contributions from the sublayer to be neglected.

quiescent stream. Applied to the calculations shown in Figs 3b-3d, equation (14) suggests that $\tilde{u}/u_e$ would need to be of order 3½% to produce the 25% increase in ℓ/δ which had the same effect on H as a threefold increase in Reynolds number. Of course, equation (14) is at best an informed guess, and no real substitute for the experimental results that are needed here.

5.4 Acoustic disturbances

In the working sections of most transonic wind tunnels, the flow disturbances are predominantly acoustic[14] - ie pressure fluctuations radiated from the slotted or perforated tunnel walls rather than vorticity fluctuations convected from the settling chamber. These two types of disturbance clearly cannot interact with a turbulent boundary layer in the same way, but both could be significant in many modern transonic wind tunnels unless the influence of pressure fluctuations is an order of magnitude weaker than that of vorticity fluctuations. This is another topic which needs experimental investigation, though simulation of the acoustic source provided by transonic tunnel walls may present difficulties. It is arguably the topic most urgently in need of preliminary study, to establish at an early date the order of magnitude of the influence of acoustic disturbances.

5.5 Compressibility effects

The experiments discussed in section 2 and the calculations of section 3 are for incompressible flow. The available evidence suggests[15] however that the basic structure of turbulence is not significantly influenced by compressibility effects, even at fairly high supersonic speeds. Hence, in relating the conclusions of sections 2 and 3 to flow at subsonic and transonic speeds, no first-order correction for the effect of compressibility is thought necessary.

5.6 Atmospheric turbulence

Since the object of wind tunnel testing is to simulate flight through the atmosphere, the question arises as to whether we should expect the level of turbulence encountered in the atmosphere to have any significant effect on boundary-layer structure. Recalling the comments in section 5.1 on the effect of turbulence scale, it seems probable that the kind of influence discussed here will be wholly insignificant. For a large subsonic transport aircraft at cruise the rms velocity fluctuation over an octave bandwidth centred on a wavelength of 0.3 m (the order of δ over the rear upper surface of the wing) will be only 0.03% of free stream velocity in 'heavy' turbulence[16]. Moreover, any such fluctuations will invariably be accompanied by fluctuations much larger in both amplitude and wavelength so that, if our speculation of section 5.1 is correct, the prime influence on the boundary layer will be large scale unsteadiness of the flow. From our present viewpoint, therefore, the atmosphere is thought always to be quiescent.

6 CONCLUSIONS

In zero pressure gradient, published measurements show that a small increase in free stream turbulence $\tilde{u}/u_e$ has the same effect on the shape of the boundary-layer velocity profile as a fractional increase in Reynolds number $\Delta R/R$ roughly 60 times as great.

Calculations for lifting wings suggest that the same effect occurs in flows in pressure gradients, with an increase in turbulence level delaying separation onset. By comparison, the effects of turbulence on wing drag and viscous loss of lift are calculated to be small.

These tentative deductions are relevant to the design of new, high Reynolds number wind tunnels. It is clear that we must have a better understanding of the influence of tunnel turbulence before we can say with any precision what the 'effective' Reynolds number in any particular wind tunnel is. It is equally clear that the target turbulence level in any projected new tunnel, particularly one intended to measure the influence of Reynolds number, should be low: for uncertainty in 'effective' Reynolds number to be less than 5%, free stream turbulence may need to be less than 0.1% (although, noting Bradshaw's argument cited in section 2, the precise influence of very low levels of turbulence remains in doubt). It is not so clear that enhancing the 'effective' Reynolds number of a tunnel by artificially increasing its turbulence level will prove a valid experimental technique, although for economic reasons it is worth investigation. Even so, to use such a technique in a controlled manner, it would again be necessary to achieve a very low datum turbulence level in the 'undoctored' tunnel.

Some of the most important gaps in our knowledge, from the practical viewpoint, are discussed in section 5. Given the large capital cost of any major new wind tunnel, research into any of these problems would be a worthwhile investment.

REFERENCES

1. "AGARD Study of High Reynolds Number Wind Tunnel Requirements for the North Atlantic Treaty Organisation," by the AGARD Fluid Dynamics Panel HIRT Group, Paper 32 in AGARD CP-83-71.

2. "Facilities and Techniques for Aerodynamic Testing at Transonic Speeds and High Reynolds Number," AGARD Specialists' Meeting, Göttingen, April 1971, AGARD-CP-83-71.

3. Large Windtunnels Working Group of the AGARD Fluid Dynamics Panel, (see AGARD Report 588, 1971).

4. Charnay, G., G. Compte-Bellot and J. Mathieu, "Development of a Turbulent Boundary Layer on a Flat Plate in an External Turbulent Flow," Paper 27 in AGARD CP 93, 1971.

5. Huffman, G.D., D.R. Zimmerman and W.A. Bennett, "The Effect of Free Stream Turbulence on Turbulent Boundary Layer Behaviour," presented at AGARD Specialists' Meeting,"Boundary Layer Effects in Turbomachines,"Paris, April 1972.

6. Coles, D.E., "The Turbulent Boundary Layer in a Compressible Fluid," USAF Project Rand Rept. R-403-PR, 1962.

7. Nash, J.F., and A.G.J. Macdonald, "A Turbulent Skin Friction Law for use at Subsonic and Transonic Speeds," ARC CP No 948, 1966.

8. Green, J.E., D.J. Weeks and J.W.F. Brooman, "Prediction of Turbulent Boundary Layers and Wakes in Compressible Flow by a Lag-Entrainment Method," RAE Technical Report 72231, 1972.

9. Weeks, D.J., "Some Applications of Boundary Layer Theory in the Design of Aerofoil Sections for High Lift," RAE unpublished paper.

10. Blackwell, J.A., Jnr, "Preliminary Study of the Effects of Reynolds Number and Boundary Layer Transition Location on Shock-induced Separation," NASA TN D-5003, 1969.

11. Green, J.E., "Some Aspects of Viscous-inviscid Interaction at Transonic Speeds, and their Dependence on Reynolds Number," Paper No 2 in AGARD CP-83-71.

12. Bearman, P.W., "Some Measurements of the Distortion of Turbulence Approaching a Twodimensional Body," Paper 28 in AGARD CP 93, 1971.

13. Bradshaw, P., D.H. Ferriss and N.P. Attwell, "Calculation of Boundary Layer Development using the Turbulent Energy Equation," J. Fluid Mech, 28, 593-616, 1967.

14. Mabey, D.G., "Flow Unsteadiness and Model Vibration in Wind Tunnels at Subsonic and Transonic Speeds," ARC CP 1155, 1971.

15. Bradshaw, P., and D.H. Ferriss, "Calculation of Boundary Layer Development using the Turbulent Energy Equation: Compressible Flow on Adiabatic Walls," J. Fluid Mech, 46, 83-110, 1971.

16. Jones, J.G., Private Communication, RAE, 1972.

ACKNOWLEDGEMENT

This paper is British Crown Copyright reproduced by permission of the Controller of Her Brittanic Majesty's Stationery Office.

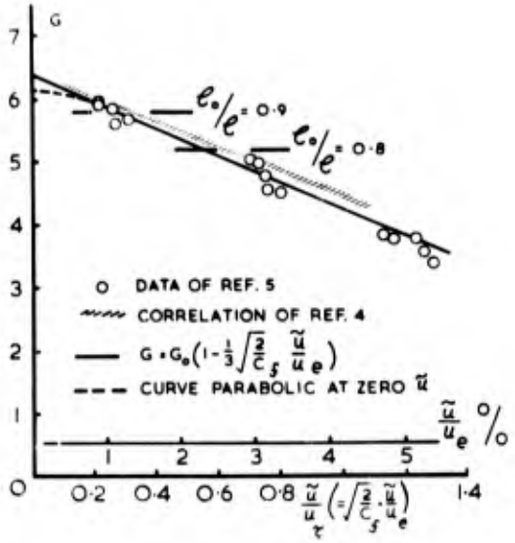

FIG.1 INFLUENCE OF FREE STREAM TURBULENCE ON THE SHAPE PARAMETER G IN ZERO PRESSURE GRADIENT

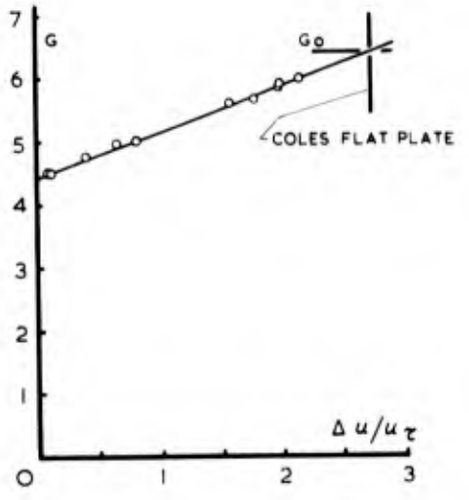

FIG.2 ESTIMATION OF G_o FROM WAKE COMPONENT IN THE EXPERIMENTS OF HUFFMAN

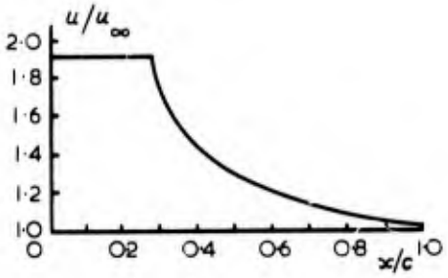

FIG. 3a Streamwise velocity distribution

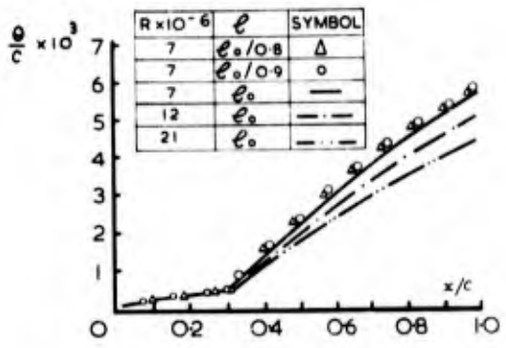

FIG. 3b Momentum thickness distribution

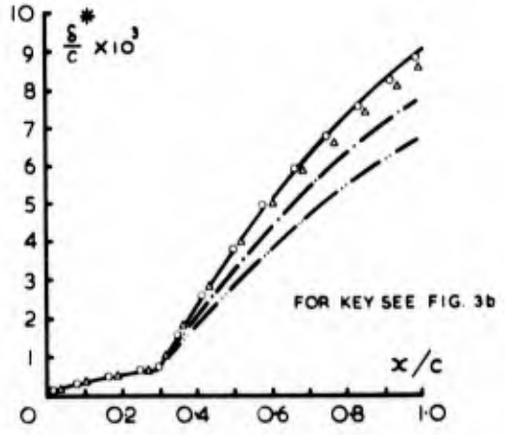

FIG. 3c Displacement thickness distribution

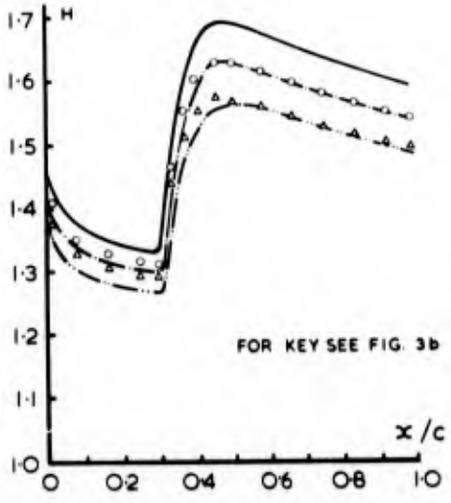

FIG. 3d Shape parameter distribution

FIG. 3 CALCULATED INFLUENCE OF MIXING LENGTH AND REYNOLDS NUMBER ON BOUNDARY-LAYER DEVELOPMENT ON AN AEROFOIL UPPER SURFACE

EFFECTS OF TURBULENCE AND NOISE ON WIND-TUNNEL MEASUREMENTS AT TRANSONIC SPEEDS

by

Adalbert Timme
Deutsche Forschungs- und Versuchsanstalt
für Luft - und Raumfahrt e.V.
Institut für Turbulenzforschung
1 Berlin 12, Müller-Breslau-Str. 8
W.Germany

SUMMARY

A review is given of current knowledge of the effects of flow unsteadiness on steady and dynamic measurements on models in windtunnels at transonic speeds. In most cases the influence of the pressure or velocity fluctuations on flow patterns such as boundary layers with transition or separation, bubble flow or shock interaction is quantitatively known from experiments only for particular parameter combinations. No universal information about the turbulence effect in different situations is available nor is there a general theory including all observed effects at conditions of interest. Only in the case of a turbulent boundary layer at zero pressure gradient a quantitative relation is known between the turbulence in the free stream and the boundary layer development. It is concluded, therefore, that new experimental work using advanced measuring techniques and a secured theoretical background is urgently needed for planning new windtunnels for transonic testing at high Reynolds numbers. As long as our knowledge is incomplete the lowest possible level of flow unsteadiness over the whole frequency range should be achieved.

1. INTRODUCTION

The problems concerning the influence of flow unsteadiness on windtunnel measurements at transonic speeds are manifest and to some extent thoroughly discussed in the literature as far as the effects on the result of measurements are concerned. A detailed summary on this field exists in the reference 1 by D.G. Mabey which is the basis of this report. But the situation changes when we look at the physical mechanism of the effect of unsteadiness, i.e. velocity, pressure and temperature fluctuations, on the flow pattern. There is very little information available about the basic structure of these fluctuations, as e.g. amplitude, frequency and phase relation, space and time correlation. In contrast for the growing subsonic shear layer we have an almost complete catalogue of experimental data. Our theoretical knowledge of the disturbance mechanism at transonic speeds is trivial compared to that of subsonic shear layer. As long as we don't understand completely and in detail the interference of flow unsteadiness and noise of aerodynamic measurements one can only follow the suggestion of Mabey to achieve the lowest possible level of flow unsteadiness in the design of a new transonic windtunnel.

2. DEFINITION AND MEASUREMENTS OF FLOW UNSTEADINESS

Aerodynamic theory normally postulates for a given flow problem a certain speed in a certain direction at a certain pressure and temperature. But in reality there exist always fluctuations of speed, direction, pressure and temperature, only the level, the character and the mutual order of magnitude may be different in different cases. If the pressure fluctuations are predominant, the phase velocity corresponds with the speed of sound and the fluctuation pattern shows a wave form, one speaks of noise or acoustic disturbances. If the fluctuations are more stochastic in space and time, and the phase velocity so far detectable equals a fraction of the flow velocity, we speak of turbulence. But the boundaries between these two types of disturbances are somewhat vague because the phase velocity due to acoustic sources only corresponds in the far field with the speed of sound. In a turbulent flow according to the Lighthill theory the acoustic sources are in a near field and the mean phase velocity is very difficult to define. On the other hand, even a turbulent flow may have a wave form character as we know from the correlation measurements in a free jet of Fuchs [2]. A single probe can never distinguish between turbulence and noise, therefore one needs at least two probes and a correlator. Thus in doubtful cases one should follow the suggestion of Mabey and use the more general term, unsteadiness.

The measurement of velocity fluctuations at transonic speed is extremely difficult, even in continuous facilities. Contrary to the low subsonic range, where the hot wire is the most powerful tool for the measurement of velocity fluctuations down to the order of cm/s, the hot wire in the transonic range becomes very unsensitive. Spangenberg [3] shows that the interpretation of the signals as well as the handling of the probes becomes very difficult. Hot wires at atmospheric pressure tend to fatigue rapidly because of aerodynamic buffeting (the critical Mach number of a circular cylinder is about $M = 0.5$). In addition, there is aerodynamic interference at transonic speeds from the prongs which support the hot wire. On the other hand there are some other techniques which may permit velocity fluctuation measurements. There is the corona probe [4] and the laser-doppler method [5, 6] which should be tried. The corona probe has no breakable wire between the prongs but nevertheless the interference is still a problem. The latter method works on a optical principle and therefore with the minimum perturbation at the measuring location. The results of the actual windtunnel measurements of reference strongly substantiate the feasibility of utilizing the laser-doppler-velocimeter as an operational instrument.

Igoe [7] measured the lateral components of turbulence derived from differential-pressure yawmeters. The rms incidence fluctuations vary from about $0{,}25^\circ$ to $0{,}5^\circ$ in the Langley 16 ft transonic tunnel, and rms fluctuations of $0{,}3^\circ$ have been measured in the NAE 5 ft tunnel [8]. Hills [9] used a similar device in the ARA transonic tunnel. However, it is difficult in yawmeter measurements to decide whether the pressure difference is due to a change of the angle of attack, that is the presence of a lateral velocity component, or whether additional gradients of the velocity in the u - direction or the static pressure fluctuations are more responsible for the signal.

But even in the low subsonic regime where lateral velocity fluctuation measurements are very easily performed, it is very difficult to get from them enlightening information about a turbulent flow field because of the vector character of the velocity and the tensor character of the turbulence quantity $v_i\, v_j$.

Therefore it is more promising to deal with a scalar quantity as e.g. the pressure, the temperature or the density. No temperature fluctuation measurements at transonic speeds are known to the author, but the new crossed beam method [10, 11] enables the measurement of density fluctuations without flow perturbation, hence no correction factors are required. Certainly, both the laser-doppler method and the crossed beam method may be expensive and not applicable for the whole flow field - at least not in the shadow path of the model. Yet for very sensitive flow configurations this method is of great promise confirming the measurements of the flow in the absence of any probe.

The measurement of the third scalar quantity, the static pressure, is most commonly used in transonic facilities. Mabey [12] compared the static pressure fluctuation on a body of revolution on the tunnel centre line with the pressure on the sidewall of the tunnel. He found the level of both pressure fluctuations nearly identical, whereas McCanless [13] for several large American tunnels suggests that the centre line pressure fluctuations may vary from 70 % to 100 % from those of the sidewall. The problem in measuring the true static pressure is the influence of the turbulent velocity components perpendicular to the pressure orifices. Siddon [14] and Fuchs [15] have proven the possibility of such measurements in the lower subsonic regime with the restriction to a turbulence level below a critical value, but still more basic experiments at higher speeds are missing. The upper limit for the probe used by Lau [16] was about M = 0.7.

Even if there are some doubts about the absolute level of the pressure fluctuations in the centre line in comparison to the sidewall, important information about the phase and the coherence should be available.

From dimensional analysis we know that the only significant nondimensional form of rms pressure fluctuation $\tilde{p}$ is the relation to the kinetic pressure $q(=\frac{1}{2}\rho V^2)$ that is $\tilde{p}/q$, either as a function of the dimensional frequency f (or better $f \cdot \Delta f$) or as an integral of the measured spectrum.

Many measurements are given in the literature. In his basic report Mabey [1] adopted a form introduced by Owen [17] who made specific tunnel data more general by replacing the dimensional frequency by the Strouhal number $n = f\ l/V$ (where l is a representative length and V the free stream velocity) and introducing a spectrum function $F(n)$, such that $F(n)\,\delta n$ is the contribution to $(\tilde{q}/q)^2$ in the frequency range between n and $n + \delta n$. Thus

$$\delta\left(\frac{\tilde{p}}{q}\right)^2 = F(n)\,\delta n = n\,F(n)\,\delta(\log n)$$

The results of spectrum analysis can therefore be plotted in the form $F(n)$ against n, or $nF(n)$ against $\log n$. The integration over any range of frequency gives the corresponding mean-square intensity of the fluctuation. The total area under such curve is equal to the total intensity, for

$$\left(\frac{\tilde{p}}{q}\right)^2 = \int_0^\infty F(n)\,dn = \int_{-\infty}^{\infty} n\,F(n)\,d(\log n)$$

Corrections may be needed because of mechanical vibrations of receiver surroundings (probe or sidewall). In the high frequency range there is a contribution due to the fully developed turbulent boundary layer of approximately $\tilde{p}/q = 0.006$. Alternatively Lilley suggested [18] $\tilde{p}/q = 2{,}5 \times C_f$, where C_f is the skin friction coefficient, estimated to be about 0.002 to 0.003 for tunnel boundary layers.

3. INFLUENCE OF FLOW UNSTEADINESS ON:

3.1 Development of boundary layer

In rather similar experiments on flat plates with turbulent boundary layers at zero pressure gradient Charnay, Compte-Bellot and Mathieu [19] and Huffmann, Zimmermann and Bennett [20] have shown the influence of free-stream turbulence on the development of the boundary layer. An increase in free-stream turbulence level leads to an increase in skin friction coefficient, a fuller velocity profile (the shape parameter H is reduced), and a thicker boundary layer. Charnay et al found that the velocity profiles could brought to coincidence only by scaling in the form

$$\frac{u_e - u}{u_\tau - \alpha\tilde{u}} = f\left(\frac{y}{\delta}\right)$$

where $\tilde{u}$ is the rms fluctuating component of the velocity, u_e the velocity at the edge of the boundary layer, u_τ the friction velocity $(=\sqrt{\tau_w/\rho_w})$ and α an empirical constant. This means that the otherwise common velocity-defect law is a function of the turbulence level. With the results of refs. 19 and 20 and the skin friction relation of Nash and McDonald [21], Green [22] calculated the influence of the free-stream turbulence level on the skin friction coefficient C_f, the shape parameter H and the Reynolds number based on the momentum thickness R_θ:

$$\frac{\Delta C_f}{C_f} = 4.8\,\frac{\tilde{u}}{u_e}$$

$$\frac{\Delta H}{H} = -\left\{2.4 - 0.25\,H\right\}\frac{\tilde{u}}{u_e}$$

$$\frac{\Delta R_\theta}{R_\theta} = -\left\{\frac{0.27}{C_f} - 0.97\sqrt{\frac{2}{C_f}}\right\}\frac{\tilde{u}}{u_e}$$

Thus, a free-stream turbulence of 0,2 % will result in a value of C_f roughly 1 % greater than in quiescent air, and value of H roughly 0,005 lower. Green defines an "effective" Reynolds number of the boundary layer in a turbulent stream as the Reynolds number at which the same value of H would be obtained with a quiescent external flow. Then, from the last equation, one sees that not only is the effective Reynolds number highly sensitive to turbulence - the fractional increment in R_θ is 60 times that in $\tilde{u}/u_e$ for the data of refs. 20 and 21 - but also that this sensitivity increases with increasing Reynolds number. Calculations by Green for lifting wings suggest that the same effect occurs in flows in pressure gradients, with an increase in turbulence level delaying separation onset. By comparison, the effects of turbulence on wing drag and viscous loss of lift are calculated to be small.

3.2 Transition

The transition from laminar to turbulent flow depends on multiple parameters in a complicated way which is summarized in refs. 23 to 26. In ref. 27 Morkovin points to the major open question influence of free-stream disturbance fields and the variations of transition and the receptivity of the boundary layer to all disturbance modes. Thus, without a complete understanding of the physical phenomena one can only list the known facts.

For the instability of a boundary layer, theory and experiment indicate a multiplicity of competing modes (generalized Tollmien-Schlichting twodimensional waves, Mack's higher "acoustic" modes, obliques waves, cross-flow modes, nonlinear vorticity stretching etc.) each of which can independently or cooperatively with others grow to the selfregeneration threshold and generate a local spot at a certain position. The process of assimilation of the free-stream unsteadiness into the various unstable modes remain essentially unexplored, theoretically and experimentally.

Spangler and Wells [28] measured in the low subsonic speed range the flat plate boundary layer transition with zero pressure gradient at different free-stream disturbance levels, in the range from $\tilde{u}/u_e$ = 0.04 % to 0.33 %. Fig. 1 shows the result of their measurements with a transition Reynolds number of 5.25×10^6 for the lowest possible disturbance of their facility. This Reynolds number is almost twice as great as the well known value found by Schubauer and Skramstad [29]. Transition turns out to be very sensitive to grid produced turbulence with a broad spectrum. In contrast pure acoustical disturbances produced by an air-driven rotating-vane sound generator influence the transition only if the fundamental frequency or the first harmonics lie within the critical frequency range, which is for this case approximately 10 to 80 Hz. In other measurements of Miller and Fejer [30] at a level of disturbance two orders of magnitude higher ranging in amplitude from 8.0 to 67 % of the free-stream velocity, the transition Reynolds number depends only on the amplitude of the oscillations whereas the nondimensional transition length is a function only of the frequency (Fig. 2). One explanation of this contrast is, according to Spangler and Wells [31], the enormous level of the free-stream oscillation produced by the rotating shutter valve in the experiments of Miller and Fejer. Transition may indeed be a function of disturbance amplitude only and not of frequency, when the free-stream disturbance is large enough to impose directly on the boundary layer rate of shear high enough to cause breakdown.

In the supersonic and hypersonic speed range $3 < M < 4.5$ Pate and Schueler [32] and Pate [33] investigated the transition on twodimensional sharp leading-edge models and sharp cones. These transition measurements show conclusively a significant and continuous increase in transition Reynolds numbers with increasing tunnel size. This increase in Re_t was explained by a decrease in the radiated aerodynamic noise emanating from the tunnel wall turbulent boundary layer. Including the data of eleven different windtunnel facilities covering a Mach number range from 3 to 14, they developed a correlation of transition Reynolds number independent of Mach number and unit Reynolds number and dependent only on the aerodynamic noise parameter established by Pate and Schueler for planar data. (Fig. 2 c).

These results provide convincing evidence that tunnel noise or turbulence substantially reduces transition Reynolds number in these two speed ranges. The same phenomenon would be expected at transonic speeds probably to a higher degree because of high enviromental noise in transonic windtunnels. Thus, Cunning and Low suggest that the measured drag with free transition on a model of the F 1-11 aircraft was influenced by disturbances generated by the walls of the working section. The model was tested at identical conditions in a windtunnel which could be fitted with either porous or slotted walls. The minimum drag of the model was much higher with porous walls than with slotted walls which could be explained with a different position of the transition point.

Because of the gap in basic information in the transonic speed range Credle and Carleton [35] performed detailed transition measurements on a 10 deg total-angle cone in two different windtunnels. To determine the influence of the free-stream disturbances the overall noise of the tunnel, as well as the pressure fluctuations on the surface of the cone in two different positions were measured. It was concluded that the overall rms levels measured on the cone were controlled by the tunnel noise (both wall and free-stream). To obtain a correlation between transition and noise they crossplotted the variation of transition Reynolds number with Mach number for fixed unit Reynolds number, and the variation of the nondimensional noise level with Mach number for the same unit Reynolds numbers, as seen in Fig. 3. It shows the same trend as in Fig. 1 although the difference in notation (velocity and pressure fluctuations) and the difference in absolute level should be considered.

However, for force test of aircraft models, transition generally is fixed by boundary layer trips at a location representative of the flight condition so that a known reference is available for extrapolation of skin friction drag. Hence unknown variations should not occur with angle of attack, as

Lloyd Jones [36] suggested.

3.3 Bubble flow and trailing edge separation

In a bubble flow a laminar boundary layer separates due to a positive pressure gradient and a free shear layer is formed around the dividing streamline of the separation. The shear layer is several orders of magnitude more unstable than the laminar boundary layer before separation. Consequently, transition often occurs in the portion of the free shear layer near the dividing streamline, and very shortly after the separation point. When such a transition occurs, the mixing in the layer near the wall is greatly increased and this leads to reattachment in a short distance. At high Mach numbers sometimes the reattachment zone is still laminar and followed by transition further downstream. Tani [37] has compiled various kinds of bubbles (long and short bubbles, two- and threedimensional) and their correlation for the case of airfoils.

It is likely that such a stream pattern is sensitive to flow disturbances and especially the pressure fluctuations in the separation region, as Mabey [38] suggested. He assumes that the bubble flow is ruled by a feedback process between conditions at separation and reattachment, and that the strength of the wake component of the boundary layer, and hence the low-frequency pressure fluctuations, may be altered by the free-stream disturbances.

In nozzles transition bubbles can have significant effects too. Even though the oncoming flow is turbulent, relaminarization often occurs in the converging section of nozzles due to the very high accelerations. When relaminarization of the boundary layer occurs in the converging section, a local separation bubble probably occurs in the local adverse pressure gradient near the wall just past the throat. Transition to turbulent flow then occurs in the bubbles.

Wills [39] also showed that the first diffuser of a low speed windtunnel may introduce spurious low-frequency pressure fluctuations into the working section. However, the level of these spurious pressure fluctuations required to influence the spectra generated by separated flows has not yet been established.

Separation in general is assumed to be sensitive to flow disturbances e.g. separation generating leading-edge vortices on slender wings and the wake system of these vortices, but no detailed information is available to the author.

3.4 Intake flows

Very little is known about the influence of free-stream unsteadiness on the flow through intakes as ref. 40 stated. The only example given there shows the noise level inside the intake along the centre-line with the characteristic jump on the position of the shock, but no recommendation about the expected effect of free-stream unsteadiness variation is given. The buzz boundary of supersonic inlets can be obscured by a high level of tunnel turbulence, as Stewart and Fisher [41] showed.

3.5 Shock interaction

The influence of flow unsteadiness on shockwave boundary layer interaction has to be seen in connection with what is known from the boundary layer development and transition. There we have seen that the shape of the boundary layer can be altered by flow unsteadiness as well as the position of the transition point. Thus, it is to be expected that under certain circumstances the interaction of the shock with the boundary layer (whether the shock causes only thinning of the laminar boundary layer or separation with or without transition and with or without reattachment) can be shifted to another type of interaction by the influence of free-stream disturbances. Moreover, not only is the type of shock wave interaction likely to be sensitive to unsteadiness, but also the position of the shock itself and therefore the surface pressure distribution upstream and downstream of the shock as reported by Robertson [42]. In Robertson's experiments with missiles at high transonic speeds the flow stays almost attached at the junction between nose and body but the terminal shock downstream of the junction oscillates upstream and downstream and causes large pressure fluctuations which were controlled by the flow unsteadiness. Robertson assumes that these oscillations in free flight are controlled by atmospheric turbulence or the vibration of the missile.

According to Mabey a typical example for the assumption of a control mechanism is Fig. 3 from ref. 1 based on Figs. 17a and b, ref. 42. It shows the spectral amplitude distribution of the pressure fluctuations measured on the surface of the missile model near the mean position of the terminal shock (continuous curve) and the free-stream turbulence measured without the model on the centreline of the AEDC 1 ft perforated tunnel at M = 0.9 (dotted curve). In the frequency range below 100 Hz the model pressure fluctuation level is almost one order of magnitude higher than the tunnel level but of the same shape. This could be interpreted as a broadband amplification mechanism of the shockwave interaction. In the frequency range above 100 Hz unfortunately the tunnel level is so high that no definite information is available whether the amplification process is overloaded or, as is more likely, the model transducer measures the tunnel unsteadiness only. Although the region of these pressure fluctuations is restricted, Mabey points out that they will still make a significant contribution to the loads on the model.

In his considerations about future concepts of design pressure distributions of aerofoils Küchemann [43] emphasizes the significance of shock position and the flow patterns at the foot of the shock which are sensitive to flow disturbances. In Fig. 5a to d four different types of design pressure distributions are shown which represent the various kinds that are being considered nowadays. In all four examples the mainstream Mach number is M_o, the curves marked 1 are the pressure distributions at design condition with fully attached flow, the full lines marked 2 the distributions at off-design conditions where the postulated type of flow can no longer be maintained and gross departure must be expected to occur (such as severe buffeting). Küchemann defines a limit for these conditions which are represented by the full lines. The dotted line marked 3 are the pressure distributions beyond these limits and unacceptable for engineering applications. Without going in all the details of the distributions it may be pointed out that the bubble at the foot of the shock which may in the limiting case either: a) have lengthened and be about to burst (Fig. 5a, type A flow ref. 44) or b) there may be an incipient rear separation (Fig. 5b and

presumably in Figs. 5c and 5d, type B flow ref. 44) According to Küchemann in all the unacceptable cases marked 3, a large bubble beginning at the shock and extending beyond the trailing edge is assumed to have occurred. But these are flow patterns which are sensitive to flow unsteadiness. And therefore one has to expect that these advanced pressure distribution concepts are possibly sensitive to turbulence level, or scale or frequency.

3.6 Wing buffeting and flutter

Mabey [1] mentions in his report that in many cases dynamic measurements of wing buffeting are masked by turbulent pressure fluctuations and therefore difficult to detect, or that the buffet boundaries are changed with changing turbulence level. He explains this interference with a shifting of the mean shock position changing the severity of buffeting. In extensive measurements of windtunnel unsteadiness in different facilities he derived summary criteria [12] for the influence of turbulence on buffeting measurements which are shown in Fig. 6.

As a typical example for shifting of the buffet boundaries due to different turbulence levels, he shows in Fig. 7 the comparison of measurements on a transport aircraft model in the RAE 3 ft x 3 ft tunnel with a higher turbulence level ($\sqrt{nF(n)} = 0.006$ to 0.008) and in the HS 2 ft x 2 ft tunnel with a lower turbulence level ($\sqrt{nF(n)} = 0.001$ to 0.002) in contrast to free flight measurements. Fig. 7 establishes better agreement with the flight results at transonic speeds with the lower turbulence level.

In another example Mabey changed the level of tunnel unsteadiness by opening or closing the slots of the working section, resulting in higher or lower unsteadiness level respectively. Fig. 8 shows the wing-root strain signal of a fighter aircraft model at subsonic speeds ($M = 0.6$) where the turbulence level influences only the level of model response but not the buffet onset significantly [45]. In contrast, at transonic speeds ($M = 0.8$) the buffet onset occurs more suddenly and at a much higher angle of incidence with the lower turbulence level, and in a better agreement with flight tests. In similar measurements Mabey [46] found the buffet boundary very sensitive to flow unsteadiness, especially in the speed range $M = 0.8$ to 0.9, and better agreement with flight tests when the turbulence level was lower.

Even more difficult are flutter tests in the presence of turbulence not only because of the masking effect, but also by the possible excitation of response modes which can be mistaken for flutter modes, as Mabey points out. The upper limit of turbulence level for flutter tests at zero lift is according to BAC Filton [1] $\sqrt{nF(n)} = 0.004$ if great care is taken. But, as Mabey suggests, future flutter tests may have to be made on lifting models close to the buffet onset boundary or above it and these tests will be hazardous to the model and might require a turbulence level below this value.

The method for the determination of flutter modes used by BAC is the vector response of the model to a sinusoidal excitation. For the free decay method of testing, commonly used at supersonic speeds, a lower level of unsteadiness is needed. Reference 47 cites an example when this method could not be used at transonic speeds, because the unsteadiness level was too high.

3.7 The measurement of pressure fluctuations

In the foregoing sections we spoke about turbulence effects where the level of the turbulence possibly might change the results. Beyond that, there are cases where the presence of flow disturbances prevents the measurement of the wanted intensity, or falsifies the results by other causes than aerodynamic ones.

It is clear that one can never measure pressure fluctuations of a level below the free-stream turbulence level of the windtunnel (at least as long as there are no known frequency correlations). In a comparison of windtunnel and flight measurements of surface pressure fluctuations for attached and separated boundary layers on an ogive-cylinder model, Lloyd Jones [36] showed the severity of this problem. These tests were conducted in various Ames windtunnels and on a nose boom of a F - 104 aircraft. With attached boundary layers at transonic speed the level of nondimensional pressure fluctuations $\tilde{p}/q$ was in the tunnel experiments more than one order of magnitude higher than in flight which means that in the tunnel the model acted as a pressure probe for measuring the tunnel noise. With separated boundary layers the differences became smaller but nevertheless , the tunnel measurements are still doubtful, as Lloyd Jones suggested.

Free-stream disturbances can excite model vibrations and therefore restrict the use of a windtunnel, as in the case of the 3 ft x 3 ft transonic working section of the RAE 3 ft tunnel [48]. Thus, the vibrations can cause fatigue failures in the balance system [49] or overload the amplifiers connected with balance straingauges [50]. These effects restrict the use of existing windtunnel facilities. They will become more serious in new facilities operating at much higher pressures and therefore higher model stress limits unless radical improvements of the electronic and mechanical design of future balances alleviate the problem.

4. GENERATION AND SUPPRESSION OF TURBULENCE AND NOISE

In an extensive study of the flow unsteadiness in the RAE 3 ft x 3 ft transonic tunnel and in a 1/9 scale model of this tunnel, Mabey [12] shows in a sketch (Fig. 9) the principal sources of flow unsteadiness. Since these disturbances, and the model vibrations excited, impeded static and dynamic measurements of subsonic and transonic speeds, Mabey improved the level of disturbances by successive modifications to the balance section and diffuser. In both tunnels he found flow instabilities with separation and resonances with organ pipe frequencies which could be eliminated by the installation of a diffuser fairing and a revised balance section without a centre body. In the slotted working section operated by diffuser suction unsteadiness came from the extraction region. By covering the slots with perforated screens the level of unsteadiness was reduced but not down to the level of the closed or perforated working section (which had nearly the same unsteadiness). In the final version of the perforated working section with 60° inclined holes the hole geometry had to be modified because of the occurence of edge tones.

Similar problems with the generation of discrete frequencies by wall holes are reported by Credle [51] from the Propulsion Windtunnel (16 T) and Aerodynamic Windtunnel (4 T) of AEDC. In the tunnel 16 T was a critical Mach number range in which a wall hole frequency was in acoustic resonance with a compressor blade frequency. Credle suggests in this case the installation of a silencer. For other frequencies, and in the tunnel 4 T, noise reduction was achieved by the installation of acoustic insulation on the interior walls of the plenum cavity. He found that the noise level varies slightly with wall angle and significantly with Mach number and wall porosity. Thus, for subsonic Mach numbers optimal noise reduction was achieved with a modified wall geometry, and the porosity adjusted for optimum aerodynamic conditions. For some conditions the resultant noise levels were found to be equal to those of a smooth wall tunnel. For maximum reduction of noise generated by inclined holes both Mabey [12] and Credle [51] recommend rounding the edge of each hole thus allowing every hole no distinct length in flow direction for the frequency determination of the feedback system inside the hole.(Details of this problem are reported by Cox elsewhere). Further, Credle recommends the serration of the lip of each hole which recalls the experiments of Neuwerth [52] with free jets impinging a flat plate. In the distance range from 1.2 to 6 nozzle diameters a feedback mechanism generates an enormous pressure fluctuations level which can be suppressed by shifting a small pin on the end of the nozzle through the shear layer. The length of pin needed for a complete suppression is not more than 1/20 nozzle diameter.

Also important, but not of the same severity, is the reduction of turbulence level upstream of the working section at lower velocities. In extensive investigations Loerke and Nagib [53] measured the efficiency of various turbulence damping devices such as screens, perforated plates, porous foam, and honeycomb-like matrices formed with closely packed plastic drinking straws. In a comparison (Fig. 10) of various combinations of these devices the quantitative turbulence generating and damping effect is shown as a function of the downstream distance. They confirm that combinations of matched manipulators in series are more effective in suppressing free-stream turbulence than any individual manipulator of equal pressure drop.

5. CONCLUSION

It has been shown in a series of examples that by free-stream flow disturbances - they may be called turbulence or noise - the measurement of both static and dynamic quantities may be altered in a scale and direction which is known and calculable only in very few cases. In view of a need for higher accuracy in transonic windtunnel measurements and the ability to relate the test results to aircraft in flight, it should be worthwhile to discuss the most efficient way to overcome the present scarcity of reliable information. One way to go is to stop this gap by numerous experiments with the variation of all related parameters and configurations. This is an assured, approved, but laborious and protracted path. The other way consists in making only a restricted number of basic investigations, including the measurement of all related parameters, in order to get a better understanding of the physical mechanism of interaction between turbulence and noise on the one side and boundary layer development, transition and separation including shock interference on the other side. Instead of compiling and plotting hundreds of details it seems better to correlate in a few basic experiments all needed data with advanced theoretical concepts. This appears to the author a more economical way.

What Tollmien-Schlichting and Schubauer-Skramstad did for the wall boundary layer, what Michalke and Freymuth did for the free shear layer, that is what the situation demands.

One possible aspect of this problem is the search for any structure in the turbulent flow pattern of a transonic flow field. As Fuchs [2] has shown for the subsonic free jet, there is evidence of a strong coherence within the turbulent jet for at least 8 diameters downstream from the nozzle, although this flow pattern is commonly described as truly turbulent i.e. of random character (Fig. 11). For at least one source of unsteadiness in a transonic windtunnel Cox [54] has proven a regular pattern of coherent sound wave fronts radiated from the perforated sidewalls. He suggests that the coupling is caused by disturbances propagating along the surface of the liner. Results from individual holes indicate that the mechanism for production of sound waves is similar to that observed from twodimensional cavities. Apparently it is the same feedback mechanism of the flow through a sharp edged cylindrical nozzle described by Heller [55, 56]. In both flows disturbance travelling downstream or a vortex generates a sound wave on the end of the system which, in turn radiated upstream, coincides with the next disturbance. For this cycle the frequency law of Heller is well confirmed by the results of Cox.

For this source of unsteadiness we know now the regular pattern, but one should check by the use of two pressure probes or one probe and one sidewall pressure hole and a correlator whether in general the turbulence in a transonic windtunnel has certain coherence lengths and if so how the structure can be changed in frequency and wave length. And further having in mind from the investigations of Pfizenmaier [57] that only frequencies at a certain range are really harmful for the growth of a shear layer, whether to some extent a shift to harmless frequencies is possible.

Admittedly, for the present moment we need rather suggestions about the acceptable level of tunnel unsteadiness as e.g. proposed by Mabey [1, 12] with $\sqrt{nF(n)} = 0.002$ for the detection of light buffeting for past designs and even lower level for future designs, than speculations about a futuristic research strategy. But the question is whether we are really realistic in the assessment of one perhaps important parameter of complex flow patterns with an unknown variety of factors, which are not yet fully understood.

In some discussions with Professor Cox, Mr. Mabey and Mr. Hill an agreement was reached about the most desirable future basic research aims which may be listed as follows:

The influence of flow disturbances (i.e. frequency, amplitude, phase and coherence distributions) revealed with unobstructive measurement technique, should be thoroughly studied in:

i laminar boundary layers,
ii turbulent boundary layers,
with transition or separation
without and with separation

} at constant pressure, without shocks

iii, iv } as in i and ii, with pressure gradient

v, vi } as in iii and iv, with shock interaction

Further points of interest:

vii In the case of interaction of an oscillating shock associated with separation (and reattachment): Is this flow pattern restricted to swept wings (from where it is known) or transferable to flat plates with pressure gradient?

viii flow around leading edges at varying angle of incidence.

ix bubble flow: distribution of mean pressure, distribution of fluctuating pressure } as function of turbulence level

x the influence of ultra high frequency sound waves on transition of the boundary layer

But as long as we don't understand the complex aerodynamic mechanism of turbulence we should follow the suggestion by Mabey in the design of a new transonic windtunnel, namely to achieve the lowest possible level of flow unsteadiness over the whole frequency range of the measurable spectrum.

REFERENCES

[1] D G Mabey — The influence of flow unsteadiness on windtunnel measurements at transonic speeds. LaWs-Paper Nr. 38

[2] H V Fuchs — Über die Messung von Druckschwankungen mit umströmten Mikrophonen im Freistrahl. DLR-FB 70-22 (1970), Dissertation, TU Berlin, 1969

[3] W G Spangenberg — Heat-Loss Characteristics of Hot-Wire Anemometers at Various Densities in Transonic and Supersonic Flow. NACA TN 3381, 1955

[4] W Fucks — Messung der Turbulenz und von Turbulenzkomponenten mit Hilfe der Koronaentladung. Z.Phys. 137, Berlin 1954

[5] B S Rinkevichyus — Measurement of local velocities in flows of liquid and gas according to the Doppler effect. Teplofizika Vysokikh Temperatur, Vol 8, No. 5, pp. 1073-1082, 1970

[6] A E Lennert, R L Parker, F H Smith — Application of dual laser doppler velocity-meters for windtunnel measurements. AGARD-LS-49, 1971

[7] W B Igoe — Windtunnel buffeting measurements on two wing-end plate airplane model configurations. NASA TMX 1454

[8] W B Igoe — Dynamic flow characteristics of the transonic test section of the 5 ft tunnel. Report DME/NAE 1968 (4) P 59

[9] R Hills — To be published

[10] M J Fischer, K D Johnston — Turbulence measurements in supersonic, shock-free jets by the optical Crossed-Beam method. NASA TN D - 5206 (1970)

[11] R J Damkevala, K A Kadrmas — Turbulence measurements with infrared Crossed-Beam system near 4.3 microns. AIAA Paper No. 70-235, Sciences Meeting, N.Y. 1970

[12] D G Mabey — Flow unsteadiness and model vibration in windtunnels at subsonic and transonic speeds. ARC CP 1155

[13] G F McCanless, J R Boone — Noise reduction in transonic windtunnels

[14] T E Siddon — On the response of pressure measuring instrumentation in unsteady flow. UTIAS Report 136

[15] H V Fuchs — Measurements of pressure fluctuations within subsonic turbulent jets. Journal of Sound and Vibration 22 (3), 1972, 361-378

[16] J C Lau — The coherent structure of jets. Univers.South., Ph.D.Thesis, 1971

[17] T B Owen — Techniques of pressure fluctuation measurements employed in the RAE low speed windtunnels. AGARD Report 172 (ARC 10780) (1950)

[18] G M Lilley — On wall pressure fluctuations in turbulent boundary layers. ARC 24241 (1962)

[19] G Charnay, G Comte-Bellot, J Mathieu — Development of a Turbulent Boundary Layer on a Flat Plate in an Exterral Turbulent Flow. Paper 27 in AGARD CP 93, 1971

[20] G D Huffmann, D R Zimmermann, W A Bennett — The Effect on Free Stream Turbulence on Turbulent Boundary Layer Behaviour. Presented at AGARD Specialists' Meeting "Boundary Layer Effects in Turbomachines", Paris, April 1972

[21] J F Nash, A G J Mcdonald — A Turbulent Skin Friction Law for use at Subsonic and Transonic Speeds.

[22] J E Green — On the influence of free stream turbulence on a turbulent boundary layer, as it relates to windtunnel testing at subsonic speeds. LaWs Paper No. 104

[23] M V Morkovin — Critical Evaluation of Transition from Laminar to Turbulent Shear Layers with Emphasis on Hypersonically Traveling Bodies. AFFDL TR 68-149 (March 1969)

[24] L M Mack, M V Morkovin — High-Speed Boundary-Layer Stability and Transition. Notebook for the AIAA Professional Study Series, AIAA (June 1969)

[25] L M Mack — Boundary-Layer Stability Theory. Jet Propulsion Laboratories, Tech Report 900-277 (1969)

[26] M V Morkovin — Critical Evaluation of Laminar-Turbulent Transition and High-Speed Dilemma. Vol 13 of Progress in Aerospace Sciences, D. Küchemann, Editor, Pergamon Press (1972)

[27] M V Morkovin — Open Questions Transition to turbulence at high speed. AFOSR - TR - 70 - 1731, 1971

[28] J G Spangler, C S Wells, Jr. — Effects of Freestream Disturbances on Boundary-Layer Transition. AIAA Journal, Vol. 6, pp. 543-545 (1968)

[29] G B Schubauer, H K Skramstad — Laminar boundary layer oscillations and transition on a flat plate. Rep. 909, 1948, NACA

[30] J A Miller, A A Fejer — Transition phenomena in oscillating boundary layer flows. JFM, Vol. 18, Pt. 3, 1964

[31] J G Spangler, C S Wells — Reply by Authors to J A Miller. AIAA Journal Vol. 6, No. 12, p. 2461, 1968

[32] S R Pate, C L Schueler — An Investigation of Radiated Aerodynamic Noise Effects on Boundary-Layer Transition in Supersonic and Hypersonic Windtunnels. AIAA Journal Vol. 7, p. 450 (1969)

[33] S R Pate — Measurements and Correlations of Transition Reynolds Numbers on Sharp Slender Cones at High Speed. AIAA Journal Vol. 9, p. 1082 (1971)

[34] D P Cumming, W H Lowe — Experimental wall interference studies in a transonic windtunnel. AIAA Paper 72-292

[35] O P Credle, W E Carleton — Determination of transition Reynolds number in the transonic Mach number Range. AEDC-TR-70-218, 1970

[36] J L Jones — Transonic testing in existing windtunnels. Paper 19 AGARD CP 83-71

[37] I Tani — Low-speed flows involving bubble separations. Progress in Aero. Sciences 5. Pergamon Press, Oxford

[38] D G Mabey — Pressure fluctuations caused by separated bubble flows at subsonic speeds. RAE TR 71-160

[39] J A B Wills — Spurious pressure fluctuations in windtunnels. NPL Aero 1273, July 1967, Journ.Acoustical Scociety of America Vol. 43 P 1049-1054 (1968)

[40] Report of AGARD Ad Hoc Committee on Engine/Airplane Interference and Wall Corrections in Transonic Windtunnel tests.

[41] P G Steward — Instability and turbulence in supersonic air intakes - the effects of free stream turbulence, Reynolds number and surface roughness on some axisymmetric intakes at M = 1.8 and 2.2.
ARL/ME 129, November 1970

[42] J E Robertson — Unsteady pressure phenomena for basic missile shapes at transonic speeds.
AIAA Preprint 64-3

[43] D Küchemann — Fluid mechanics and aircraft design.
Journal of the Aeron. Soc. of India, Vol. 22, No. 3, 1970

[44] H H Pearcey, J Osborne, A B Haines — Interaction between local effects at the shock and rear separations - a source of significant scale effects in windtunnel tests on aerofoils and wings.
NPL Aero 1071 (ARC 30477) September 1968

[45] D G Mabey — Measurements of wing buffeting on a Scimitar model.
ARC CP 1171

[46] D G Mabey — A hypothesis for the prediction of flight penetration of wing buffeting from dynamic tests on windtunnel models.
RAE Technical Report 70-189
ARC CP 1171

[47] W P Hanson, R V Doggett — Windtunnel measurements of aerodynamic damping derivatives of a launch vehicle vibrating in free - free bending modes at Mach numbers from 0.70 to 2.87 and comparisons with theory.
NASA TND 1391, October 1962

[48] E P Sutton, M T Caiger, A Stanbrook — Performance of the 36 x 36 in slotted transonic tunnel of the RAE Bedford 3 ft windtunnel.
ARC R&M 3228 (1960)

[49] E Huntley — Details of the fatigue failure of a windtunnel drag balance.
RAE Tech Memo 641 (1959)

[50] L C Squire — Further experimental investigations of the characteristics of cambered gothic wings at Mach numbers from M = 0.4 to 2.0.
ARC R&M 3310 (1961)

[51] O P Credle — Perforated wall noise in the AEDC-PWT 16 ft and 4 ft transonic tunnels.
AEDC-TR-71-216, 1971

[52] G Neuwerth — Akustische Rückkopplungserscheinungen am Unter- und Überschall-Freistrahl, der auf einen Störkörper trifft.
Reprint of the 5. DGLR-Jahrestagung, Berlin 1972

[53] R I Loerke, H M Nagib — Experiments on management of free stream turbulence.
LaWs Paper No. 48

[54] M M Freestone, R N Cox — Sound fields generated by transonic flows over surfaces having circular perforations.
AGARD-CP-83-71 pp. 24-1

[55] H Heller — Tonbildung bei der Durchströmung scharfkantiger Düsen mit hohen Unterschallgeschwindigkeiten.
DLR-FB 65-70, 1965, Dissertation, TU Berlin, 1965

[56] H H Heller, D G Holmes, E E Covert — Flow-induced pressure oscillations in shallow cavities.
Journ. of Sound & Vibr. 18 (4), pp. 545-553, 1971

[57] E Pfizenmaier — Experimentelle Untersuchung der Druck- und Geschwindigkeitsschwankungen im schallbeeinflußten Freistrahl.
7. Internat. Congress on Acoustics, Budapest, 1971.
Pap. 23N3, 1971

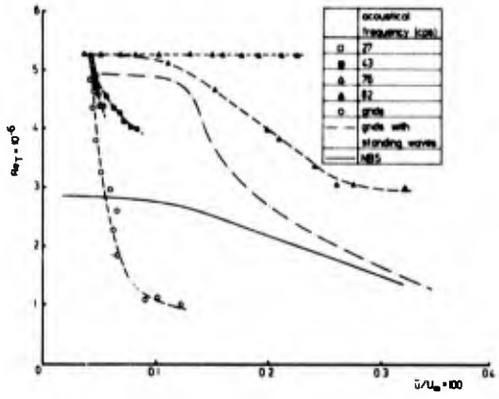

Fig. 1 Transition Reynolds number as function of free-stream dusturbance intensity. (U_o/ν = 2.4 x 10^7/ft; U_o = 38.5 fps). From Spangler and Wells, Ref 28, taken from ref. 27

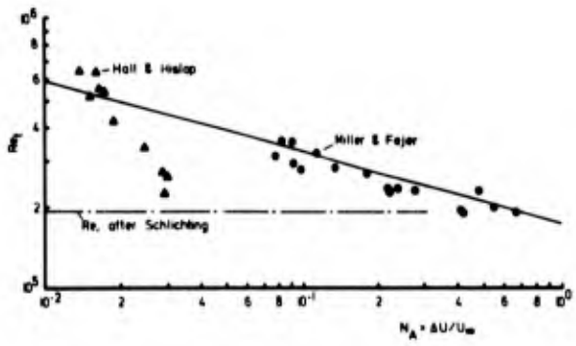

Fig. 2a Effect of the amplitude parameter, $\Delta U/U_\infty$, on the transition Reynolds number from ref. 30

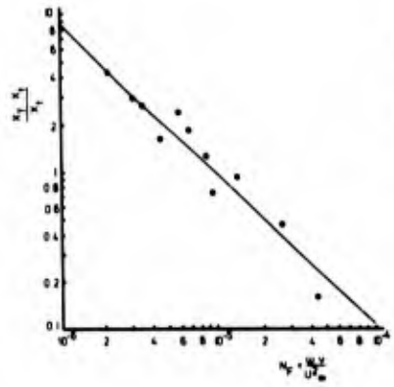

Fig. 2b Effect of the frequency parameter, $\omega\nu/U^2_\infty$, on the transition length, from ref. 30

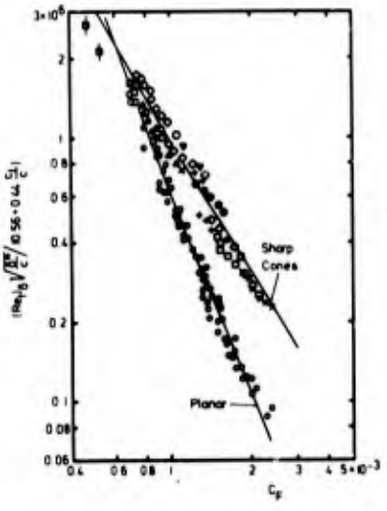

Fig. 2c Correlation of planar and sharp slender cone transition Reynolds numbers; from ref. 33

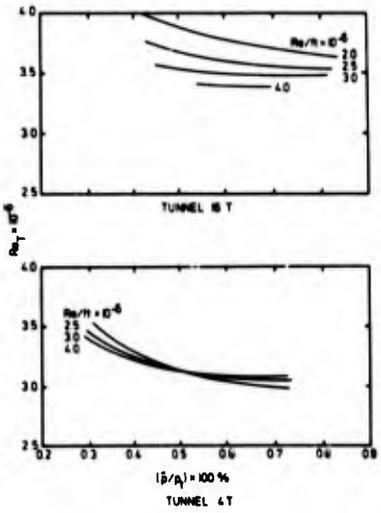

Fig. 3 Correlation of transition Reynolds number and test section noise levels in tunnels 16 T and 4 T, $0.60 \leq M \leq 1.00$ from ref. 35

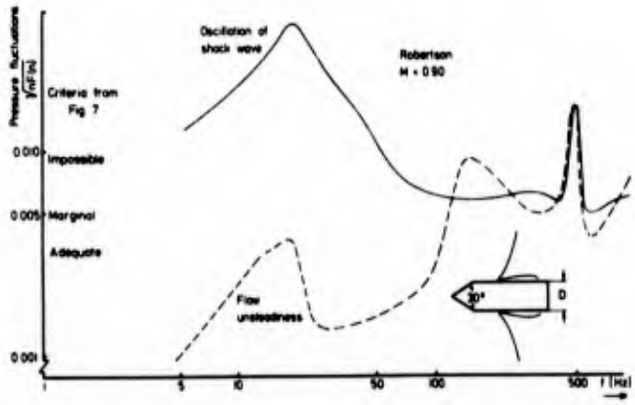

Fig. 4 Influence of flow unsteadiness on oscillation of terminal shock, from ref. 1

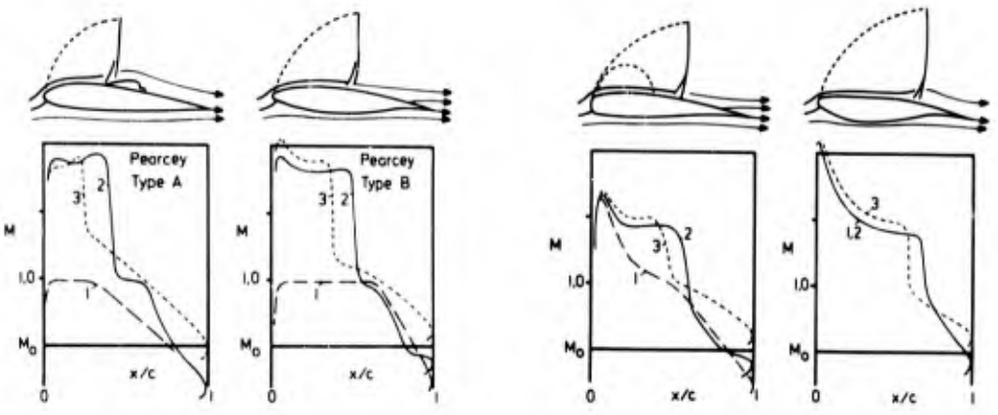

Fig. 5a Short roof top (a) 5b Long roof top (b) 5c Shockless compression (c) 5d Shockless compr. and shock (d)

High-subsonic pressure distributions
from ref. 43

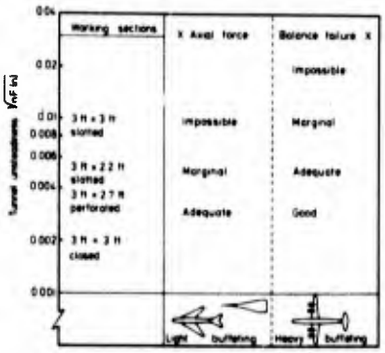

Fig. 6 Tunnel unsteadiness criteria for buffeting tests from ref. 12

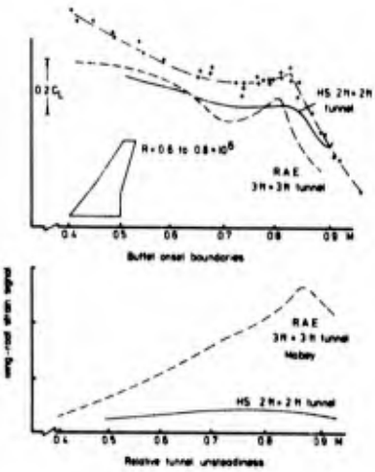

Fig. 7 Transport Aircraft - Influence of tunnel unsteadiness on wing buffeting from ref. 1

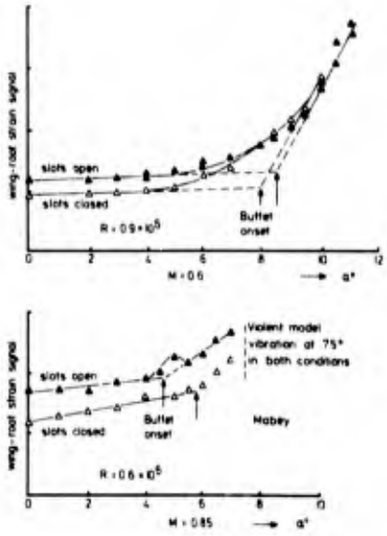

Fig. 8 Fighter aircraft model - influence of tunnel unsteadiness on wing buffeting from ref. 1

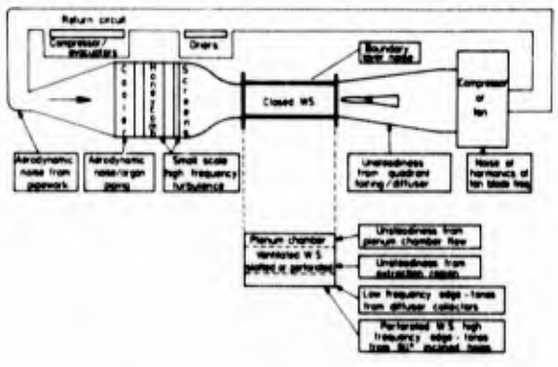

Fig. 9 Sources of unsteadiness in transonic tunnels, from ref. 12

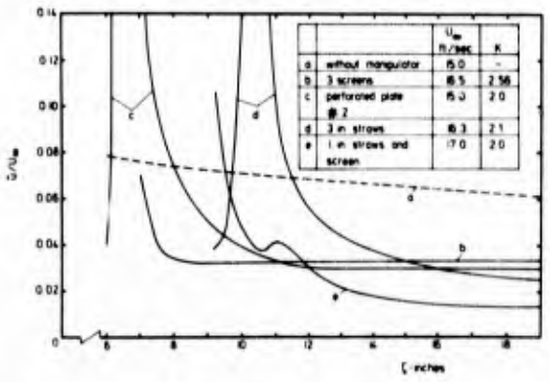

Fig. 10 Comparison of turbulence damping for manipulators of almost equal pressure drop coefficient, from ref. 53

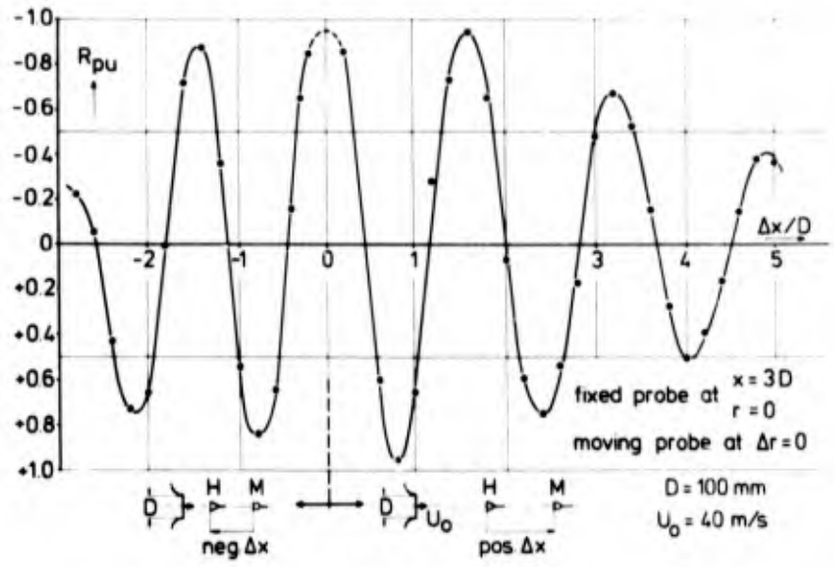

Fig. 11 Two-point longitudinal cross correlations in a jet (pressure and velocity signals filtered at f_m = 200 Hz Δf = 10 Hz) from ref. 2

DESIGN OF VENTILATED WALLS WITH SPECIAL EMPHASIS ON THE ASPECT OF NOISE GENERATION

R. N. COX and M. M. FREESTONE
Department of Aeronautics,
The City University,
St. John Street,
London, EC1V 4PB,
England

SUMMARY

Brief reviews are given of the parameters influencing the design of ventilated walls in current use and of noise generation by such walls. By drawing an analogy between results from flows past two-dimensional cavities and the discrete frequency tones generated by perforated walls, some suggestions are made about the mechanisms responsible for the tones. Finally some possible methods of reducing unwanted noise from tunnel walls are discussed.

1. INTRODUCTION

The object of using ventilated walls in a transonic wind-tunnel is to reduce the effect of wall constraints so that as large a model as possible can be used up to high angles of incidence in a working section of given dimensions. Ideally, the method chosen should accomplish this over the whole of the test Mach number range (subsonic, transonic and supersonic) with a single type of liner for the test section walls; if adjustments do have to be made, they should be kept as simple as possible.

Basically, two types of ventilated walls are used at the present time in transonic tunnels; longitudinal slotted walls, employed mainly for subsonic and near sonic flows, and perforated walls, used over the whole Mach number range up to about 1.3. The latter are superior to slotted walls for supersonic wave cancellation.

Current designs of slotted walls normally have an open area ratio between 1 and 3%, or up to around 6% with up to 6 slots per wall, and methods of wall correction are available up to near-sonic speeds if the model incidence and blockage ratio are not too large.

Slotted liners can also be employed up to about $M = 1.2$ if too great an accuracy is not demanded, although difficulties may arise because of the upstream propagation in the open slots of the effects of shock boundary-layer interactions.

An advantage of slotted walls over perforated walls at subsonic Mach numbers is that if a wall configuration giving zero lift and blockage corrections for a given model can be established at $M = 0$, this will normally be valid over the whole Mach number range. To keep the corrections small for a perforated wall, the open area ratio needs to be varied with Mach number. An AEDC arrangement for achieving this is shown in Fig. 1.

For both slotted and perforated walls, the wall configurations for minimum lift and blockage corrections are not the same as for minimum pitching moment corrections. Recent work (Refs. 1 and 2) has suggested that this apparent defect can be remedied by longitudinal variation of the open area ratio.

Perforated walls have been developed to deal principally with shock and expansion wave cancellation at the wall for supersonic flows. Earlier tunnels used normal holes with a porosity of about 20%, but recent practice is to employ holes slanted at 60° and having a maximum open area ratio of 6% (based on the drill area) in a plate of thickness normally about equal to the hole diameter (Fig. 1). Values of open area ratio of 6% or less also lead to reasonably small subsonic flow corrections, and for blockage of 1% or less, most groups do not apply any corrections. The main development work for the 60°/6% slanted hole configuration was carried out at AEDC.

The requirement for supersonic wave cancellation is to reproduce at the tunnel walls the relationship between the pressure coefficient and flow inclination which would occur in an unbounded stream. The required $C_p - \theta$ variation may be obtained theoretically for a range of model shapes and blockage ratios.

The characteristics of the holes, which must include the effects of parameters such as boundary-layer growth, hole size and angle, and plate thickness, are determined experimentally. The $C_p - \theta$ relationship produced is strongly dependent on the ratio of boundary-layer thickness to hole diameter and, as the boundary-layer thickness increases, the cross-flow behaviour becomes increasingly non-linear, and shock/boundary-layer interaction effects become more marked. Lukasiewicz (Ref. 3) suggested that the hole diameter should always be more than twice the boundary-layer displacement thickness. (Some control over the boundary-layer thickness can be obtained both by adjusting the plenum chamber pressure and by varying the inclination of the walls to the flow; inclinations of the order of $\pm$ 40 minutes are often used.)

Another design requirement which influences the hole size is that the steady flow disturbances produced by the holes should not cause too great a spatial variation in Mach number in the test region. The amplitude of this disturbance field increases as the Mach number increases and as the wall boundary-layer thickness decreases; it also decreases with increasing distance from the wall. The criterion suggested by Lukasiewicz (Ref. 3) is that, for 60° slanted holes, the hole diameter should be less than 1/100 of the smaller working section dimension. This criterion has been satisfied in most perforated wall tunnels built in recent years.

2. TURBULENCE AND NOISE GENERATION FROM VENTILATED WALLS

There are a number of types of disturbance likely to be present in a ventilated-wall tunnel. The main ones are (a) low-frequency unsteadiness associated with the large-scale features of the tunnel circuit and plenum chamber, (b) high-frequency turbulence and noise arising from the ventilated tunnel walls (and possibly from the compressor), (c) low-frequency noise induced by high frequency oscillations, (i.e. cross-tunnel modes driven by wall-generated disturbances), and (d) low-frequency disturbances in the working section consisting of the unsteady waves either reflected back from a downstream sonic throat at subsonic and transonic test-section Mach numbers or, in the absence of a second throat, waves moving upstream from a diffuser.

Slotted liners can lead to noise generation from eddies caused by the shearing action between the air in the test section and that in the plenum chamber. Low-frequency oscillations resulting from these have given trouble during the development stage of a number of slotted wall tunnels but can usually be reduced satisfactorily by alterations in the geometry of the tunnel (Ref. 4). Some tests made in the RAE Bedford 3 ft x 2.7 ft wind-tunnel showed that, over a limited frequency range of 20 - 2000 Hz, the noise level with top and bottom walls slotted was only slightly higher than the level with four perforated walls (Ref. 4).

For perforated wall liners, recent U.S. tests show that in addition to low-level broad-band fluctuations over a wide range of frequencies, typically having a fluctuating wall r.m.s. pressure coefficient δC_p of from 0.01 to 0.02, there are narrow-band high-level fluctuations with δC_p from 0.03 to 0.06. δC_p values measured at the tunnel centre line may normally be as much as 50% lower than those measured at the wall, although a few measurements have been reported in which they were higher (Ref. 5).

Fig. 2 gives a typical frequency spectrum for a perforated wall test section taken from Ref. 5. Normally, the power of one or perhaps two of the discrete tones is dominant, but six or even more frequency components can sometimes be identified.

McCanless (Ref. 6) has given a summary of the results of frequency analyses performed (by different agencies) in nine perforated-wall wind-tunnels. The discrete frequencies of the noise measured in all but the two smallest test sections he presents in terms of Strouhal number, S, defined by:

$$S = \frac{fh}{U_\infty},$$

where h is the major axis of the ellipse formed on the liner surface by drilling at an angle to the wall normal. A re-plotting of McCanless's data points is shown in Fig. 3. Also shown on this figure are some results obtained with isolated holes (Ref. 7).

The main features to note from Fig. 3 are that there is a tendency for the Strouhal numbers to lie in fairly well-defined bands, and that the general trend for each band is for S to decrease somewhat with increase of M_∞.

Furthermore, the median Strouhal numbers for the four identifiable bands are, at a Mach number of unity, approximately 0.08, 0.25, 0.5 and 0.75.

McCanless (Ref. 6) associates the four discrete frequencies of the perforated wall sound with the four stages of edge tones described in detail by Brown (Ref. 8), but apparently discovered by Sondhaus (Ref. 9). (In fact, the quadruplicity of neither phenomenon can be accepted.) One can readily draw an analogy between, on the one hand, jet instability and the essential presence of an edge for edge-tone existence and, on the other hand, shear-layer instability and the essential presence of the downstream end of the hole for perforation tone existence.

There have been several relevant studies on unsteady (isolated) cavity flows. Principally, such cavities have been rectangular and have differed from liner perforation flows also in being formed by blind holes (i.e. without connection through to a plenum chamber). A typical study was that made by Rossiter (Ref. 10) and, based on a simple theoretical mechanism involving phase matching between vortex cores progressing downstream and acoustic pulses moving upstream, he suggests that the Strouhal numbers for the discrete tones are given by the relation:

$$S = \frac{fL}{U_\infty} = \frac{m - \gamma}{\frac{1}{H} + M_\infty}, \qquad (1)$$

where m is any positive integer, γ is the fraction of the core wavelength travelled downstream by a core before its resulting acoustic pulse, effective in initiating a further vortex core, commences its travel upstream, L is the cavity length and HU_∞ is the effective downstream core convection velocity across the cavity mouth.

The factor H varies with the ratio of the wall boundary layer thickness to the cavity width. γ, although also varying, is a small fraction. Taking a measured mean value of $\gamma = 0.05$ and H limits of 0.35 ($\delta^*/L \simeq 0.3+$) and 0.57 ($\delta^*/L \simeq 0.01$), the Strouhal numbers expected for the spectrum peaks are shown in Fig. 4. A typical frequency spectrum of pressure fluctuations measured by Rossiter in a rectangular cavity with $L/D = 1$ and $M_\infty = 0.9$ is shown in Fig. 5.

The resemblance between the levels and variations of the Strouhal numbers for perforations and for cavities is striking (Figs. 3 and 4), and it seems likely that the second, third and fourth perforation tones noted by McCanless (Ref. 6) can be associated respectively with the 'quasi edge tone' m = 1, 2 and 3 modes observed by Rossiter and others.

It seems unlikely, though, that the first perforation tone can be produced solely by the 'quasi-edge-tone' type of mechanism.

There is, in fact, a marked difference shown in results presented by Mabey (Ref. 4) between the variation of power with Mach number of the two lowest frequency perforation modes. He found that the first perforation tone reduced in amplitude and then vanished as the tunnel unit Reynolds number was increased, and that when δ^*/d in the test section was below 0.4, the first tone was absent. This first tone could also be suppressed by sliding a thin plate, attached to the liner on the plenum chamber side, in the downstream direction until the holes were approximately half covered. Mabey suggested that for $\delta^*/d > 0.4$ when, with a conventional perforation, the shear layer might not reattach to the hole interior, sliding of the plate downstream by a certain amount would result in shear-layer attachment. The first perforation tone might therefore be associated with a secondary instability of the outflow.

An important feature of these discrete frequency fluctuations is that they can form coherent unsteady wave fronts crossing the working section; that is to say, the fluctuations from individual holes are phase locked. Such waves (shown in Fig. 6) have been observed in spark schlieren photographs in tests at The City University, London (Ref. 7) and at NASA Langley (Ref. 11).

Although the influence of the high-frequency fluctuations on model tests is not known in detail, it is noted that their amplitudes may be several times higher than those normally present in turbulent boundary layers, and comparable with the pressure fluctuations present under oscillating shock-waves on a body. It is therefore highly desirable to reduce the amplitudes as much as possible.

Various methods of reducing unwanted high-frequency noise are worth exploring. The upstream covering of the holes mentioned above may reduce the level of the first perforation tone, although it is thought that this mode is only present for $\delta^*/d > 0.4$. On the other hand, partially covering the bottom of the holes by a plate moved in the upstream direction proved effective in reducing the amplitude of the second perforation tone in tests at The City University. This solution was also suggested by Credle (Ref. 5). It may be noted that one way of suppressing edge tones is to replace the knife edge by a cylinder. The implication for the perforation tones is that the downstream hole edges should be rounded off. In tests at The City University, in which the rear edge was bevelled, it was found that the sound intensity was not much reduced. The drawback to all these methods of sound reduction is that they may result in the cross-flow characteristics of the perforations being altered, and there could be a conflict between the methods for reducing sound, and the choice of geometry for good correction characteristics of the liners.

3. CONCLUSIONS

In spite of the large amount of development work on both slotted and perforated tunnel walls over the past twenty years, one is left with the impression that their designs still represent a compromise solution valid only for small blockage ratios and moderate angles of attack. Current work on the variation of longitudinal porosity should result in some improvement in obtaining conditions for minimising wall corrections.

It is clear also that further work is needed on elucidating the behaviour of both isolated hole and hole array sound fields and their effect on model testing.

4. REFERENCES

1	Pindzola, M.	Transonic Wind Tunnels. VKI Lecture Series 42 (1972)
2	Lo, Ching-Fang	Wind Tunnel wall interference reduction by streamwise porosity distribution. AIAA Journal Vol. 10 No. 4 (1972)
3	Lukasiewicz, J.	Effects of boundary layer and geometry on characteristics of perforated walls for transonic wind tunnels. Aerospace Eng. Vol. 20, No. 4 (1961)
4	Mabey, D. G.	Flow unsteadiness and model vibration in wind tunnels at supersonic and transonic speeds. ARC CP-1155 (1971)
5	Credle, O. P.	Perforated wall noise in the AEDC-PWT 16-ft and 4-ft transonic tunnels. AEDC-TR-71-216 (1971)
6	McCanless, G. F.	Additional correction of 4% Saturn V protuberance test data. Technical Report HSM-RI-71. NAS8-30517 (1971)
7	Freestone, M. M. & Cox, R. N.	Sound fields generated by transonic flows over surfaces having circular performations. AGARD CP 83 Paper 24 (1971)
8	Brown, G. B.	The vortex motion causing edge-tones. Proc. Phys. Soc. Vol. 49, p 493 (1937)
9	Sondhaus, C.	Uber die beim Ausströmen der Luft entstehenden Töne. Ann. Phys. (Leipzig), Vol. 91, pp 126 & 214 (1854)
10	Rossiter, J. E.	Wind-tunnel experiments on the flow over rectangular cavities at subsonic and transonic speeds. R & M No. 3438 (1966)
11	Karabinus, R. J. & Sanders, B. W.	Measurements of fluctuating pressures in 8 by 6 ft supersonic wind tunnel for Mach number range of 0.56 to 2.07. NASA TM X 2009 (1970)

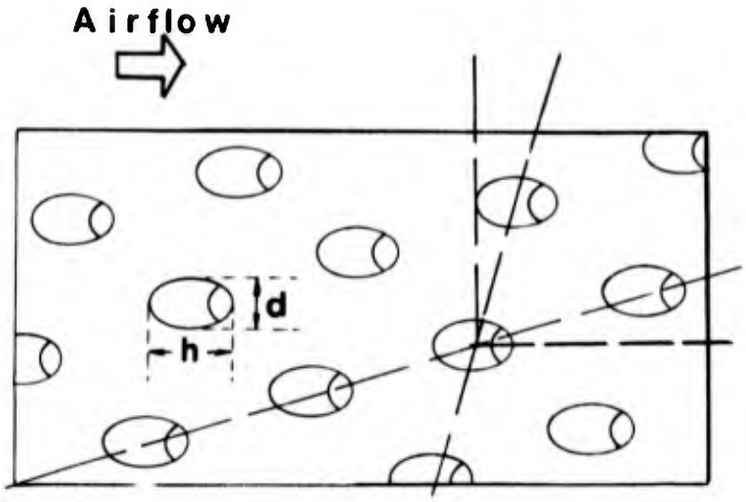

Fig. 1a Typical array of liner perforations

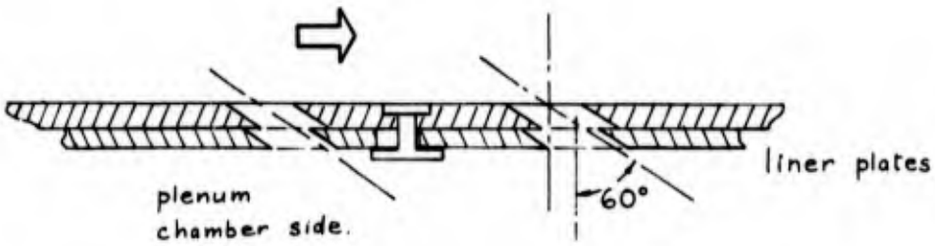

Fig. 1b Liner plates showing means of varying open area ratio

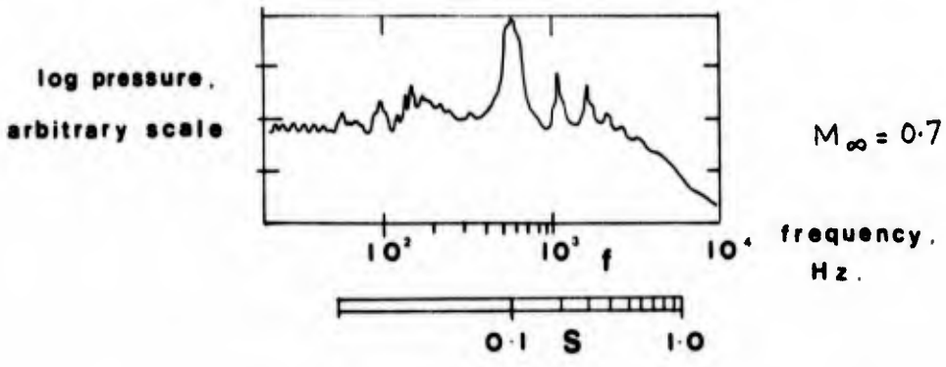

Fig. 2 Typical frequency spectrum of pressure variations measured on a test cone in the centre of a wing tunnel. (After Credle, Ref. 5)

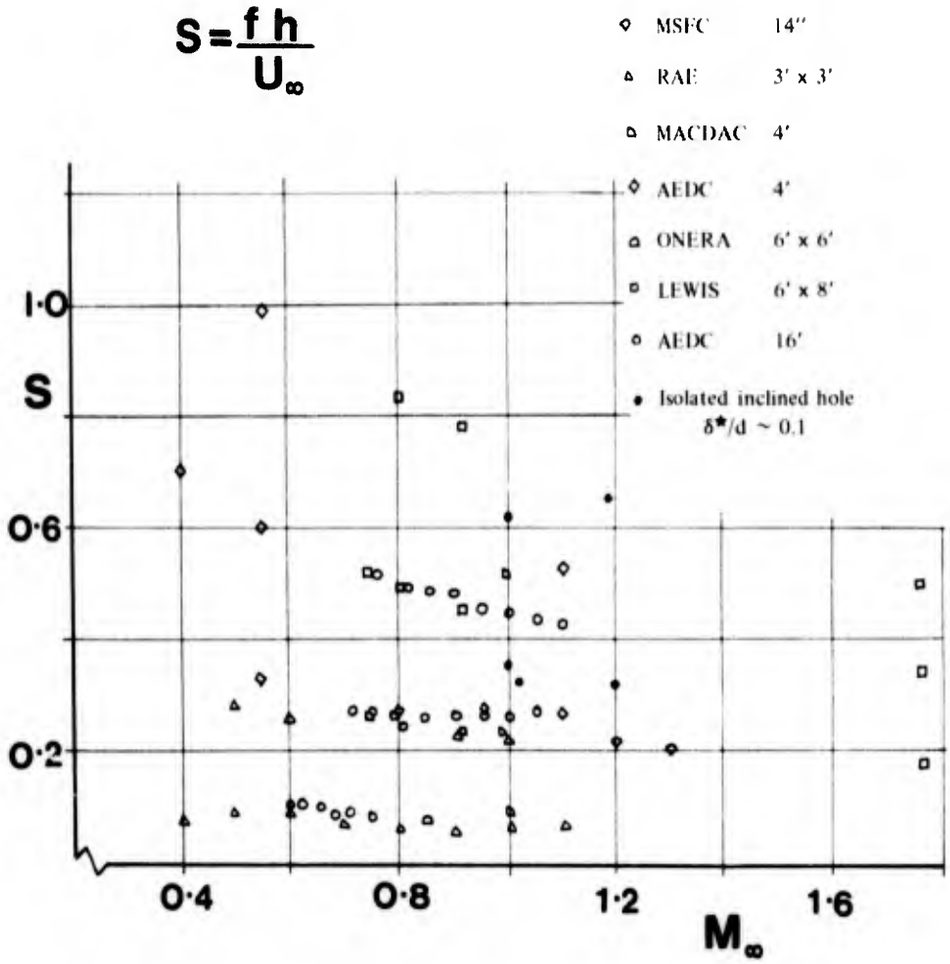

Fig. 3 Strouhal numbers of narrow band perforated liner sound measured in several wind tunnels.
(From McCanless, Ref. 3)

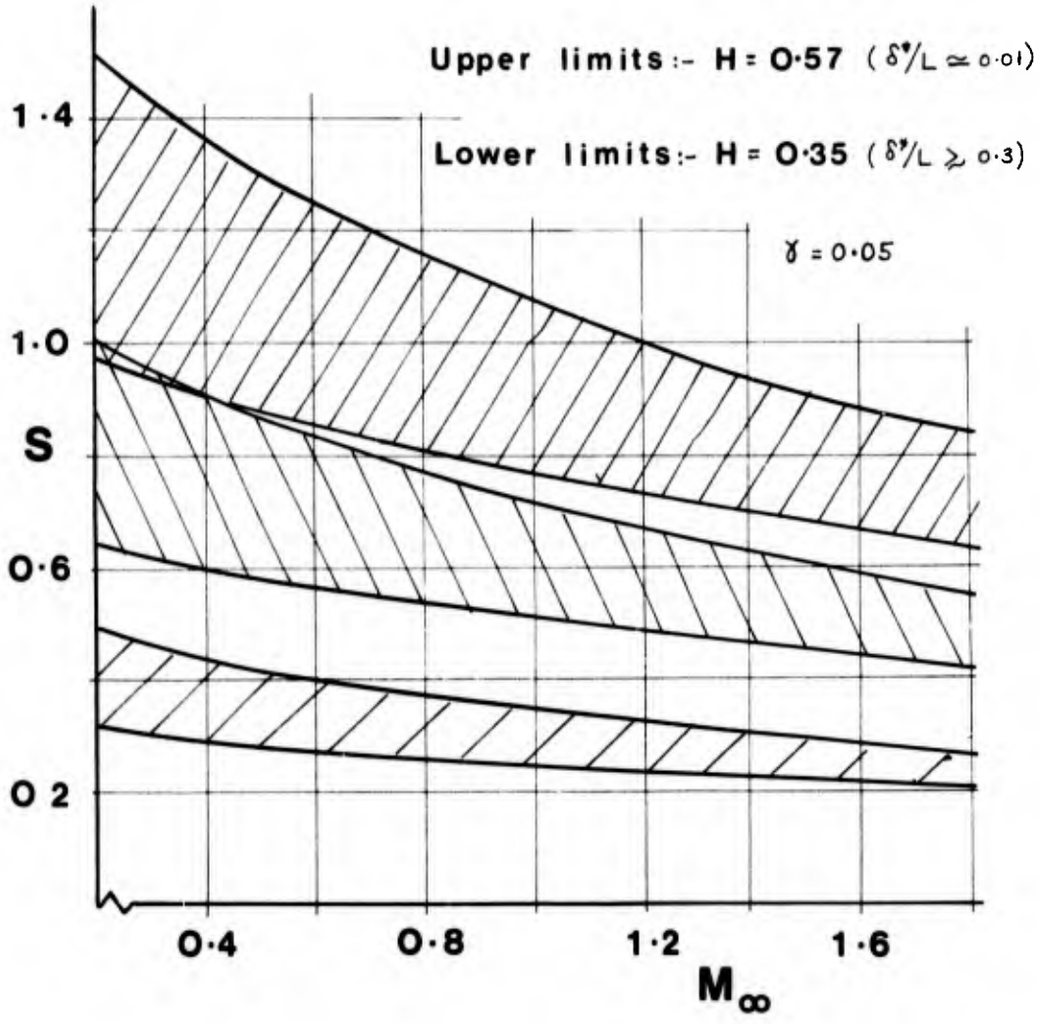

Fig. 4 Variation of Strouhal number with Mach number according to equation 1, relating to cavity tones.

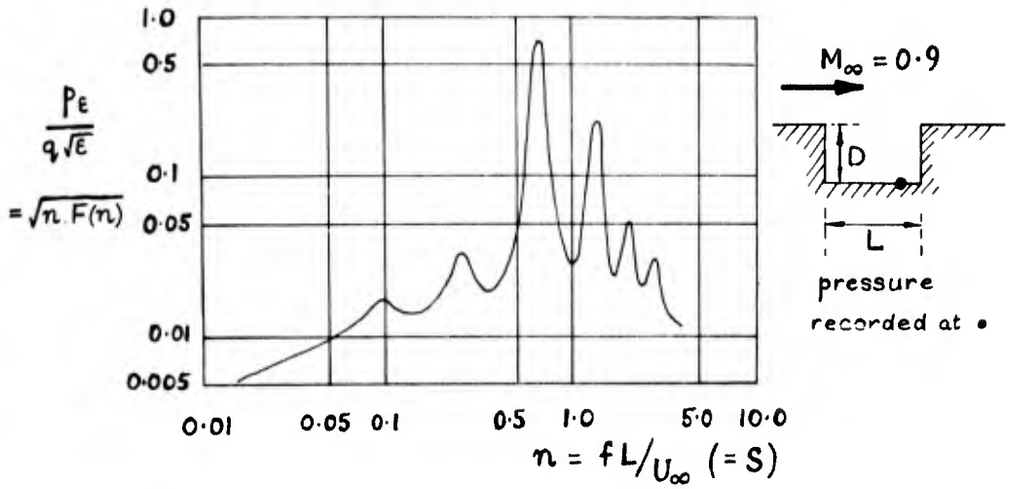

Fig. 5 Typical frequency spectrum of pressure variations measured in a rectangular cavity
($L/D = 1$, $M_\infty = 0.9$. See Rossiter, Ref. 10)

Fig. 6 Spark schlieren photograph of sound waves emanating from a single streamwise row of liner holes ($M_\infty \sim 1.2$)
(For test details see Ref. 7)

APPENDIX I

This Report is one of four issued as documents complementary to Advisory Report 60 of the Large Wind Tunnels Working Group of the AGARD Fluid Dynamics Panel. The other reports in the series are as follows:

AGARD REPORT No.598

EXPERIMENTS ON MANAGEMENT OF FREE-STREAM TURBULENCE by R.I.Loehrke and H.N.Nagib.

AGARD REPORT No.600

PROBLEMS OF WIND TUNNEL DESIGN AND TESTING

Some considerations of future low-speed tunnels for Europe: by A.Spence and B.M.Spee.

Project study of a large European transonic Ludwieg Tube wind tunnel: by H.Ludwieg, H.Grauer-Carstensen and W.Lorenz-Meyer.

The development of an efficient and economical system for the generation of a quiet transonic flow suitable for model testing at high Reynolds numbers: by P.G.Pugh.

Induction transonic wind tunnel: by P.Carrière.

Soufflerie à compresseur hydraulique: by M.Ménard.

Testing at supersonic speeds: by Ph.Poisson-Quinton.

Facilities for aerodynamic testing at hypersonic speeds: by F Jaarsma and W.B. de Wolf.

AGARD REPORT No.601

PROBLEMS IN WIND TUNNEL TESTING TECHNIQUES

Review of some problems related to the design and operation of low-speed wind tunnels for V/STOL testing: by M.Carbonaro.

Survey of methods for correcting wall constraints in transonic wind tunnels: by J.C.Vayssaire.

Interference effects of model support systems: by E.C.Carter.

Minimum required measuring times to perform instationary measurements in transonic wind tunnels: by J.W.G.van Nunen, G.Coupry and H.Förscher.

Some considerations of tests under dynamic conditions in low-speed wind tunnels: by D.N.Foster.

Use of model engines (V/S/CTOL): by E.Melzer and R.Wulf.

Wind tunnel requirements for helicopters: by I.A.Simons and H.Derschmidt.

Acoustic considerations for noise experiments at model scale in subsonic wind tunnels: by T.A.Holbeche and J.Williams.